

## Clay–Organic Interfaces for Design of Functional Hybrid Materials

Pilar Aranda<sup>1</sup>, Margarita Darder<sup>1</sup>, Bernd Wicklein<sup>1</sup>, Giora Rytwo<sup>2</sup>, and Eduardo Ruiz-Hitzky<sup>1</sup>

<sup>1</sup>Materials Science Institute of Madrid, CSIC, c/ Sor Juana Inés de la Cruz 3, 28049 Madrid, Spain

<sup>2</sup>Environmental Physical Chemistry Laboratory, MIGAL- Galilee Research Institute of Environmental Sciences, Tel-Hai College, Upper Galilee, 12201, Israel

### 1.1 Introduction

#### 1.1.1 Clay Concepts, Definitions, and Classification

Clay minerals represent a wide family of natural silicates that are essentially related from the structural point of view with 2D solids, being arranged in a layered stacking (phyllosilicates) and showing unique colloidal and surface properties of crucial importance for the life in Earth [1]. They constitute a key reference not only as structural models and other basic aspects but also regarding their role in agronomy, industry, and environmental features influencing human activities of global concern. Clay-sphere represents a vast domain belonging to the Earth geosphere, mainly being associated with soil, which in turn can be regarded as a sort of *magic skin* of our planet. According to Kutílek and Nielsen [2], soil – and indeed clay minerals as one of its essential component – started its critical role when macroscopic life moved from oceans to mainland, roughly 500 million years ago. The support of and the interaction with micro- and macroorganisms is in a large extent deserved by clay mineral components that represent one of the most ample group of inorganic solids that interact with the biosphere. Even more, it has been invoked by diverse authors that clays have played an essential role in the origin of life in close interaction with organic precursors [3].

From the structural point of view, clay minerals appear mainly organized as hydrous phyllosilicates whose elemental layers have one dimension (the thickness) in the nanometer range, and therefore they can be considered as nanomaterials. According to the silicate layers nature, clay minerals can be classified as 1 : 1 (or TO) and 2 : 1 (or TOT) phyllosilicates representing the stacking of tetrahedral (T) and octahedral (O) layers, which can be considered as building blocks that combined between them lead to a huge diversity of layered silicates. Typical examples of 1 : 1 phyllosilicates are kaolinite and serpentine with octahedral

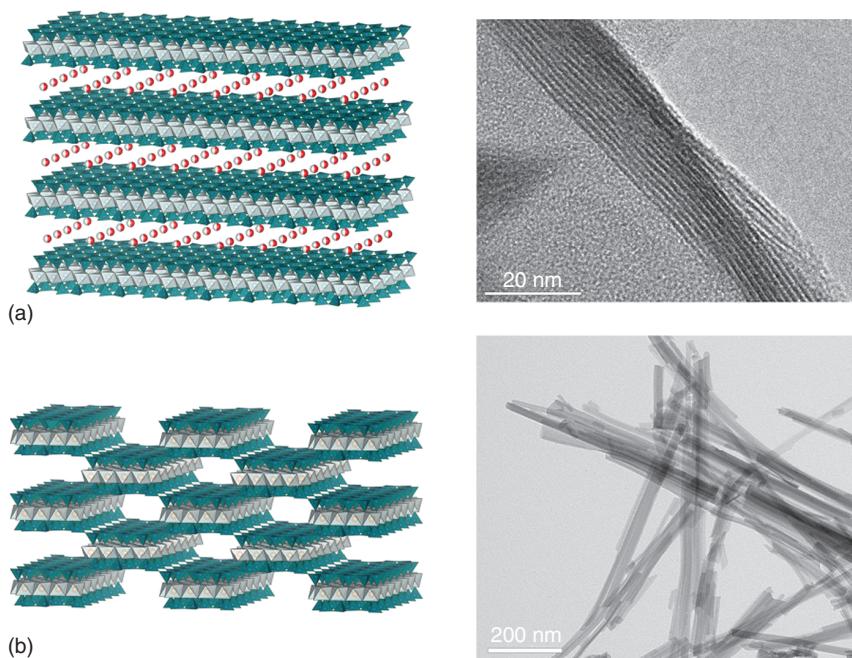


**Figure 1.1** Schematic representation of clays structure with (a) layered habit (montmorillonite) showing on the right column the cross section of the silicate layers and (b) fibrous morphology (sepiolite) showing the organization of silicate fiber dimension.

layers composed of aluminum (dioctahedral silicate) and magnesium (trioctahedral silicate), respectively. Typical examples of 2 : 1 phyllosilicates are pyrophyllite and talc, with octahedral layers composed of aluminum (dioctahedral silicate) and magnesium (trioctahedral silicate), respectively. In this case, the structure of 2 : 1 phyllosilicates is composed of two tetrahedral Si sheets sandwiching the Al or Mg central octahedral sheet.

Clay minerals are often associated with smectites and particularly with montmorillonites (MMT), the main component of bentonites of great interest for diverse industrial applications. Smectites are dioctahedral aluminosilicates belonging to the 2 : 1 phyllosilicate structure with isomorphous substitutions of aluminum by magnesium ions, giving rise to negatively charged layers that are compensated with cations in the interlayer space (Figure 1.1a). These cations, named exchangeable cations, can be easily replaced by treatment with salt solutions of metal or organic cations, leading to homoionic smectites. Many other related structural 2 : 1 silicates such as beidellite, saponite, nontronite, hectorite, and so on are known, where isomorphous substitutions could also affect the cationic replacement in the tetrahedral layer (e.g.,  $\text{Si}^{4+}$  by  $\text{Al}^{3+}$ ). Vermiculites are a family of 2 : 1 phyllosilicates with an isomorphous substitution degree higher than in smectites, therefore showing a more elevated net layer charge per formula unit (0.6–0.9) than in smectites (0.2–0.6) [4].

MMT and related smectites exhibit significant characteristics/properties with particles of colloidal size, high degree of layer stacking disorder, elevated specific

surface area (SSA), large cation exchange capacity (CEC), and a variable interlayer separation that depends on the nature of interlayer cation and relative humidity [1]. However, the most interesting feature of these 2D solids is definitely their capacity to intercalate many diverse species, neutral or charged, inorganic or organic, and even macromolecules of relatively high molecular mass. As will be discussed later, the nature of the interface at the interlayer space in these systems is determinant for the intercalation processes, as well as for the arrangement and stability of species in the resulting intercalation compounds.

Typical morphology of clay minerals corresponds to platelike crystallites of micrometer size. However, in certain circumstances special structural arrangements determine other conformations, as it is the case of halloysite that can exhibit a nanotubular morphology due to the rolling of 1 : 1 aluminosilicates such as kaolinite, leading to a multiwalled system. Halloysite nanotubes have characteristic inner diameter in the order of 15 nm, their lumen facilitating the access of organic species with the formation of hybrid organic–inorganic materials [5]. Certain 2 : 1 phyllosilicates such as sepiolite (Figure 1.1b) and palygorskite show a fibrous habit with a continuous tetrahedral silica layer and a discontinuity of the octahedral sheet due to the periodic inversion of the apical oxygen atoms of the tetrahedra in every two (palygorskite) or three (sepiolite) silicate chains [1, 6]. As a consequence of this structural arrangement [7], both types of silicates show an alternation of blocks and cavities named *tunnels* [8], which are oriented along the *c*-axis, that is, in the fiber direction (Figure 1.1b). The fiber length varies depending on the origin of the fibrous silicates, typically the fibers of sepiolite from Vallecas-Vicálvaro deposits in Spain being between 1 and 5  $\mu\text{m}$ . The structural blocks are composed of two tetrahedral silica sheets sandwiching a central sheet of magnesium oxide–hydroxide in the case of sepiolite and of magnesium and aluminum oxide–hydroxide in the case of palygorskite. Due to the periodic discontinuity of the silica sheets, silanol groups ( $\equiv\text{Si}-\text{OH}$ ) are covering the “external surface” of the silicate fibers [8, 9]. The tunnel dimensions are in the nanometer range (0.37 nm  $\times$  1.06 nm, in sepiolite and 0.37 nm  $\times$  0.64 nm in palygorskite), allowing the entrance of small molecules such as  $\text{N}_2$ ,  $\text{H}_2\text{O}$ ,  $\text{NH}_3$ ,  $\text{CH}_3\text{OH}$ , and others to the interior of the silicates, that is, these molecules can be adsorbed at the internal surface of sepiolite and palygorskite [8].

The surface and the interface chemistry of the different types of clay minerals – and indeed essential properties inherent to these silicates – are determined by various factors such as:

1. The chemical composition and the nature of the surface (mainly oxygen atoms, water molecules, and hydroxyl groups)
2. The type, extent, and localization of the electrical charge in the silicate
3. The nature and CEC in the external and intracrystalline regions
4. The extent (SSA) and reactivity of the planar external surface, the internal surface (interlayer space), and the edge of the clay particles

In this way, the surface activity toward adsorption and other interactions of diverse compounds with clay minerals can be modulated by the aforementioned features.

### 1.1.2 Clay–Organic Interactions: Clay–Organic Interfaces and Functionalization of Clay Minerals

The history of well-defined organic–inorganic hybrid materials starts with the assembling between organic compounds and clay minerals, which took place in the intercalation of organic cations in smectite phyllosilicates by ion-exchange processes replacing interlayer cations by alkylammonium species, as reported by the first time by Giesecking [10]) and Hendricks [11]. Since these early reports, many different types of organic cations, such as alkyl- and arylammonium species, cationic dyes, amino acids, charged peptides and proteins, cationic pesticides and surfactants, and so on, have been intercalated in smectites and vermiculites [12]. Clearly, electrostatic bonding mechanisms between the organic cations and the charged clay layers can be here invoked, although, strictly speaking, non-coulombic attractions such as van der Waals forces must be also considered. Nowadays, long-chain alkylammonium species belonging to the cationic surfactants group represent from far the most remarkable organic compound used for the preparation of so-called organoclays of great importance in diverse applications. As initially reported by MacEwan, non-charged, that is, neutral, molecules can also be accommodated in the interlayer region of smectite and vermiculite layered silicates in interaction with interlayer cations and oxygens belonging to the internal surface of these solids [13]. Since this last discovery, a huge number of neutral compounds of different functionality have been intercalated in layered clays involving diverse host–guest mechanisms in those clay–organic interactions: amines by proton transfer reactions; hydroxyl compounds such as alcohols, polyols, and phenols by H bonding; aromatic compounds by electron transfer mechanisms; macrocyclic compounds such as crown ethers by ion–dipole interactions; and so on [12].

Surface modifications by clay–organic interactions give rise to hybrid organic–inorganic materials, where the introduced organic functionality leads to complementary properties to those inherent to the silicate substrate. In this way, combination of the exchangeable ability of the interlayer cations, the adsorption capacity and certain colloidal characteristics of clays with the hydrophobic character, chemical reactivity, and specific functionality of the organic component result in extraordinarily versatile organic–inorganic materials provided with modulated physical and chemical predetermined behaviors.

Most of the resulting organic–inorganic systems are derivatives of layered silicates belonging to smectite clays (e.g., MMT), more rarely to vermiculites, and even in minor extent to kaolinite and related aluminosilicates [14]. X-ray diffraction (XRD) technique is in these cases the determinant tool to show the penetration of organic species in the interlayer space of the layered silicates, producing an increase of the basal distances due to the expansion along the *c*-axis that depends on the molecular size and disposition of the guest molecule. Only in few cases the crystallinity of these hybrids allows approximations toward the partial resolution of their crystal structure by means of one-dimensional X-ray Fourier analysis. Dichroism studies of infrared (IR) absorption bands were applied to ascertain the orientation of intercalated molecules with respect to the silicate plane. A salient example of application of these two techniques corresponds to the



determination of pyridinium ion orientation in layered silicates of different charges, that is, MMT and vermiculite. In MMT (lower charge) the pyridinium rings are arranged with their planes parallel to the silicate layers, whereas in vermiculite (higher charge), the pyridinium ions are disposed perpendicular to the layers [15, 16].

Increasing interest is currently being paid to clay–organic hybrids derived from clays showing different structures and morphologies, such as the fibrous, or rather expressed the needlelike, sepiolite and palygorskite silicates as well as the nanotubular halloysite. The lumen of this last silicate allows the access to diverse reactive compounds to the interior of the nanotubes whose internal surface is covered by aluminol groups ( $=\text{Al}-\text{OH}$ ). These groups are able to interact with diverse compounds and, in some cases, could generate stable derivatives where the organic component is attached to the clay through covalent bonds. Ionic liquids can be grafted, forming stable  $\text{Al}-\text{O}-\text{C}$  bonds, the resulting species being able to selectively support deposited palladium nanoparticles (NP) inside the nanotubular halloysite lumens [17].

Sepiolite and palygorskite contain intracrystalline cavities extended along the fiber axis ( $c^*$ ) but showing a reduced cross-sectional size ( $a$ - and  $b$ -axis), which allows only the access of small molecules (*vide supra*) [8]. The internalized molecules can be often stabilized inside the structural tunnels by hydrogen bonding with the water molecules coordinated to Mg(II) ions at the edge of the octahedral layer in the structural silicate blocks. This is, for instance, the case of pyridine–sepiolite hybrids, in which H-bonded pyridine heated at  $140^\circ\text{C}$  leads to the elimination of water molecules, being directly coordinated to the Mg(II) edge cations through unusual, but here stable, Mg–N bonds [18]. Contrarily to the case of layer silicates, hybrids derived from fibrous and nanotubular clays cannot be characterized by XRD patterns, but multinuclear nuclear magnetic resonance (NMR) is here a powerful technique allowing to clarify clay–organic interaction mechanisms of organic species located at the interior of the silicates as well as at their external surfaces [18].

As indicated earlier, silanol groups are present at the external surface of sepiolite and palygorskite [8, 9]. They play an essential role in the interaction of fibrous clay minerals with organic compounds that could result in organic derivatives of those silicates through covalent bonds by reaction with organosilanes, epoxides, and isocyanates [19–21]. The grafting reactions on sepiolite using alkylsilanes, such as trimethylchlorosilane, produce hydrophobic organic–inorganic materials, whereas the use of silanes containing functional groups (benzyl, amino, mercapto, etc.) modifies the inherent chemical reactivity of this silicate [12]. As an example, the use of aryl-containing organosilanes results in sepiolite derivatives allowing further reactions of the aromatic rings, leading to functional hybrid materials whose interphase can contain, for instance, sulfonic groups provided with strong acidity [22, 23]. Many other types of organic compounds interact with sepiolite mainly by physical adsorption at the exterior of the silicate surface, producing a perturbation of IR bands assigned to Si–OH groups. Cationic surfactants such as alkylammonium species interact with sepiolite in a similar way than that reported for smectites but, in this case, only affecting the external surface of the fibrous clay. The resulting organosepiolites can be easily

dispersed in low-polar organic solvents [24], allowing diverse industrial applications. One of them is their use as nanofiller in the preparation of polymer–clay nanocomposites, making the polarity of the polymer matrix and the modified sepiolite compatible, enhancing their miscibility and improving therefore the material characteristics [25].

Clay modifications to prepare conventional organoclays are based on electrostatic mechanisms, but they can be also driven by using a broad variety of organic functional compounds involving diverse bonding mechanisms in their interaction with the silicate surfaces, resulting in organic–inorganic materials of variable stability. For instance, neutral polar molecules (alcohols, phenols, amines, etc.) interact with clay surfaces through hydrogen bonding and water bridges (i.e., water molecules coordinated to interlayer cations in smectites and at the crystal edges in sepiolite and palygorskite). Also, interaction mechanisms can be based on ion–dipole and direct coordination of molecules acting as ligands, as it is the case of intracrystalline complexation of interlayer cations with crown ethers and cryptands [26, 27]. Finally other clay–organic interaction mechanisms are based on the transfer of protons and electrons. Protonation of organic bases, as it is the case of clay–amine interactions, has been ascribed when the clay surface exhibits enough acidic character mainly correlated with the nature of interlayer cations (e.g.,  $\text{Al}^{3+}$  ions). Transition metal interlayer cations can induce the formation of  $\pi$ -bonds in clay–aromatic compounds (e.g., benzene) interactions as firstly reported by Doner and Mortland [28]).

### 1.1.3 Clay–Organic Materials and Interfaces: Design and Preparation of Nanostructured Hybrids with Functional Properties

Interaction of clay minerals with organic compounds is the basis for the design and fabrication of hybrid materials having incidence in critical areas such as agriculture (e.g., interactions of soils and clays with pesticides and fertilizers), environment (e.g., air, water, and soil protection and removal of pollutants), health and hygiene (e.g., sequestering of mycotoxins, antimicrobial activity, drug delivery systems (DDS), and carriers for vaccines and other bioactive species), industry (e.g., adsorbents, separation, catalysis, and sensors), building and transportation (e.g., polymer–clay nanocomposites and ultra-lightweight materials), and energy (e.g., generation of carbon–clay materials of interest as elements for batteries and supercapacitors). In general these interactions take place at the nanometer level, and therefore the nanotechnology concepts can be applied to clay minerals to develop advanced nanomaterials via functionalization, that is, through the deliberated introduction of suitable properties giving rise to novel functional nanoarchitectures.

The most extensively investigated, widely applied, and expansively commercialized organic–inorganic hybrids derived from clay minerals are undoubtedly the materials named as “organoclays,” in view of their importance to many applications [1, 12, 14, 29]. As mentioned earlier they result from the ion exchange of the original interlayer cations in smectites for long-chain alkylammonium quaternary ions. Therefore, organoclays exhibit an organophilic interface useful for many diverse applications from removal of organic pollutants in water to fillers

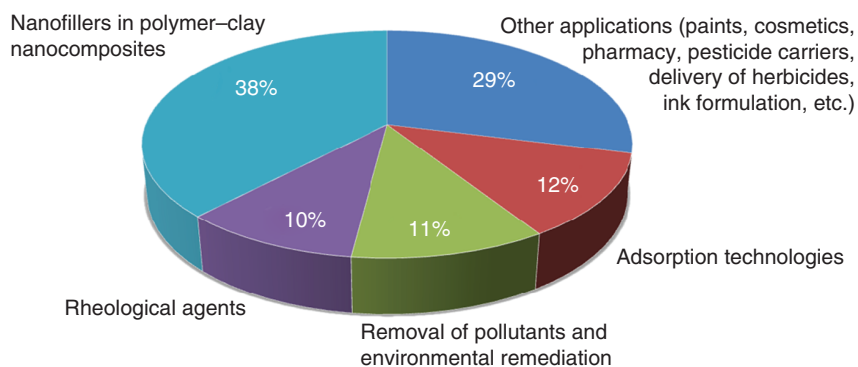


**Figure 1.2** Distribution of application fields of organoclays elaborated with data from the ISI Web of Science (Thomson Reuters) accessed on July 13, 2016.

in polymer-clay nanocomposites. In fact, this last topic represents about 38% of articles dealing with organoclays, which corresponds to a total of 6864 articles, according to data accounted from the ISI Web of Science (Thomson Reuters) accessed on July 13, 2016. Other important applications of organoclays are related to adsorption technologies (12% of total articles), removal of pollutants, and environmental remediation (11%) as well as rheological agents (10%) and in minor extent as components of paints, cosmetics, pharmacy, pesticide carriers, delivery of herbicides, inks formulations, and so on (Figure 1.2).

As the alkylammonium surfactants exhibit toxicity, in order to prepare benign organoclays, the replacement of this type of organic cations for other nonhazardous ones should be investigated. In this way, phosphatidylcholine (PC), one of the main constituents of the cell membranes, has been considered as a promising alternative to alkylammonium compounds [29]. This last compound is a zwitterion that, in a controlled manner, can be intercalated as a cation in MMT, leading to organic-inorganic materials whose interfaces appear as “supported biological membranes” [30]. These lipophilic interfaces are useful for certain applications, for instance, in mycotoxin sequestration [31].

As already indicated, the main investigations on organoclays are addressed to their use as fillers in polymer-clay nanocomposites (Figure 1.2) due to the compatibility between the organically modified clays and the organophilic polymers. Polymer-clay nanocomposites result from the interaction of clays – and organoclays – with monomers followed by polymerization or directly with polymers, which in the case of layered clays gives rise to delamination or exfoliation phenomena, resulting in uniformly dispersed silicate nanolayers within the polymer matrix. These systems investigated for the first time by the Fukushima’s team at the Toyota Central Labs [32] exhibit unique properties, in general improving considerably mechanical properties of the polymer matrix, even involving a very low content of the clay component (<3 wt%). The topic has received in the last two decades a huge dedication by many scientists and engineers with an extensive number of publications and patents. Most of the reviews on polymer-clay nanocomposites (see, for instance, Refs. [33–40]) deal with applications related to structural properties and, in minor extent,

to functional materials. As the aim of this chapter is to focus on functional hybrid materials, we will here emphasize on nanocomposites based on clays of diverse characteristics and polymers, or biopolymers, whose assembly leads to hybrids provided with functional properties. The main procedures of polymer intercalations are experimentally conducted by direct adsorption of the polymer from water – especially in the case of hydrogels – or from organic solvents, as it is the case of soluble polymers – see, for instance, the intercalation of poly(ethylene oxide) (PEO) in clay smectites [41, 42]. Alternatively, melt intercalation processes can produce the intercalation/exfoliation of layered clays as firstly reported by Vaia *et al.* [43]. This last procedure has been largely applied for low-polar polymer matrices (e.g., polypropylene (PP) and polystyrene (PS)) in which many diverse organoclays are delaminated and homogeneously distributed among the entire matrix as a nanofiller that enhances mechanical and rheological properties [36].

Also sepiolite and palygorskite fibrous clays can offer organic–inorganic interfaces for assembling polymers, giving rise to polymer–clay nanocomposites. This type of clay minerals has attracted increasing interest as nanofiller in the preparation of diverse types of polymer–clay nanocomposites [1, 25, 44–46]. Interesting effects of these clays in the reinforcement of a large variety of polymers have been reported, although as they are two-nanodimensional particles usually show scarce efficiency for improving barrier properties compared with 2D clays such as smectites and vermiculites. The high hydrophilic character of the external surface of sepiolite and palygorskite determines poor compatibility with polyolefins and many other polymers (e.g., thermosetting resins such as epoxy and polyurethane), disfavoring their homogeneous distribution and interaction with the polymeric matrix. Therefore, in most cases a previous modification of the clay is necessary to create compatible interfaces and to improve their adhesion with the polymers. For this reason, organoclays prepared by treatment of these clays with diverse cationic surfactants and specially with coupling agents (organochlorosilanes and organoalkoxysilanes) through reactions with the clay  $\equiv\text{Si}-\text{OH}$  groups afford suitable interfaces to reach higher compatible nanofillers [36]. The modification of the clay can be done prior to the incorporation in the polymeric matrix, or the modifiers can be added during the *in situ* formation of the polymer, for instance, polyethylene [47]. The nature of the organic–inorganic interface stabilized by electrostatic interactions, as in the case of cationic surfactants, or by covalent bonds, as occurs in the case of fibrous clays treated with organosilanes, influences the characteristics of the nanofiller. For instance, epoxy resins incorporating palygorskite modified by reaction with aminopropyltrimethoxysilane show its maximum reinforcement effect at about 2 wt% loading, but the use of an organoclay prepared by ion exchange with hexadecyltrimethylammonium (HDTMA) ions allows the incorporation of higher amounts of nanofiller without severe degradation of the mechanical properties [48]. In another case, the modification of the clay with organosilanes bearing reactive groups, for example, 3-methacryloxypropyltrimethoxysilane, creates a reactive interface useful for further copolymerization with diverse unsaturated monomers, for instance, acrylamide, leading to very stable polyacrylamide (PAAm) nanocomposite hydrogels [49].

Biopolymer–clay nanocomposites, called as *bionanocomposites*, are biohybrid materials resulting from the assembly between natural polymers (polysaccharides, proteins, nucleic acids, etc.) and layered or fibrous clays [50]. In the first case, biopolymers such as positively charged chitosan can be intercalated in one or various layers in smectites (e.g., MMT) [51] or assembled to the external surface of fibrous clays [52], resulting in functional clay-based bionanocomposites.

The aforementioned considerations give us an idea of the importance of the clay–organic interactions that will be discussed in detail in this chapter, highlighting the role and significance of the interfaces in organic–inorganic functional materials based on clay minerals.

## 1.2 Analytical and Measuring Tools in Clay–Organic Hybrid Interfaces

Analysis of hybrid clay–organic materials is in most cases complicated. Since those materials are usually prepared in order to perform a specific task, there are several stages that are required in order to fully elucidate the suitability of the material prepared. In general such analysis can be divided in different categories, and the required analytical tools should be able to answer three different questions:

1. *Composition*: What is the ratio between the organic compound(s) combined and the clay mineral(s) used?
2. *Structure*: What is the physicochemical structure of the hybrid material prepared?
3. *Activity*: Are the hybrid material prepared adapted to the task it is expected to be used for?

It is obvious that any list of methods will be far from being complete, as the ingenuity of material scientists will always force them to discover and imply new techniques to elucidate the influence of and changes caused while preparing hybrid materials. However, in this section we will try to describe at least part of the widely used analytical methods capable of answering the three questions stated previously.

### 1.2.1 Composition

While combining organic compounds with clay minerals, the first question to be answered is, “What is the ratio between the components?” In some cases the hybrid material is prepared by introducing low amounts of clay to an organic matrix: Toyota Research Lab [32, 53] developed a reinforced nylon-6 smectite material by adding MMT or saponite at 2–8% wt to the polymeric matrix. In such cases the clay–polymer ratio is determined *a priori* by the composition introduced to the mixture. Another similar application of *a priori* determined composition is the preparation of clay–polymer nanocomposites for the removal of suspended solids in water treatment, where polydiallyldimethylammonium chloride (poly-DADMAC) or chitosan is added to clay minerals at 0.04–4 g polymer



per gram clay, according to the colloidal charge of the effluents to be treated [54–56]. However in several other cases, the amount of organic material combined with the clay mineral must be determined after performing the initial “mixing”. Thus, the organic compound is prepared by the relevant technique in case, and the amount of organic compound bound to the minerals is evaluated by a specific analytical technique. Such techniques either measure the remaining “nonreacting” organic participant, and might be considered as “indirect” methods, or can measure directly the amount of organic and/or mineral content in the hybrid (“direct” methods).

### 1.2.1.1 Indirect Methods

In the indirect methods the measurement is performed on the remaining organic compound in the preparation material. In all those cases the evaluation is performed similarly, and the amount of organic compound adsorbed on the mineral is determined from the expression below [57], in a procedure known as *mass balance*:

$$[\text{amount adsorbed}] = \frac{[\text{added concentration}] - [\text{remaining concentration}]}{[\text{mass of sorbent}]}$$

For example, when preparing dye–clay organocomplexes for the adsorption of herbicides [58] or priority pollutants [59], the remaining amount of dye in the preparation solution was used to evaluate the adsorbed amount of dye. Since dyes can be measured with high sensitivity by ultraviolet–visible (UV–Vis) spectroscopy, this was the approach adopted by those studies. The same approach and analytical technique might be used for the preparation of dye-based hybrid materials used in controlled-release herbicide formulation [60]: prepared metolachlor herbicide formulations, and the amount of berberine in the hybrid initial based on berberine–MMT compound was determined in the same way. A similar approach might be taken, but using other analytical quantitative techniques: for example, carbamate adsorbed on a berberine–bentonite organoclay was quantified by measuring by high performance liquid chromatography (HPLC) carbamate concentration in the supernatant [61]. Similarly, to prepare sulfosulfuron formulations based on clay–octadecyltrimethylammonium (ODTMA) ion micelles, the quantification was, again, performed in the supernatant by mass balance – but in this case HPLC was used to measure the remaining non-bound pesticide, whereas fluorescence measurements were used to evaluate the amount of ODTMA that was not intercalated in the complex [62]. In a previous study by the same research group on the preparation of a sulfometuron formulation on ODTMA or HDTMA micelle–clay matrix, the amount of non-bound surfactants (ODTMA, HDTMA) was evaluated by drying the supernatant by evaporation and measuring the precipitate remains by C/N/H/S analysis [63].

Thus, “mass balance” is considered a very widely used approach. However, one of the problems of such techniques is that several other processes that reduce concentration in equilibrium solution might be wrongly ascribed as “adsorption,” yielding an overestimate of the amount of organic component in the hybrid material [64]. For example, Rytwo and coworkers [65] described

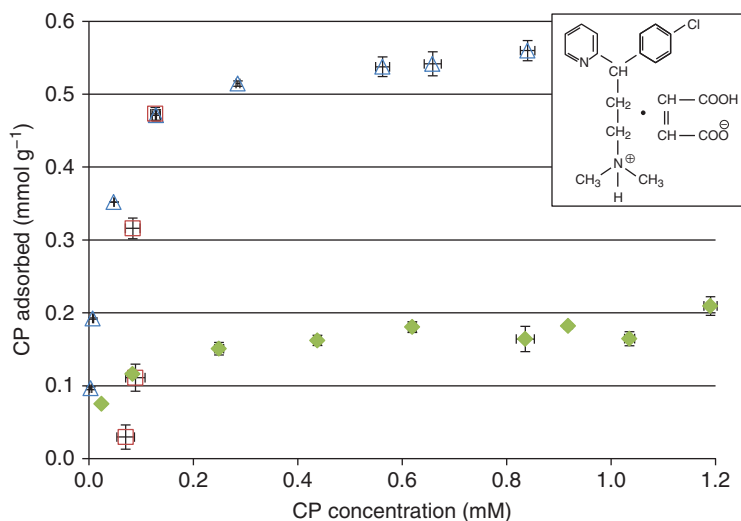


**Figure 1.3** Adsorption of the cationic pharmaceutical chlorpheniramine (CP) on SWy-2 clay (triangles), SWy-2 with inefficient separation between the colloids and the supernatant due to low centrifugal acceleration (squares), and CP adsorbed on a neutral organoclay based on SWy-2 modified with TPP (full rhombus).

apparent “adsorption” of crystal violet (CV) on Texas vermiculite that after a more detailed analysis happened to be degradation of the dye on the surface of the mineral. Overestimated adsorbed amounts may also stem from precipitation or evaporation of the adsorbate in case. For example, in early works with berberine clay, adsorption of the dye was assumed to reach 150–175% of the CEC [66], whereas later studies show that several commercial clays absorb berberine at amounts that are directly related to the CEC of each clay [67]. The discrepancy is ascribed presumably to the fact that the previous study was performed at concentrations 20-fold above the solubility of berberine [68], and at such conditions precipitation is prone to occur. Other effects might yield underestimate: for example, if separation between the clay–organic particles and supernatant is ineffective, due to low centrifugation velocities and small colloidal organoclay particles, analytical techniques might measure bound organic component as “free,” yielding calculated organic compound/clay ratios that are lower than the real values. Figure 1.3 (based on [69]) shows adsorption of the cationic pharmaceutical chlorpheniramine (CP) on SWy-2 clay (triangles), SWy-2 with inefficient separation between the colloids and the supernatant due to low centrifugal acceleration (squares), and CP adsorbed on a neutral organoclay based on SWy-2 modified with TPP (full rhombus), as described in [59]. It can be seen that raw clay adsorbs CP at amounts considerably larger than TPP–clay. This can be ascribed to the fact CP is a cationic compound with large affinity to the negatively charged raw clay. On the other hand, inefficient separation appears as higher remaining concentration in the supernatant, erroneously leading to underestimates of the amounts adsorbed.

Thus, even though indirect quantification is in most cases an accurate approach, care should be taken, and in some cases other complementary evaluations must be performed.

#### 1.2.1.2 Direct Methods

Erroneous quantifications might be minimized by measuring the adsorbate content not in the supernatant, but directly on the hybrid material prepared. This approach can be performed by several analytical techniques, depending on the adsorbed chemical and the type of mineral. The most widely used analytical approach is based on the fact that clay minerals have very low contents of C, N, and S, whereas those elements are main constituents of any organic compound. Evaluation of the organic compound/mineral ratio can be done by means of a CHNSO analyzer [30, 70, 71]. In cases where the sorbent contains some of those elements, more cumbersome evaluations can be performed to take that in consideration [60]. Another option, in cases where the adsorbed organic compounds contain relatively large amounts of heavier elements that do not appear in the lattice of the clay mineral (Fe, Ti, Cr, Zr, etc.), is to measure the total dry material by X-ray fluorescence (XRF) [72]. It should be mentioned that in several cases, large discrepancies between methods based on elemental analysis and other techniques were reported: Aznar *et al.* [70] had shown a 20% difference between CHNSO and mass balance by UV–Vis. Another problem with measurements based on elemental analysis and not on the specific structure of the bound organic compound is that element analysis will not detect degradation on the surface, if the products remain bound to the clay [65].

As for methods able to describe the hybrid materials at a molecular level and relate the measurements specifically to molecular structure of the compound adsorbed, Fourier transform infrared spectroscopy (FTIR) [73] and NMR [74] are the most notorious. NMR can be very useful for the elucidation of the specific interactions between organic molecules and the environment [75]. It can be used in semiquantitative and in specific cases even quantitative evaluations of the ratio between components in a hybrid material [76–78].

FTIR spectrum is used as a fingerprint technique for identification [79]. In clay mineralogy it helps to derive information concerning their structure, composition, and structural changes upon chemical modification [80], due to the fact that it is a rapid fast and cheap technique that yields unique information about mineral configuration [81], including quantitative mineral analysis [82, 83], water content and influence on the minerals [84, 85], interactions between adsorbed organic molecules and clay sorbates [60, 86], and even in-plane or out-of-plane organic orientation of molecules on the clay surface [16, 87]. In recent studies [64], the use of attenuated total reflectance (ATR)-FTIR was used to quantify the amount of several organic compounds adsorbed on clay minerals, compared with other techniques (gravimetric, UV–Vis, CHNSO), yielding similar results and even describing similar effects of saturation or desorption. Its main advantage is that it allows the measurement of dispersions, gels, liquids, and pastes very fast, with no extra preparation procedures [81].

As an example of the use of the last method, Figure 1.4 (based on [88]) shows amounts of olive oil adsorbed on clays and organoclays when added at several

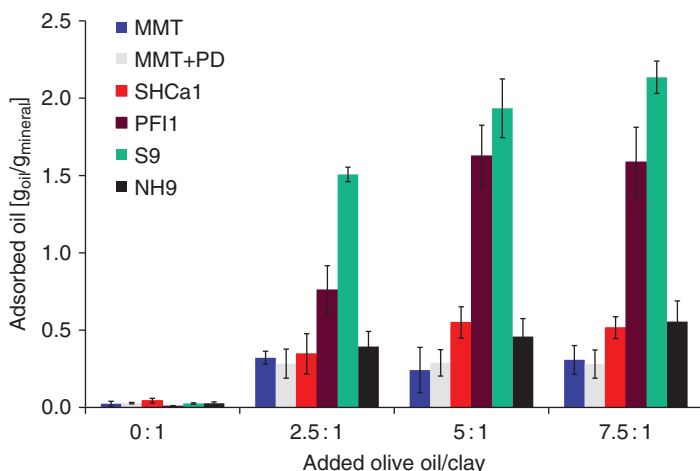


**Figure 1.4** Amount of olive oil adsorbed on clays and organoclays at several mass to mass ratios: montmorillonite (MMT), poly-DADMAC-modified MMT (MMT + PD), hectorite (SHCa1), palygorskite (PFI-1), sepiolite (S9), and chitosan–sepiolite nanocomposite (NH9).

mass to mass ratios. Measurements were performed after removing excess of oil by washing and centrifugation: the free oil “creams” up to the top of the test tube, and the sediment contains the clay with the bound oil. ATR-FTIR ratios between IR absorption bands of olive oil ascribed to absorption of the symmetrical and asymmetrical methylene ( $\text{CH}_2$ ) stretches ( $2865$  and  $2925\text{ cm}^{-1}$ , respectively) and the  $\text{C}=\text{O}$  group at  $1710\text{ cm}^{-1}$  to the clay peaks of the  $\text{Si}-\text{O}$  stretch ( $1020$ – $1100\text{ cm}^{-1}$ , depending on the mineral) and the sharp band at  $3570$ – $3630\text{ cm}^{-1}$  ascribed to  $\text{OH}$  stretching structurally coordinated with  $\text{Mg}$ ,  $\text{Al}$ , or  $\text{Si}$  atoms in the lattice of the mineral allow detailed quantification.

Averaging the information of all those ratios yields adsorbed amounts of oil (in gram oil per gram sorbent) shown in Figure 1.4, indicating that (a) smectites like MMT or hectorite (SHCa-1) adsorb olive oil at very low amounts; (b) fibrous clays as sepiolite (Pangel S9) or palygorskite (PFI-1) adsorb considerably larger amounts (5–8-fold) of oil, which increase with the added amount; and (c) montmorillonite poly-DADMAC (MMT-PD) yields similar results to the original clay (MMT), whereas chitosan–sepiolite (NH9) nanocomposites adsorbs more oil than MMT but considerably less than fibrous clays. All of these effects can be explained by the fact that fibrous clays (unlike MMT and most other clays) adsorb non-charged molecules in relatively large amounts on neutral silanol sites [89]. Adsorption to such sites has been proven by changing a doublet ascribed to the structural  $\text{O}-\text{H}$  at about  $780\text{ cm}^{-1}$  to a single band and shifts of an absorption band at  $3690\text{ cm}^{-1}$  bathochromically to lower energies [90, 91]. Indeed, the same effect was observed in this study, when olive oil adsorbs on sepiolite or palygorskite, whereas in the nanocomposites, it seems that chitosan “covers” the silanol sites. Thus, on the one hand, a more organophilic surface is formed by the covering of chitosan. On the other hand, silanol sites are no longer available for adsorption of the oil.

## 1.2.2 Structure

In this subsection we will describe shortly part of the methods used to determine the physicochemical structure of the hybrid material prepared. It should be emphasized that even though in some cases a single method is used [92], in most cases determination of the structure is done by combination of several techniques (e.g., [93–97]).

### 1.2.2.1 Visualization Methods

Methods based on direct or indirect visualization of the obtained hybrid are widely used: optical microscopy allows observing macroscopic arrangements and formation of large aggregates [98]. When used with oriented films and polarized light, anisotropic light properties (“birefringence”) might be observed [95] or the formation and size of polymer crystallites in the nanocomposite structure [99]. A direct visualization of labeled clays into polymer matrices can be obtained by fluorescence imaging through a confocal microscope, providing pictures with bright particles accounting the dispersion level of the platelets [100]. Atomic force microscopy (AFM) allows to elucidate surface morphology of hybrid materials in general [101] and clay–organic materials in particular: when used in the “tapping mode,” the cantilever oscillates vertically close to its resonance frequency and contacts the sample surface briefly in each cycle of oscillation. As the tip approaches the surface, characteristics of the cantilever oscillation are modified due to tip–sample interactions. Thus, the surface can be imaged as “height” at the nanometric scale along the path of the cantilever [95], yielding a visual three-dimensional (3D) picture of the general structure. For example, AFM allowed differentiating architecture of monolayers of several clay minerals interacting with rhodamine B octadecyl ester perchlorate: lath-like structure for hectorite, plates for Wyoming bentonite, a mixture of laths and plates for saponite, and aggregates of very small layers in Laponite® [92].

However it seems that from all visualization methods, electron microscopy is by far the most widely used. The electron microscope uses a beam of electrons to create an image of the sample. Visible light wavelength photons are in the range of 350–700 nm, whereas wavelength of an electron can be several orders of magnitude shorter than that. Thus, an electron microscope is capable of much higher magnifications and has a greater resolving power than a light microscope, allowing it to see much smaller objects in finer detail [102]. In *transmission electron microscopy* (TEM), the electron beam that has been partially transmitted through a very thin sample carries information about the structure of the specimen. In *scanning electron microscopy* (SEM), the electron beam is scanned across the surface of the sample in a raster pattern, with detectors building up an image by mapping the secondary electrons that are emitted from the surface due to excitation by the primary electron beam. TEM resolution is usually about an order of magnitude better than the SEM resolution; however because the SEM image does not rely on transmission, preparation is simpler and SEM is able to image bulk samples with a greater depth of view, yielding a good representation of the 3D structure [102]. Improvements in the technology allow the measurement of wet samples (in environmental scanning electron microscopy – known



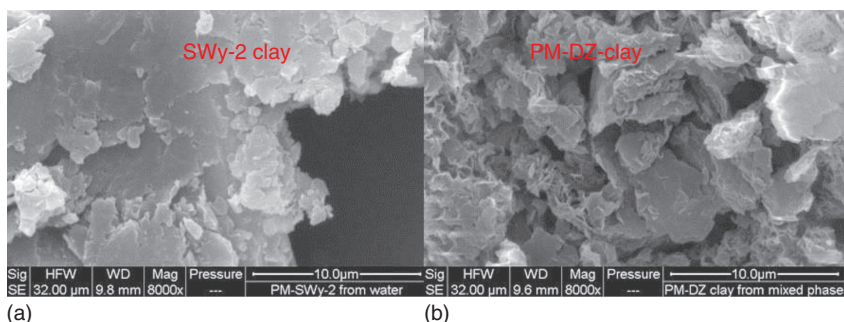


**Figure 1.5** SEM images of the pristine SWy-2 clay (a) and a formulation of the herbicide pendimethalin (PM) prepared on difenzoquat (DZ)/SWy-2 organoclay.

as ESEM) or increased resolution to magnifications that can reach  $50 \times 10^6$  times in high-resolution transmission electron microscopy (HRTEM).

For example, the use of the latter technology allowed to obtain detailed microstructural analysis of fluridone–organoclay nanocomposites [103]. In some cases combining different techniques delivers complementary information: in a study that addressed the role of natural clay–organic complexes in cementing sand [104], SEM of the air-dried samples exhibited high porosity even though TEM of the water suspensions showed a network texture. In several cases electron microscopy is simply used to demonstrate the changes in the microstructure imposed by the binding of an organic compound to a clay mineral (e.g., [67, 105–108]). For example, Figure 1.5 (based on [109]) shows SEM pictures of microstructure and microporosity scanning of different materials. Whereas the crude MMT (SWy-2) clay (Figure 1.5a) shows an almost plane surface, when a formulation of the herbicide pendimethalin (PM) is prepared on an organoclay based on difenzoquat (DZ) adsorbed on SWy-2 up to the CEC of the clay (PM/DZ/clay; Figure 1.5b), a flaky appearance with considerable larger external surface and large micropores is observed.

### 1.2.2.2 Structure Determination

An overlook on clay–organic hybrid publications will easily show that the most broadly used method to determine the structure of minerals in general and clays in particular is XRD, denoted also sometimes as “wide-angle X-ray diffraction (WAXD).” Since the classic publication by George Brindley describing the techniques and discussing applications and effects with other eminent clay scientists as Mac Ewan and Bradley [110], the general idea of the method remained even though the instruments improved and today “desktop” XRD are available at affordable cost, allowing the use of such instruments for all scientists. The principle is that a monochromatic and collimated beam of X-rays generated by a cathode ray is directed toward the sample. When conditions satisfy Bragg’s law ( $n\lambda = 2d \sin \theta$ ), there is an integer relationship between the wavelength of the beam ( $\lambda$ ), the lattice spacing ( $d$ ) in a crystalline sample, and sinus of the incident angle ( $\theta$ ), and constructive interference occurs. These diffracted X-rays are then detected, processed, and counted. By scanning the sample through a range

of incident  $2\theta$  angles, all possible diffraction directions of the lattice should be attained due to the random orientation of the powdered material [111]. Angles are then converted to spacing between lattice surfaces. Determination of such spacings allows evaluating the distribution of the organic compound on the clay when forming the hybrid material. Data on the raw clay minerals can be widely found in literature (e.g., [112]), and the modifications on those original spacings were reported in thousands of studies and summarized in dozens of review papers [29, 35, 113–115]. The rationale is that the nanocomposite structure (“intercalated” or “exfoliated”) may be identified: in an “exfoliated” nanocomposite, the extensive layer separation associated with the delamination of the original silicate layers in the polymer matrix results in the eventual disappearance of any coherent XRD from the distributed silicate layers. In “intercalated” hybrid nanocomposites, the finite layer expansion associated with the polymer intercalation results in the appearance of a new basal reflection corresponding to the larger gallery height [35].

Thermal analysis methods are also applied to determine stability and other important properties related to the structure of the hybrid materials. The term *thermal analysis* covers a range of techniques used to determine physical or chemical properties of a substance as it is heated, cooled, or held at constant temperature. Using this technique it was possible to determine, for example, the marginal thermal stability of the quaternary ammonium organoclays [116] compared with that of phosphonium [117] or dye-based [118] organoclays.

Differential thermal analysis (DTA) method for studying materials is based on the suggestions made by Le Chatelier in 1887. The method consists of heating a small amount of the substance at a constant rate as close to fusion as is possible experimentally and recording the endothermic and exothermic effects that take place in the material [119]. The technique uses a known substance, usually inert over the temperature range of interest and with thermal properties similar to that of the sample as reference material [120].

In thermogravimetric analysis or thermal gravimetric analysis (TGA), changes in the mass of the sample are measured with an accurate balance as a function of increasing temperature. The method can deliver details on phase transitions (vaporization, sublimation), adsorption processes (desorption, chemisorptions), desolvation (especially dehydration), decomposition, and solid–gas reactions (e.g., oxidation or reduction) [121]. This method can also be performed while comparing to a reference material (differential thermogravimetric analysis (DTG)) with known properties.

The third widely used thermal method is differential scanning calorimetry (DSC) in which the energy needed to establish a nearly zero temperature difference between the sample and an inert reference material both subjected to the same identical temperature regimes in an environment heated or cooled at a controlled rate is monitored [122]. Monitoring can be performed by power compensation where temperatures of the sample and reference equaled by varying the power input to the two furnaces, and the energy required to do this is a measure of the enthalpy or heat capacity changes in the sample relative to the reference. Another method is based on measuring the heat flux between the sample and reference that are connected by a metal disk and heated in a

single furnace. Enthalpy or heat capacity changes between the sample and the reference cause differences in temperature that are monitored and related to enthalpy change in the sample using calibration experiments.

An interesting setup known as *thermo-XRD analysis*, combines the two methods mentioned in this subsection. It is based on performing a series of XRD measurements at different temperatures and monitor changes in the spacings of the material [66]. Such combination allowed, for example, to determine changes in the structure of tactoids of quaternary ammonium organoclays with temperature [123].

There are of course several other methods that can deliver very important information on the structure. As mentioned in the previous section, NMR can be used to analyze the ratio between the organic compound and the mineral, but some researchers also consider it as the most powerful tool for the determination of complex structures and interactions, with the additional advantage that can be performed on components with various physical phases (solids, gels, liquids, and gases) [75]. Other common quantification techniques can yield important structural information: metachromasy of organic dyes adsorbed on clays as measured by UV–Vis spectroscopy is in several cases ascribed to the configuration of the dye molecules as those interact between themselves in the interlayers of the minerals: whereas a bathochromic shift (absorption peak shifted to lower energies) is ascribed to “head-to-tail” aggregation (J-aggregates), hypsochromic shift (absorption peak shifted to higher energies) is generally related to “sandwich”  $\pi$ – $\pi$  aggregation (H-aggregates) [124–128]. However, there are studies that show metachromasy when the dye–clay ratio is very low, and dye aggregates on the surface does not appear to occur [109, 129]. In such cases  $\pi$  interactions between the oxygen plane of the silicate layer of the clay mineral and the aromatic parts of the dye or local influences of surface acidity might be a more logical explanation for the metachromasy effect [130–132]. IR spectroscopy can demonstrate direct interaction between the organic adsorbate and the clay sorbate [60, 73, 86, 133], and in several studies it has even been used as a proof of modification or degradation of the organic compound attached to the clay [65]. Combination with polarizers allowed to deduce the in-plane or out-of-plane orientation of the organic molecule [16, 134–136], whereas mathematical deconvolutions of the amide absorption peaks in proteins [137, 138] allow to evaluate the specific structure of proteins adsorbed on clays [107, 139–141].

### 1.2.3 Activity

The last question to be answered is – “Are the hybrid material prepared adapted to the task it is expected to be used for?” The answer to the question depends on the expected role of the material. If the hybrid prepared is expected to act as a fire retardant, for example, relevant experiments on such property are prepared, and thermal analysis techniques and calorimetry methods are applied [142–144]. When influence on the electric conductivity is expected, the property is specifically measured at different compositions or clay–organic contents [145, 146]. Influence on optical properties as the preparation of nonlinear optical hybrids [147], photochromism (isomers exhibiting different absorption spectra) [148],

optical anisotropy (different absorption spectra depending on the direction and/or polarization of the light) [149], Förster or fluorescence resonance energy transfer (FRET) effects (where energy passes from a donor to an acceptor in a non-radiative form) [150], or similar effects are evaluated by light absorption, emission, or dispersion using suitable spectrophotometers, fluorimeters, or photometers. Influence on physiological properties such as adsorption of oil or cholesterol can be measured by *in vitro* or *in vivo* experiments on mice [88]. Measurements of the influence on the charge particles can be made by several ways [151], even though care has to be taken in differentiating the “intensity” factor known as *zeta potential* from the “capacity factor,” that is, the actual charge to be neutralized, usually measured by other methods such as titration with a “streaming current detector” [152]. Similarly, other properties of the method to be used strongly depend on the conditions of the preparation, and the decision on the exact application to be made has to consider that, since in such cases large discrepancies between the different methods might occur. Readers should not expect that we will present conclusive remarks, but we will discuss the polemic of the different methods for (i) particle size and (ii) surface area.

#### 1.2.3.1 Particle Size of the Hybrids

Several publications have focused on the differences between particle-size-determination techniques (e.g., [153, 154]), and it is clear that each of them has its advantages and limitations. Even instrument manufacturers denote that the only techniques that can fully describe particle size are microscopy or automated image analysis [155].

When particles range from hundreds of nanometers up to several millimeters in size, as it is the case in most clay–organic hybrids, laser diffraction is a widely used method (e.g., [156, 157]). It measures the light scattered as a laser beam passes through a dispersed particulate sample. Large particles scatter light at small angles relative to the laser beam and small particles scatter light at large angles. By performing analysis of the angular scattering intensity data, the size of the particles responsible for creating the scattering pattern can be calculated using the Mie theory of light scattering. Mie theory requires knowledge of the optical properties (refractive index and imaginary component) of the sample being measured, along with the refractive index of the dispersant [158]. Even though large databases on those parameters can be found, it is not obvious that a new hybrid material will fit parameters found in previous studies. Although Fraunhofer’s approximation does not require exact knowledge on refractive indexes for particles smaller than tens of microns, transparent materials are prone to artifacts.

It should be emphasized that all particle-size-determination techniques make a broad set of assumptions. A comparative study [159] between a laser blocking instrument, a “time-of-flight” instrument, and three different laser diffraction instruments based on Fraunhofer’s approximation showed that the results obtained by the various methods are generally not in good agreement and that the first two methods produce results that are consistent with one another and with microscopy, while on the other hand the Fraunhofer diffraction instruments yield particle size distributions that may vary significantly from each other and

from that observed via image analysis. This study suggests that the investigator must carefully select the appropriate particle size equipment for a given application and verify using another independent method to ensure against the presence of instrumental artifacts. They also emphasize that as all methods were highly reproducible, reproducibility of a given method is not a sufficient criterion. They conclude that it does not appear to be possible to make particle size measurements that are completely independent of the apparatus. Another study performed 2 years later comparing microscopy with laser diffraction using the more accurate Mie theory [153] led to similar conclusions: the laser diffraction instruments gave results that were both dissimilar to the microscopy measurements and to each other. The optical model employed affected the calculated particle size distribution but in a non-predictable manner, and the Mie optical model did not assure more accurate results. Similar conclusions are given in another study that compared sedimentation techniques based on “Stokes’ law” with laser diffraction measurements in 42 California soils [160]: they conclude that the relationship between the sedimentation data and the laser diffraction data for the different size fractions was less than satisfactory.

Even though there are other technological principles for particle size determination, we almost could not find such instruments in use in the research of clay–organic hybrids. In a study on the preparation of organoclay-based herbicide formulation, the differences in the particle sizes for dried or wet berberine–MMT were reported based on an “EyeTech” laser obscuration time instrument [60]. The method is based on the interaction of a rotating laser spot with a particle, which creates the “obscuration time” pulse. Analysis of the pulse duration yields the size of the particle. The obscuration time combined with the known rotation velocity of the laser beam makes it possible to calculate the particle diameter. The obtained images of shadows of the particles give a clear description of the shape of the particles, enabling evaluation of the aspect ratio (ratio of the length and width), distance between surface and boundaries, and other important geometric parameters. Authors concluded that non-dried hybrid particles have larger sizes, with a mean size of almost 62  $\mu\text{m}$ , compared with less than 30  $\mu\text{m}$  for the dried particles. Thus, the non-dried organoclay forms more aerated flocs allowing in that case to more herbicide to adsorb to the compound.

Another instrument for the determination of the particle size distribution in the range between hundreds of nanometers to hundreds of microns was developed by LUM GmbH. It combines two different approaches and is based on measuring light transmission at three different wavelengths, all along the test tube while sedimentation by gravity occurs (“LUMiReader”). The differences in the transmission of the three different wavelengths allow avoiding the need of applying Mie theory and consequently refractive indexes for the determination of volume weighted particle size distribution [161]. A similar instrument (LUMiSizer) introduces centrifugal acceleration instead of gravity, allowing monitoring of smaller particles. One of the advantages of the instrument is that it can measure very concentrated suspensions, whereas the need for significant dilutions is one of the handicaps of laser diffraction instruments that might influence directly on the particle size, for example, in micelles, where dilution



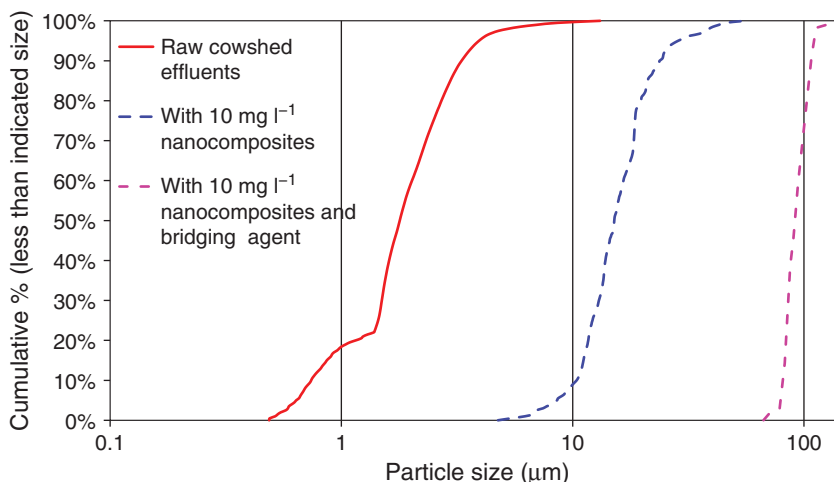


**Figure 1.6** Particle size distribution of untreated and treated cowshed effluents.

can reduce concentration below critical micelle value. Figure 1.6 exhibits particle size distribution of untreated and treated cowshed effluents, which contain more than  $10000 \text{ mg l}^{-1}$  (1%) suspended particles (based on [98]) measured by such instrument. Considering the high amount of suspended solids, it would be impossible to perform non-diluted measurements of such effluents with laser diffraction. Raw effluents consist of very small, negatively charged colloidal particles, almost all of them  $<2 \mu\text{m}$ , which remain in a stable suspension, making water treatment almost impossible. Addition of suitable clay–cationic polymer nanocomposites changes completely the distribution. Cationic charges of the nanocomposite neutralize and bind the negative colloids, forming flocs of  $10\text{--}30 \mu\text{m}$  that sediment in minutes. Adding to that also a bridging polymer that meshes the flocs together leads to formation of very large aggregates that can reach more than  $100 \mu\text{m}$  and might be easily filtered.

### 1.2.3.2 Specific Area of the Hybrids

The SSA is a very important and commonly used property to describe a powder or porous solid [162]. As in particle sizing, discrepancies between methods are also very common. The most widely used techniques is nitrogen adsorption at 77 K analyzed based on the Brunauer–Emmett–Teller (BET) theory and a standard cross-sectional area of a single molecule ( $0.162 \text{ nm}^2$ ) to extract the desired surface area [163]. The main disadvantage of this technique is the need to use dry samples. For example, surface area of standard sodium MMT clay (SWy-1), when measured with this technique, yield tens of square meters per gram, whereas the theoretical values presented in the literature are several hundreds of square meters per gram. These large values are generally confirmed by adsorption experiments in solutions [164]. Such discrepancies lead to the conclusion that surface area of swelling smectites such as MMT cannot be measured by gas adsorption on powdered aggregates, because the drying processes forms tight tactoids, with areas inaccessible to the nitrogen gas [165].

Although performed on clays and not on hybrid materials, an interesting study [166] compared the SSA as measured by AFM measurements of several particles,  $N_2$  adsorption, and the relatively simple method based on adsorption of ethyl glycol methyl ether (EGME) [167]. When compared with AFM,  $N_2$  adsorption yielded underestimates (50% for illite and only 17% for MMT), whereas EGME adsorption yielded a 35% overestimate for both minerals. Similar large discrepancies were observed when comparing  $N_2$  to methylene blue adsorption [168]. However, in this latter study it can be seen that when measuring non-expandable clays such as kaolinites, similar values were obtained by both methods. Thus, discrepancies strongly depend on the general structure of the minerals: for the fibrous clays sepiolite and palygorskite,  $N_2$ , methylene blue, and EGME adsorption yielded less than 10% difference. Studies performed on hybrids based on zeolite indicate also that in non-swelling minerals,  $N_2$  SSA measurement yield similar hundreds of square meters per gram values, before and after modification [169, 170].

An interesting new method to evaluate surface area in suspensions is based on NMR relaxation time. The principles of the method for general colloids in general [171] or clays in particular [172] had been published several years ago; however, inexpensive low-resolution NMR instruments developed in the last few years enable its application [173]. The rationale is that adsorbed water molecules have shorter relaxation decay time than those in bulk fluid. Considering that the fraction of adsorbed water is directly correlated to the area of the particles coming into contact with the liquid (the wetted area), evaluation of relaxation times can yield a direct evaluation of the wetted area. Obviously, calibration is needed for the specific material and the liquid in case, and after making several assumptions, measured relaxation time can be used to find the surface area of an unknown sample of the same material used for the calibration [174]. Thus, in the preparation of new hybrid materials, the need for a known calibration sample is a limiting factor. However, it can also be an advantage because changes in the surface properties that influence the *wetting* area (e.g., increase in hydrophobicity) will yield changes in relaxation times for the same solid-to-solvent ratios that might be ascribed to a direct modification of the surface [152]. To summarize, for SSA, as in the case of particle size measurements, it is strongly recommended to adapt the method used to the need of each specific research and to apply a criticist observation when reaching conclusions from the results measured.

### 1.3 Nanoarchitectures from Organic–Clay Interfaces

Among other uses, organic–clay interfaces have been employed for developing diverse type of porous nanoarchitectures based on clays of exceptional relevance in adsorption and catalytic applications. Essentially, “nanoarchitectures” or “nanoarchitectonics” [175] are nanostructured materials that result from the assembly of structural units organized at the nanometer scale in which the resulting “nano-organization” procures specific functionality. Typical clay-based nanoarchitectures come from the organization of clay platelets in view of procuring materials of regular and predetermined porosity, being the most classical

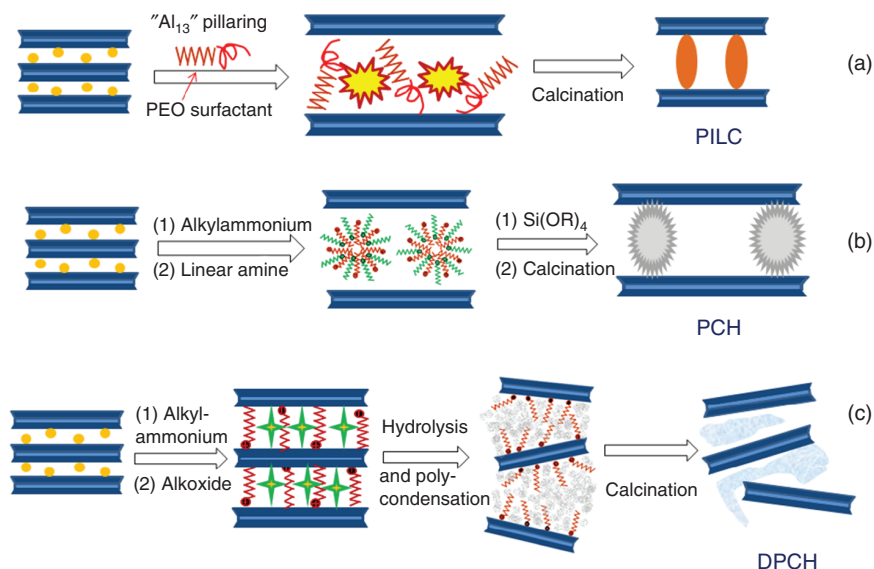


**Figure 1.7** Schematic representation of the use of organoclay interfaces in the formation of diverse clay-based nanoarchitectures: (a) use of PEO-based surfactants to produce PILC, (b) use of organoclays incorporating amines to prepare PCHs, and (c) use of organoclays as interfaces for controlling hydrolysis–polycondensation of silicon and metal alkoxides in the formation of delaminated clay heterostructured materials.

example the so-called pillared clays (PILC) group [176–178]. Classical methods used in the preparation of PILC did not involve the use of organoclays but just the direct intercalation of the metal oxide precursors in the interlayer space of layered clays, and their further thermal transformation to consolidate metal oxide NP that maintained separated the silicate layers, giving rise to a gallery of interconnected tunnels at the nanometer scale. However, the necessity to control this porosity and to direct the formation of diverse type of pillars, as well as the possibility of introducing specific functionalities, drove to a research in which the incorporation of specific organic species, either in the reactive medium or the previous organic modification of the clay, gave rise to various original routes for obtaining new type of clay-based nanostructured clay materials [29, 177–180]. In this section of the chapter, it will be shortly revised the most relevant achievements related to the use of organic–clay interfaces in the formation of the most relevant types of clay-based nanoarchitectures (Figure 1.7), introducing information on the synthetic methodologies, main characteristics of the resulting materials, and some examples and perspectives related to their applications. Moreover, it will be also shown how organic–inorganic interfaces in fibrous clays, such as sepiolite and palygorskite, can be profited to produce the assembly of NP of diverse nature on the surface of the silicate fibers [179–181], which may be of interest in the application to other types of nanoparticulated inorganic solids provided as well of abundant external –OH groups.

### 1.3.1 Organic–Inorganic Interfaces in PILC and Other Related Clay Nanoarchitectures

Typical method for PILC preparation consists in the incorporation of metallic polyoxocations (e.g., the so-called “Al<sub>13</sub>” Keggin cage ([Al<sub>13</sub>–O<sub>4</sub>(OH)<sub>24</sub>(H<sub>2</sub>O)<sub>12</sub>]<sup>7+</sup>) by ion-exchange reactions. As these polyoxocations are bigger and with larger charge than common interlayer cations of clays (e.g., Na<sup>+</sup> or Ca<sup>2+</sup>), once intercalated, they produce a larger separation between the silicate layers and are also placed much more far away one to other. After a convenient thermal treatment, the polyoxocations are transformed in metal oxide NP that become attached to the silicate layers acting as pillars that produce the permanent separation between them. In general, this methodology does not allow a good control of the type of galleries that can be produced as this is slightly controlled on one side by the nature of the precursor for a given type of final metal oxide NP, which usually grow till a specific maximum size in the interlayer region, and from the other side by the silicate charge, which determines the separation between pillars. In this way, the final porous size in the resulting PILC varies always in the micropore range. To go further, Michot and Pinnavaia [182] applied a different strategy that implies the use of nonionic surfactants (e.g., PEO-based surfactants such as commercial Tergitol 15s-5) in the pillaring solution. In this case the presence of the surfactant enhanced the stability of the Al<sub>13</sub> polyoxocations in the interlayer region, giving rise to PILC with a more uniform micropore distribution in the final structure, which is relevant in view of producing more shape-selective catalysts and adsorption materials (Figure 1.7a). The explanation of this behavior has been addressed to a surfactant effect that facilitates the clay platelet flocculation, reducing also the amount of water needed in the process, which results very convenient in view of scaling up the synthesis process. In fact, when applying this methodology, the presence of alkyl polyether surfactants in different concentration affects the way it is associated with the polyoxocations, affecting the textural properties of the resulting PILC [183]. Thus, for instance, at low surfactant loadings, it bonds the polyoxocations in the interlayer region as they both intercalate simultaneously, but for surfactant loading of around 0.67 molecule per unit, the cell part of the surfactant species binds also the interlayer gallery surfaces; this also acts as a pillaring agent, provoking the increase in basal spacing from 1.9 to 2.3 nm, while for higher surfactant contents, part of it is adsorbed on the external surface of the clay [183]. The direct use of PEO of different molecular weights allowed to produce PILC of different specific surfaces after calcination that may reach clay nanoarchitectures with SSA even higher than 400 m<sup>2</sup> g<sup>-1</sup> [184]. Hence, other PILC systems using PEO related species, such as poly(ethylene glycol) (PEG) and tetraethyl orthosilicate (TEOS), have been produced by using ultrasonication treatments of the pre-intercalated clay with either hydrolyzed TEOS or PEG or with mixtures of both components, observing the formation of hybrid nanoarchitectures that show basal space distances of 3–4 nm [185]. Interestingly, not only the nanoarchitectures resulting after the thermal calcinations but also those with the presence of the organic species show interesting properties for their application in the removal of

organic pollutants such as dyes, volatile organic compounds (VOCs), and certain petroleum products.

Alternatively, surfactant species have been used with the aim to produce organic–inorganic interfaces that can be used for the convenient reorganization of intercalated polyoxometalates and other intercalated pre-pillar species and the tuning of final textural properties in the resulting materials. In this way, silica–iron oxide PILC heterostructures based on MMT with SSA as higher as  $750 \text{ m}^2 \text{ g}^{-1}$  and pore sizes of 2 nm have been reported using alkylammonium species (e.g., octadecylammonium chloride, trimethylstearyl ammonium chloride) for the treatment of freshly intercalated clay with mixed polycations containing silica and  $\text{Fe}^{3+}$  species prepared from prehydrolyzed TEOS sol and  $\text{Fe}^{3+}$  aqueous solutions [186]. Alternatively, clays previously modified with a surfactant (e.g., HDTMA bromide also known as *cetyltrimethylammonium bromide* (CTAB)) have been later treated with  $\text{H}_3\text{PW}_{12}\text{O}_{40} \cdot 6\text{H}_2\text{O}$  and TEOS to produce under hydrothermal conditions the formation of mixed PILC systems with interlayer basal spacing increases between 3 and 4 nm, materials that present interest for application as catalysts in oxidation of diesel oil [187]. Vermiculite modified with long-chain alkylammonium ions have been treated with tetramethyl orthosilicate (TMOS) solved in supercritical  $\text{CO}_2$ , the alkoxide being hydrolyzed by water molecules still remaining at the organic–inorganic interface. This methodology gives rise to the formation of regular silica pillars with a layer separation of about 3.5 nm and SSA of around  $350 \text{ m}^2 \text{ g}^{-1}$  [188]. Regular formation of mixed silica–titanium oxide pillars are achieved using adequate sol precursors incorporating a surfactant, for instance, CTAB, TEOS, and titanium tetrabutoxide mixed with suspensions of the  $\text{Na}^+$ -exchanged clay [189]. As the alkylammonium ions intercalate into the clay by ion exchange, the organic precursors become also intercalated, and when ammonia is added, the hydrolysis–polycondensation of the alkoxides in the interlayer region of the clay produces the formation of pillars of around 3 nm [189]. A similar approach has been employed to produce regular titanium oxide pillars of different height, from 2 to 3.5 nm, using alkylammonium-based surfactants of different long-chain alkyl size (e.g., dodecyldimethylbenzylammonium chloride, tetradecyldimethylbenzylammonium chloride, HDTMA chloride, and octadecyldimethylbenzyl ammonium chloride) and titanium tetrabutoxide ammonium chloride solved in ethanol and slowly added to suspension of the clay also in this alcohol [190]. The use of organoclays and titanium alkoxide sols in supercritical  $\text{CO}_2$  gives rise to mesoporous  $\text{TiO}_2$ –MMT nanoarchitectures as anatase NP of 5–20 nm diameter are *in situ* formed and keep the clay layers separated [191].

Organoclay derivatives have been also used to favor the assembly of different types of NP in the interlayer region of the clay, giving rise to diverse types of PILC-related materials of interest in diverse applications. In this way, MMT treated with a poly(oxypropylene)amine salt [192] or with cetylpyridinium chloride [193] has been used to favor the assembly of preformed magnetite NP. The way the organic–inorganic interface is prepared strongly affects the characteristics of the final materials. Thus, for instance, magnetite NP mixed in water with  $\text{Na}^+$ -exchanged MMT and further intercalated with cetylpyridinium ions results in materials containing more galleries and showing higher magnetism than those



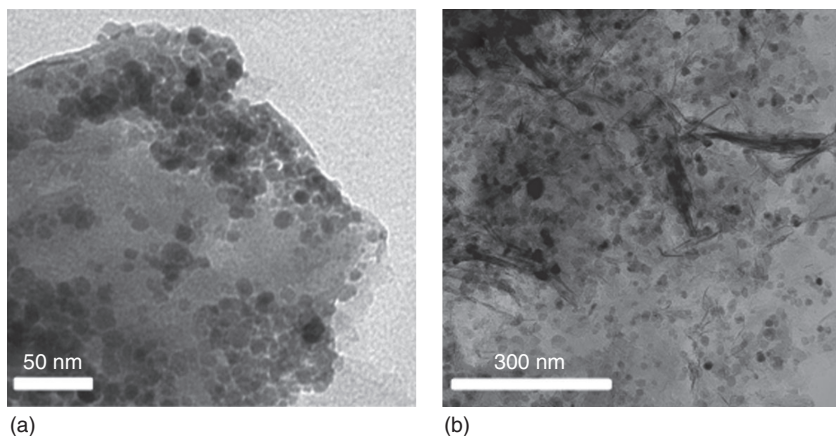


**Figure 1.8** TEM images of  $\text{Fe}_3\text{O}_4$ -smectite (a) and of ZnO-smectite (b) heterostructures prepared by assembly of  $\text{Fe}_3\text{O}_4$ -oleic acid NP and ZnO NP to an organo-smectite. (González *et al.* 2011 [196] and Akkari *et al.* 2016 [197]. Reproduced with permission of John Wiley and Sons and Elsevier.)

prepared by assembling  $\text{Fe}_3\text{O}_4$  NP to a cetylpyridinium-exchanged MMT dispersed in a mixture of ethanol in water 90% [193]. Surface modification of alumina pillared MMT with magnetic iron oxide NP has been also attained using as precursor a colloidal solution of magnetite in poly(vinyl alcohol) [194]. Alternative methodologies to produce heterostructured clay materials provided with magnetic properties can use magnetite NP modified with oleic acid. In this case, the organically modified NP shows an adequate interface to be incorporated in an organic solvent forming ferrofluids that can interact with both Na-exchanged and organically modified smectites, giving rise to magnetite–clay materials in which it is possible to control the amount of assembled NP [195]. This methodology allows the preparation, for instance, of novel superparamagnetic clay compounds (Figure 1.8a) that preserve their adsorption properties and can be easily removed from the aqueous medium with the help of a magnet once the pollutant has been adsorbed in the clay [196]. Besides magnetite, other types of metal oxide NP, for instance, ZnO, have been assembled to clays and organoclays to procure heterostructured materials of interest in photocatalysis. This can be reached either by formation of the NP in the presence of the organoclay [198, 199] or by using already preformed ZnO NP [197]. In all these cases, the use of organoclays favors the assembly of the ZnO NP, but XRD patterns do not show the presence of the particles in the interlayer region. Actually, ZnO NP remains mainly associated with the clay at its external surface (Figure 1.8b), which is very useful in view of developing active photocatalysts [197].

PILC have been also modified in post-synthesis treatments with the aim to introduce specific organic–inorganic interfaces in view of their further application in desired applications. In this way, for instance, Al-PILC has been impregnated with p-toluenesulfonic acid in view of incorporating specific functionalities for application as acid catalysts in bisphenol A preparation or in methyl *tert*-butyl ether (MTBE) synthesis [200]. Another modification to

procure organic–inorganic interfaces implies the grafting of organosilanes (e.g., trimethylchlorosilane or octadecyltrichlorosilane) to the previously formed Al–PILC to produce adsorbents for removal of VOC [201].

### 1.3.2 Organic–Inorganic Interfaces and Porous Clay Heterostructures (PCH)

Organoclays based on long-chain alkylammonium ions, typically smectites exchanged with CTAB, are used as organic–inorganic interfaces in which alkylamines are incorporated to produce interlaminar micelles that template the growth of the silica NP from alkoxy silanes (e.g., TEOS), giving rise to mesoporous materials after removal of the organic matter (Figure 1.7b). These materials known as *porous clay heterostructures* (PCH) were firstly described by Pinnavaia's group [202], and their synthesis is based on sol–gel methodologies combined with structure-directing agents; this is the approach usually employed in the preparation of periodically ordered mesoporous solids of the mobile composition of matter material (MCM) and Santa Barbara Amorphous type material (SBA), but here applied in the interlayer region of clays. Actually, that picture is not completely real, but the resulting PCH show the formation of silica NP that maintain the silicate layers about 3 nm in very well-ordered patterns separated, and their surface areas reach about  $700 \text{ m}^2 \text{ g}^{-1}$  after calcination in the case of nanoarchitectures based on smectites [203]. The porosity together with the acid character of the incorporated silica NP can be of interest in acid catalysis, for instance, in the selective dehydration of 2-methylbut-3-yn-2-ol to 2-methylbut-3-yn-1-ene [203]. The general synthetic method of PCH implies first the preparation of an organoclay by intercalation of alkylammonium species in a layered clay and its further treatment with a cosurfactant, typically a neutral alkylamine, whose interaction allows the organization of specific regions in the interlayer region of the clay to procure the formation of the silica pillars once the alkoxy silane is hydrolyzed in that environment. As already pointed out in their first publication [202], the porosity and interlayer distances in the resulting PCH are strongly influenced by the nature of the two surfactants employed in the synthesis, observing that hexadecylammonium and decylamine gave rise to materials with the highest porosity. In fact, most of the further materials developed following this synthetic approach have used those surfactants to produce the organic–inorganic interfaces. In this way, the methodology has become very popular and has been largely applied to develop porous materials from diverse smectites, such as MMT [204–206], hectorites [207], and saponites of natural origin [189, 208] or synthetic ones [209, 210], as well as other layered silicates, such as magadiite and kenyaite [211], and highly charged synthetic mica-type aluminosilicates [212] in view of producing diverse porous materials of interest mainly in catalysis.

In general, PCH are based on TEOS as the use of other metal alkoxides has proved to be less efficient to stabilize stable and organized pillared structured materials. Thus, common procedures to prepare Al-based PCH materials implies the preparation of silica-based PCH that are further treated to incorporate Al, which remain grafted to the silica via Al–O–Si bonds. In this way, post-synthesis treatment of PCH with aluminum acetylacetonate [204],  $\text{AlCl}_3$ , and  $\text{NaAlNO}_2$

[213] produces Al-doped PCH materials provided with Brönsted acid sites whose stability and specific characteristics depend on the nature and amount of the employed reagent [178]. Although post-synthesis treatment reduces the SSA of the resulting PCH, the presence of Al species may improve their catalytic activity as proven when comparing Al-PCH and PCH saponite-based catalysts in the cumene cracking reaction [213]. Zhou *et al.* show the possibility to reach the formation of mixed Al-Si-PCH using octadecylammonium MMT and dodecylamine as cosurfactant interface for the co-hydrolysis and condensation of mixtures of TEOS and aluminum isopropoxide [214]. The resulting PCH shows quite different textural properties than silica-based PCH with lower basal spacing increase and open slit-shaped pores instead of tubular pores, but the presence of Al procures Lewis acid characteristics that can be profited in catalysis, for instance, alkylation of catechol with *tert*-butyl alcohol to produce 4-*tert*-butylcatechol [214]. Incorporation of Zr into silica-based PCH has been also achieved by using mixtures of TEOS and zirconium(IV) propoxide of variable composition to react with an MMT exchanged with CTAB and treated with hexadecylamine, giving rise to heterostructures with basal spacing increase of around 4.5 nm provided with high SSA; micro-, meso-, and macroporosity; and acid properties [215]. Mixed Zr-Si-PCH have been also prepared in octadecylammonium MMT interfaces using decylamine as cosurfactant in the co-hydrolysis and condensation of TEOS and zirconium(IV) ethoxide or  $\text{ZrOCl}_2 \cdot 8\text{H}_2\text{O}$  salt [216]. Here again, textural properties deteriorate in comparison with the silica PCH, but several of the resulting heterostructures containing Zr show better properties in the separation of hydrocarbon mixtures. Similarly, the formation of the silica pillars in an HDTMA-exchanged MMT using TEOS in the presence of  $\text{Co}^{2+}$  ions (e.g.,  $\text{CoCl}_2 \cdot 6\text{H}_2\text{O}$  salt) and *n*-dodecylamine as cosurfactant has been proved effective in the development of  $\text{CoO-SiO}_2$ -MMT PCH that is active as catalyst in  $\text{NO}_x$  conversion [217]. Magnetite NP have been formed in the presence of PCH using water solutions of ferric and ferrous chloride salts and aqueous ammonium as precipitating agent [218]. The resulting PCH shows enhanced magnetic and dielectric properties in the high frequency range, for which it has been postulated as an interesting material for electronic devices in radio-frequency identification labels [218].

The presence of silica pillars in PCH materials is particularly attractive in view of developing new organic–inorganic interfaces by their further functionalization via grafting reactions with organosilanes. Thus, for instance, aminopropyltrimethoxysilane (APTMS) has been used to incorporate amine groups in the silica pillars, which can be further used to immobilize reactive coordination metal complexes [219]. Thus, for instance, chiral Mn(III) salen complexes that contains a carboxylic group are able to react with the grafted amino functionalities, producing enantioselective heterogeneous catalysts that are active and highly selective in the epoxidation reaction of styrene and  $\alpha$ -methylstyrene [219]. PCH can be also modified with phenyltriethoxysilane, mercaptopropyltrimethoxysilane, or ethoxytrimethylsilane to further immobilize diverse chiral manganese catalysts using the presence of vinyl groups in the complex to react with phenol and mercapto groups present in the functionalized PCH [220]. Depending on the experimental conditions, it is possible to tune this modification at the

external and/or internal surfaces of the PCH, which affect reactivity of the resulting nanoarchitectures as catalyst in the asymmetric epoxidation of olefins [220]. The presence of amino groups in PCH has been also used to immobilize vanadium(IV) and copper(II) acetylacetonates by refluxing these complexes with the functionalized PCH in chloroform [221]. FTIR proves the stabilization of the metal acetylacetonates through Schiff condensation of the carbonyl group in the ligand and the amino groups in the PCH, resulting in C=N bond formation. The resulting PCH containing V and Cu complexes act as heterogeneous catalysts in epoxidation reactions (e.g., geraniol) and in the aziridination of styrene, respectively [221]. Alternatively, it is possible to use organosilanes together with simple alkoxysilanes to produce directly silica pillars provided with organic functionalities. In this way, mixtures of TEOS and 1,4-bis(triethoxysilyl)benzene have been co-hydrolyzed in the interface of a smectite exchanged with HDTMA ions in the presence of octylamine or decylamine as cosurfactant [222]. The resulting functionalized PCH show different textural properties depending on the time used in the polymerization reaction; as the reaction time increases, it is incorporated with higher number of functionalities and decreases the SSA in the resulting materials. In all the cases the presence of the aromatic functionalities introduces hydrophobicity that seems useful for applications in the removal of VOCs [222]. The same methodology has been used to produce in a one-step process functionalized PCH from mixtures of TEOS and phenyltriethoxysilane using alcohol and HCl in a solvent extraction process to remove the template species [223, 224].

### 1.3.3 Organic–Inorganic Interfaces to Produce Delaminated Porous Clay Heterostructures (DPCH)

The modification of layered clays with long-chain alkylammonium ions procures to the resulting organoclays convenient properties for being dispersed in diverse organic media. These organoclays dispersed in certain alcohols, such as *n*-butanol, may suffer a sufficient expansion between the silicate layers for allowing the incorporation of certain alkoxysilanes (e.g., TMOS or TEOS) in the organophilic interface. Interestingly, Letaief and Ruiz-Hitzky [225] demonstrated that under such conditions, it is possible to produce the hydrolysis and polycondensation of the silane, prompted by the addition of small amounts of water and HCl, in a spontaneous sol–gel transition that gives rise to the formation of a polysiloxane network between the silicate layers (Figure 1.7c). In fact, the materials formed after calcination of the organic matter can be described as inorganic–inorganic nanocomposites in which the generated silica matrix provokes the delamination of the silicate as occurs in common polymer–clay nanocomposites. The nature of the starting organoclay, the involved alkoxysilane and the solvent, and other variables (temperature, amount of water, presence or not of HCl catalyst) strongly affect the sol–gel transition and in some cases impeded it, as observed, for instance, when using ethyltriethoxysilane as precursor and smectites exchanged with HDTMA ions [225]. Actually, the organic–inorganic interface plays a key role in the process as the amount and disposition of the organocations in the interlayer region may allow the more or

less efficient incorporation of the alkoxy silane and the water molecules required to produce hydrolysis for initiating the polycondensation reaction [226].

Conversely to classical polymer–clay nanocomposites, the consolidated silica–clay nanocomposites developed by this methodology exhibit enhanced SSA and porosity compared with that of the pristine layered silicates, and they have been later also named as *delaminated porous clay heterostructures* (DPCH) due to their certain resemblance with PCH [177, 178]. In fact, after calcination, some SiO<sub>2</sub>-vermiculite DPCH may reach SSA and total pore volume above 20 and 100 times to those of the parent clay, respectively [226]. As described in PCH, the presence of silica in these DPCH can be used for further functionalization of the material by reaction with organosilanes. In this way, treatment with APTMS produces hybrid DPCH provided with dual cation- and anion-exchange properties, associated with the cation-exchanged capacity of the clay and the presence of anionic species neutralizing the protonated amino groups created during the grafting reaction [226]. Thus, the presence of porosity and possibility of functionalization make this type of clay-based materials very attractive in view of their possible application as adsorbents, support of catalysts, and nanofillers of polymers.

Besides the interest of final DPCH, the intermediate phase obtained before calcination can be also used as organic–inorganic interface in view of diverse applications. In this way, hybrid heterostructures created by polycondensation of TMOS in the interlayer region of MMT treated with CTAB or with octadecylamine were further used as convenient organic–inorganic interfaces to stabilize a metallocene catalyst (i.e., bis(*n*-butylcyclopentadienyl)zirconium dichloride) commonly used as initiator in the polymerization of ethylene. The organic–inorganic hybrid material was then employed to *in situ* polymerize polyethylene that results in reinforced nanocomposites with the clay remaining well dispersed and partially exfoliated in the generated polymeric matrix [227]. More recently, hybrid heterostructures based also on smectites exchanged with CTAB have been used to produce the assembly of ZnO NP in view of developing large surface area clay-based photocatalysts [228]. In this case, the formation of the polysiloxane network exfoliates the clay, and the presence of the organocations attached to those elemental layers of the silicate favors the further assembly of freshly prepared ZnO NP. The further calcination of the material consolidates the ZnO NP within the delaminated clay and the generated SiO<sub>2</sub> matrix, resulting in materials of larger SSA and photocatalytic activity than those prepared by direct assembly of ZnO analogous to organoclays [197, 228].

The preparation of DPCH using other metal alkoxide precursors such as titanium and aluminum has also been explored [179]. In general the process implies three general steps (Figure 1.7c): (i) preparation of the organoclay exchanged with long-chain quaternary ammonium ions, typically by treatment with CTAB although even commercial organoclays have been tested as well; (ii) dispersion of the organoclay in an alcohol (e.g., *n*-butanol, isopropanol), incorporation of the alkoxide precursor (e.g., titanium tetraisopropoxide), and controlled addition of water to provoke the spontaneous heterocoagulation (sol–gel transition) of the organoclay/alkoxide mixture (usually this step is carried out at a controlled moderate temperature, about 50 °C); and (iii) calcination of the organic matter



by a thermal treatment in the presence of oxygen to produce the removal of surfactant species and condensation of the metal oxide, which could be varied in view of optimizing textural properties or to stabilize specific metal oxide phases [180].

Various authors have reported the preparation of DPCH based on layered silicates (e.g., smectites, such as MMT or beidellite, and vermiculites) and  $\text{TiO}_2$  using the aforementioned methodology with the aim to develop active photocatalysts for removal of organic pollutants in water [229–234] or for production of hydrogen from methanol, in this last case incorporating also Pd or Pt NP [235]. The methodology allows also the generation of mixed titanium–silicon oxides just by using mixtures of alkoxides (e.g., titanium tetraisopropoxide and TMOS) in the synthetic process [229]. The presence of the silica precursor favors delamination of the clays, showing the DPCH obtained after calcination enhanced textural properties compared with those incorporating only titanium oxide but impedes the crystallization of  $\text{TiO}_2$  anatase. In spite of this, both  $\text{TiO}_2$ - and  $\text{TiO}_2/\text{SiO}_2$ -clay DPCH show quite similar photocatalytic activity in the degradation of 2,4-dichlorophenol under UV–Vis irradiation, just slightly below that of commercial P25<sup>®</sup>  $\text{TiO}_2$  catalyst [229]. In fact, delamination of the clay is affected by both the length of the long alkyl chain and the amount of the surfactant incorporated in the organoclay, with the silicate expansion necessary for the incorporation of the alkoxide precursor by surfactants with a long alkyl chain of at least 16 carbons being easier to produce [231]. Moreover, the amount of surfactant may affect to the activity of the photocatalyst, with the presence of excess of surfactant species at the external surface of silicate particles being critical as it can produce a sintering of the  $\text{TiO}_2$  NP that reduces DPCH photoactivity [232]. In fact, photocatalytic activity seems to be controlled by a balance between the  $\text{TiO}_2$ -clay ratio and the available surface area [233], and it can be enhanced upon doping of the anatase, for instance, with Ce, just by adding a metal salt (e.g.,  $\text{Ce}(\text{NO}_3)_4$ ) to the sol phase [234]. Interestingly, the general methodology used to produce DPCH allows also the incorporation in the sol phase of other organometallic precursors, for instance, acetylacetonate of palladium or platinum, which become also integrated within the organophilic interface and result in the formation of DPCH that contain simultaneously  $\text{TiO}_2$  and Pd or Pt NP [235]. In fact, this procedure allows the preparation of DPCH with higher content in noble metal NP than the standard photodeposition method, resulting in materials that show higher photoactivity in the photoreforming of methanol to produce hydrogen [235].

The preparation of DPCH from aluminum alkoxides as only precursors showed difficulties due to the usually high reactivity of most of these reagents that results in their rapid hydrolysis even before they may reach the organophilic surfactant–clay interface [179]. However, it is possible to produce DPCH using mixtures of aluminum and silicon precursors (e.g., aluminum tri-*sec*-butoxide and TMOS) at different ratios at the interface of commercial organoclay (e.g., Cloisite<sup>®</sup>30B organophilic MMT) swollen in 2-propanol [236]. XRD patterns show that when the Si/Al content is 2:3 or lower, delamination does not occur but as the Si content increases, there is possibility to reach exfoliation of the clay



layers. The resulting materials after calcination contain silica-alumina mixed oxides with the presence of Si–O–Al bonds as revealed by  $^{27}\text{Al}$  NMR spectroscopy, which shows the presence of aluminum in tetrahedral coordination with an environment of  $\text{SiO}_2$  units in the heterostructured materials [236]. Textural properties of silica-alumina-based DPCH strongly vary with the Si content as well as with the drying treatment applied to the produced gels before calcination. Thus, when the intermediate phases are submitted to freeze-drying before calcination, the resulting silica/alumina/clay nanoarchitectures show higher SSA and higher mesoporosity volumes with low microporosity contents than those DPCH prepared from the same gels dried at  $50^\circ\text{C}$  in air [237]. These differences in textural properties and the possibility to change Al content, and so the acid character of the final DPCH, could be relevant in view of the use of these porous materials in catalytic applications such as conversion of limonene to *p*-cymene or the glycerol recovery reaction [238, 239].

#### 1.3.4 Assembly of Nanoparticles to Fibrous Clays Using Organic–Inorganic Interfaces

As previously mentioned, organic–inorganic interfaces of sepiolite and palygorskite can be prepared by grafting of organosilanes (e.g., chloro- and alkoxy-organosilanes) to the silanol groups ( $\equiv\text{Si-OH}$ ) at the external surface of the fibers or by treatment with cationic surfactants (e.g., CTAB) that can be stabilized via cation-exchange reaction considering that these silicates usually present cation-exchange properties (typical CEC  $< 20$  mEq/100 g). Both types of organic–inorganic interfaces have been used to develop diverse types of nanoarchitectures incorporating bonded inorganic NP either by direct assembly or by *in situ* formation [179–181]. Alternatively, the presence of organic–inorganic interfaces in the NP can be used to generate diverse inorganic–inorganic nanoarchitectures [181]. In this section, various examples showing the most common methodologies that can be used to reach this purpose as well as typical fields of application for the developed materials are introduced.

The previously mentioned sol–gel methodology can be also applied to generate diverse types of NP (e.g.,  $\text{SiO}_2$ ,  $\text{TiO}_2$ ,  $\text{Al}_2\text{O}_3$ , mixed  $\text{SiO}_2/\text{TiO}_2$ , and  $\text{SiO}_2/\text{Al}_2\text{O}_3$ ) in the presence of organosepiolite and organopalygorskite, mainly prepared by treatment of the clay with CTAB (Figure 1.9a). The use of this type of organic–inorganic interfaces was firstly applied to produce  $\text{TiO}_2$  NP on the surface of organosepiolites, the heating step being observed to be crucial to produce final nanoarchitectures with convenient textural properties and stabilization of anatase phase [241]. Actually, the addition of thiourea in the reaction medium allowed the incorporation of sulfur atoms in the generated  $\text{TiO}_2$  NP that resulted in stabilization of anatase NP chemically bonded to the silicate through the silanol groups. The same methodology has been also applied to produce diverse  $\text{TiO}_2$ –palygorskite heterostructured materials in which anatase was stabilized without using any additive in the reaction mixture [242, 243]. The presence of the surfactant clearly favors the organized growing of individual and less aggregate NP on the external surface of the clay in contrast to other methodologies that use the neat clay [180]. Both types of  $\text{TiO}_2$

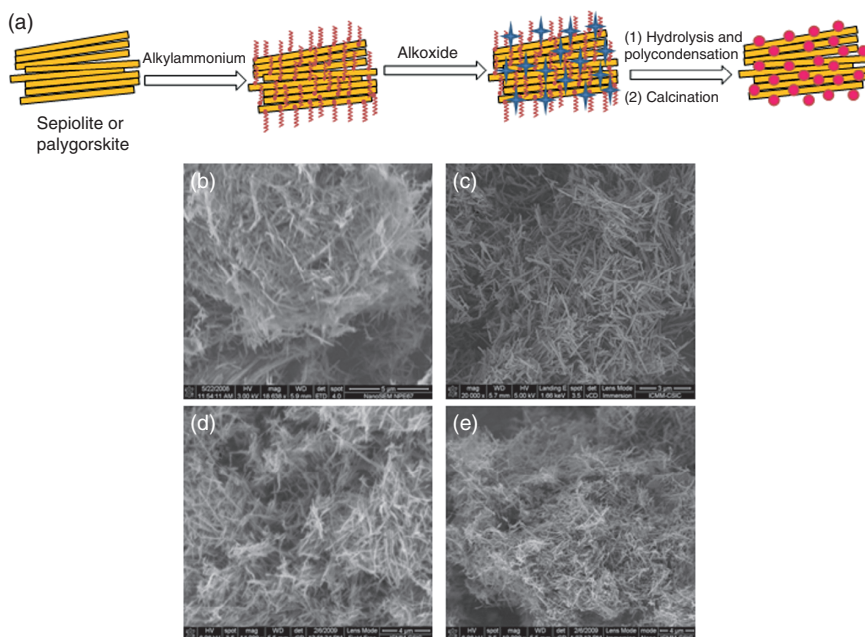


**Figure 1.9** (a) Schematic representation of use of organo-fibrous clay interfaces for *in situ* formation of NP from alkoxides and FE-SEM images of diverse  $\text{SiO}_2$ -sepiolite nanoarchitectures prepared by *in situ* growing of  $\text{SiO}_2$  NP from TMOS on organic-inorganic interfaces of sepiolite modified with propylammonium (b), hexadecyltrimethylammonium (c), didodecyldimethylammonium (d), and stadic methylbenzyl-bis-(hydrogenated tallow alkyl)quaternary ammonium ions (e) described in Ref. [240].

nanoarchitectures were tested as photocatalysts showing good properties in the decomposition of aromatic hydrocarbons and dye species [241–243]. As aforementioned, the sol-gel route allows the incorporation of mixtures of alkoxy precursors with the aim to produce NP of mixed oxides. Thus, for instance, tetraisopropoxide of titanium and TMOS mixtures have been co-hydrolyzed to produce the formation of NP with mixed titanium-silicon oxides in different ratios, although the resulting materials show inferior photocatalytic properties than the systems incorporating pure  $\text{TiO}_2$  NP [241]. During synthesis precursors of other NP, such as Pd- or Pt-acetylacetonate, can be also added, although it has been observed that the resulting Pd/Pt-doped  $\text{TiO}_2$ -sepiolite nanoarchitectures are less effective catalysts in the photoreforming of methanol compared with those prepared by photodeposition of Pd or Pt NP in the previously consolidated  $\text{TiO}_2$ -sepiolite materials [235].

In contrast to that observed in DPCH, organosepiolites treated just with aluminum alkoxides stabilize nanoarchitectures incorporating pure  $\text{Al}_2\text{O}_3$  NP. This difference could be explained considering that as the alkoxide has to reach the organic-inorganic interfaces before hydrolysis-polycondensation reactions take place, it is easier in this case than when the interface is located in the interlamellar region. Actually, the use of mixtures of silicon and aluminum alkoxides allows the formation of diverse nanoarchitectures where the generated  $\text{SiO}_2$ - $\text{Al}_2\text{O}_3$  NP

may present a Si/Al content ranging from 0 to 1 [244]. The resulting NP remain bonded to the external surface of sepiolite and develop interesting textural properties as the materials show relatively high SSA and mesoporosity. As the Si/Al ratio can be varied, it is possible to obtain materials with tuned acidity of interest in catalysis, as it has been proved in dehydration reactions of alcohols to olefins [244]. Actually, these materials can be regarded as alternative catalysts to silica-alumina, PILC, and other related materials, as they show larger SSA and mesoporosity, offering the possibility of easily tuning their acidity.

In organoclays prepared from fibrous clays, the surfactant is located at the external surface of the clay, that is, the organocations surround the fibers and procure the adequate interface where hydrolysis–polycondensation reactions of the alkoxides take place. The nature of this organic–inorganic interface clearly affects the way the NP grow as it has been shown in SiO<sub>2</sub>–sepiolite nanoarchitectures prepared from organosepiolites containing different ammonium-based organocations (e.g., propylammonium, HDTMA, didodecyldimethylammonium, and stadtistic methylbenzyl-bis-(hydrogenated tallow alkyl)quaternary ammonium ions) and TMOS as silica precursor [240]. The presence of didodecyldimethylammonium ions with branched long alkyl chains provokes the formation of thicker coatings of silica NP than HDTMA ions with only one long alkyl chain, but this last one produces nanoarchitectures that show mesoporosity with practically no microporosity. The different aspects of the generated SiO<sub>2</sub> NP (Figure 1.9b–e) clearly indicate a key role of the interface where the organocations somehow can act as “templates” of the growing polysiloxane matrix in a similar way than surfactant micelles in the template formation of silica mesoporous materials.

Moreover, it has been also shown that by varying the clay/silica precursor ratio as well as the nature of that precursor, it is possible to obtain materials with diverse textural properties [240]. Both nanoarchitectures prepared after removal of the organic matter and those in which the organocations are still present could be of interest for diverse applications, for instance, nanofillers of polymeric matrix. In certain cases the presence of the organic compound may favor the compatibility with the polymer and so the improvement of mechanical properties as it has been observed in nanocomposites based on epoxy resins [240].

Organoclays can be also used to favor the regular assembly of already formed inorganic NP. In this way, for instance, ZnO NP have been bonded to sepiolite fibers treated with CTAB, giving rise to photocatalysts that are more active than those prepared from related organoclays based on layered silicates [197]. This behavior may be related to higher availability of the ZnO NP placed on fibrous clay supports than those associated with layered clays, even if these are partially delaminated. Alternatively, metal oxide NP can be modified with a surfactant to facilitate their assembly to the silicate fibers. In this way, the formation of TiO<sub>2</sub> NP in the presence of a neutral surfactant (e.g., Triton X-100) favors their organization on the surface of palygorskite fibers [245]. In the same way, preformed Fe<sub>3</sub>O<sub>4</sub> NP surrounded with oleic acid can be dispersed in an organic solvent, for example, heptane, and the resulting ferrofluid used to facilitate the assembly of the NP to fibrous clays such as sepiolite [195]. The

resulting heterostructured materials preserve the adsorption properties of the clay and show superparamagnetic behavior afforded by the metal oxide NP as being of interest as superparamagnetic sorbents for the removal of pollutants in water [196]. Moreover, the presence of oleic acid molecules in the nanoarchitectures procures organic–inorganic interfaces that can be further used for the assembly of other organic species. In this way, PC has been associated with the production of biomimetic lipid membranes that were further stabilized by certain enzymes (e.g., cholesterol oxidase) to produce a new type of superparamagnetic bioreactors [196]. The hybrid organic–inorganic interface of these oleic acid–magnetite/sepiolite nanoarchitectures also facilitates their assembly to multiwalled carbon nanotubes (MWCNTs), producing multifunctional materials provided with electronic conductivity ( $\sim 1.5 \text{ S cm}^{-1}$  for hybrids with 5% of MWCNTs) and superparamagnetism [196].

Organoclays prepared by grafting reaction of organosilanes to fibrous clays offer also convenient organic–inorganic interfaces that can be used for the assembly of diverse types of NP. Thus, for instance, sepiolite modified with vinyl functionalities [19] shows surfaces reactive to  $\text{OsO}_4$  in which it is possible to regularly grow osmate NP [246]. The resulting materials show interesting properties as photocatalysts in the photodecomposition of water [247]. The treatment of sepiolite with AMPTS introduces amino groups that become protonated after treatment with an acid. These amino protonated groups are regularly distributed along the sepiolite fibers and favor the further assembly of gold NP to produce catalysts of interest in the acetylation of phenol derivatives [248].

## 1.4 Clay-Supported Biointerfaces and Biomedical Applications

For many practical uses it is of great advantage to support biomimetic layers and functional biological molecules on inorganic solids including natural or synthetic clays. These materials offer a robust support for handling of the delicate layers and their functional guest species, thermal and structural protection, and a large SSA, which can serve as a reservoir for uptake and release of large amounts of actives. Additionally, clays are excellent carriers and vectors that can transport the biomimetic layer and other cargo molecules to specific sites [249]. This opened the door for a large variety of biomedical applications of clays and clay–(bio)organic hybrids as detailed later.

### 1.4.1 Clay-Supported Biointerfaces

Biological interfaces have innumerable functions in the living world [250–252]. A paradigmatic interface *per se* is the cell membrane that facilitates the exchange of mass, the transformation of energy, and the transduction of signals [253–255]. Many functional proteins like receptors, transporters, or enzymes reside on the lipid membranes of cells, microorganisms, or viruses. The exploitation of their biological function is of great technological and medical interest, which has driven the biomimetic and bioinspired fabrication of membranes and interfaces

[252, 256]. Lipid membranes and other biomimetic interfaces can serve as compatibilizer between the inorganic support and immobilized biological species. This way, enzymes, proteins, viral particles, or nucleic acids can be adsorbed on clays and preserve their biological activity and thus can be employed as active phases in biosensors, biocatalysts, vaccines, transfection agents, and more.

Processes to obtain biomimetic interfaces are generally based on self-assembly approaches like the molecular self-assembly of dissolved molecules including supramolecular chemistry [257, 258] and self-assembly of preformed aggregates such as vesicles and liposomes [259, 260] or the use of Langmuir–Blodgett methods [252, 261, 262].

Self-assembled membranes are easily formed from synthetic or natural surfactants by cooperative interaction of the polar head group and the apolar tail [263–265]. Biosurfactants, produced by microorganism or extracted from biological tissue, receive special attention as they offer unparalleled advantages like inherent biocompatibility, biodegradability, and nontoxicity besides their vast structural and functional variability [252, 266, 267]. Naturally occurring biosurfactants are, for example, glycolipids, fatty acids, phospholipids, lipopeptides, and polymeric biosurfactants [268, 269].

As pointed out earlier, for practical and technological reasons, biomimetic layers are often supported on inorganic solids like clays. Clays display a variety of interaction mechanisms to form biomimetic interfaces based on (bio)surfactants and biopolymers. Such mechanism include ion exchange and intercalation into the interlayer galleries of smectic clays or layered double hydroxides (LDH), Coulombic attraction, hydrogen bonding, water bridges, or ion–dipole interactions that may also apply on the external surface of the clay particles [133, 270]. Thus, internal and external biomimetic interfaces can be designed.

The adsorption of phospholipid molecules from a methanol solution on MMT is an example of the first case, where PC intercalates into the clay driven by a cation-exchange process [30]. The acidic interlayer space of homoionic sodium-exchanged MMT was proposed to protonate the phosphate group of the lipid head group, which renders PC cationic due to the remaining positively charged choline group. The buildup of an intercalated bilayer lipid membrane could be followed by XRD showing the expansion of the interlayer region with increasing PC concentration. The basal (001) spacing is 4.2 nm, which is compatible with the typical thickness of bilayer lipid membranes.

Adsorption of lipid molecules on non-swelling clays such as the microfibrillar sepiolite clay leads to the formation of external lipid membranes [30, 271]. PC molecules were adsorbed either from ethanol or from aqueous media as preformed liposomes. Both methods followed Langmuir adsorption isotherms, resulting in similar lipid membranes with the only difference that the adsorption of liposomes is far more effective in building up supported lipid bilayers. While 1.2 mM liposomes are needed for bilayer formation, a PC equilibrium concentration of 13 mM is required in ethanol. Moreover, depending on the lipid concentration, mono- or bilayer membranes are obtained with more hydrophobic (monolayer) or more hydrophilic (bilayer) properties. NMR and IR investigations suggested hydrogen bonding between the lipid head group and the sepiolite silanol groups as the main interaction mechanisms [30].



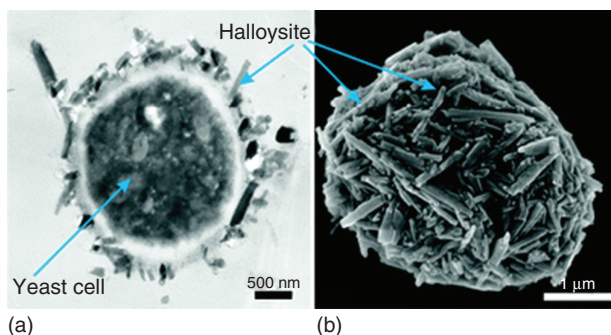


**Figure 1.10** TEM image of a yeast cell coated with halloysite clay nanotubes (a) and an SEM image of the calcinated halloysite shell replicating yeast cell morphology (b). (Konnova *et al.* 2013 [272]. Reproduced with permission of Royal Society of Chemistry.)

An inverse approach is reported by Konnova *et al.* [272], where no clay particles are coated with a membrane but yeast cells were coated with a shell of clay nanotubes. In a first step yeast cells were covered with a cationic (poly)allylamine hydrochloride (PAH) layer onto which anionic halloysite clay nanotubes were adsorbed. After removal of the cells by calcination, stable and hollow microcapsules were obtained, which resemble the original yeast cell morphology (Figure 1.10). These yeast-mimicking capsules were proposed for diverse catalysis and delivery/release applications owing to the hierarchical pore system made up of the micrometric capsule interior and the nanometric halloysite lumen. A further interest is the coating of living cells with clay nanotubes, which may provide the cells with nutrients. The authors could demonstrate high viability of living yeast cells bearing a halloysite shell, which may pave the route to more sophisticated clay/cell “cyborgs” [273].

The clay-supported lipid monolayer can be used as platform for the construction of mixed or asymmetric membranes, where both membrane leaflets consist of different lipids. For instance, the adsorption of a sugar-based surfactant like octyl galactoside onto a sepiolite-supported lipid monolayer resulted in a hybrid bilayer membrane with sugar groups on the external surface [271]. Such mixed bilayers could be used as models for cell membranes of, for instance, erythrocytes, which contain glycolipids or glycoproteins. Another interest in such interfaces displaying sugar-based surfactants is related to the antifouling properties of this type of surfactant [274, 275] or the ability to stabilize proteins [276–278].

An interesting type of solids is LDH, which are often called anionic clays and are typically synthesized by precipitation of di- and/or trivalent metal cations [279]. Guest molecules can easily be incorporated, for instance, by anion exchange or coprecipitation of the LDH structure around the molecule or polymer [280, 281]. Following the latter strategy, Wicklein *et al.* prepared lipid membranes on 2:1 Mg/Al LDH by coprecipitation of  $Mg^{2+}$  and  $Al^{3+}$  at pH 9.2 in the presence of a 0.5 mM liposome solution [282]. Contrary to the adsorption on MMT, the lipid membrane was not intercalated in the LDH, but XRD and IR spectroscopy suggested that the membrane was formed on the external surface. Based on IR analysis, it was speculated that the surface of the liposomes serves



as nucleation site for Mg/Al LDH crystallites. Hydrogen bonding between the metal hydroxides and the lipid head group may favor the growth of LDH lamellae on the liposomes, which eventually rupture and envelope the LDH platelets.

Mucous membranes are another type of biological interfaces that have attracted great attention in the area of drug delivery and tissue engineering due to their hemocompatibility and stealth effects [283, 284]. The major component of mucous membranes besides water is mucin, a high molecular weight and heavily glycosylated protein. Polysaccharides like chitosan or xanthan have now come into focus for mimicking the glycosylated structure of mucin [285, 286]. In this context the surface of sepiolite fibers was modified with the anionic polysaccharide xanthan gum [287] in order to build up an interface that mimics the ability of mucous membranes to retain viral particles [288]. Coating of the sepiolite fibers with xanthan is driven by hydrogen bonding between the hydroxyl groups of the polysaccharide and the silanol groups located at the external surface of the silicate. The resultant biohybrid shows high water retention capacity and presents a favorable environment for biological species. The negative charges originating from xanthan can interact electrostatically with the positively charged surface of the influenza viral particles. Thus, the resulting biointerface would mimic the interaction of natural mucosa with virions during infection processes.

Clays presenting biomimetic or bioinspired interfaces are frequently used to immobilize functional proteins because many proteins rapidly degenerate outside their natural environment. Biocompatible coated clays have been explored as supports of, for instance, redox proteins and to study and explore direct electron transfer processes and bioelectrocatalysis [289]. Exfoliated clay platelets of MMT were coated with biomembrane-like films of surfactants (didodecyldimethylammonium bromide) onto which heme proteins are immobilized [290]. Under preservation of their native conformation in this microenvironment, the heme  $\text{Fe}^{\text{III}}/\text{Fe}^{\text{II}}$  redox couple can be explored for biosensor and biocatalysis applications.

Another high-interest protein is hemagglutinin (HA), a surface protein of the influenza virus. Its antigenic properties make this protein interesting for the development of influenza subunit vaccines. Recombinant HA was immobilized on sepiolite–lipid biohybrids in order to mimic the viral surface of influenza A virions [282]. It could be shown that HA supported on these lipid interfaces shows similar agglutination activity as HA present in the lipid envelope of the native virus particle. This strongly suggests that influenza vaccine doses formulated on the basis of HA alone could be equally immunogenic as conventional whole virus vaccines.

The sepiolite-supported lipid interface was also shown to be well suited for the immobilization of enzymes. In a comparative study the cytoplasmic enzyme urease and the membrane-associated enzyme cholesterol oxidase were adsorbed on PC membranes and maintained their enzymatic activity over months. Contrarily, when the enzymes were adsorbed on the pristine sepiolite surface, their catalytic activity was immediately lost due to strong ionic interactions with the clay surface. The supported enzymes were also successfully implemented as the active

phase in an urease biosensor and a cholesterol batch bioreactor [271]. Alternatively, sepiolite/lipid/urease hybrids were incorporated into carbon black-doped polyvinyl alcohol foams. These nanocomposite foams show simultaneous enzymatic and conductive properties, which make them attractive candidates for bioelectrocatalysis [291].

## 1.4.2 Biomedical Applications of Clays

### 1.4.2.1 Natural Clays in Pharmaceutical Applications

The use of clay minerals for biomedical purposes is known for centuries and continues nowadays in diverse applications including pharmaceuticals, cosmetics, biomaterials, and biosensors [292]. Natural clays can be used in pharmaceutical applications as active agents or excipients. In the first case, the application can be based on their beneficial effects as antimicrobial and antifungal, antidiarrheal, and anti-inflammatory agents, as well as for skin protection [293]. Due to their nontoxicity, rheological properties, sorptive capacity, and ion exchange capacity, natural clays have been commonly used as excipients, acting as drug diluents and carriers. They can provide an emulsifying and stabilizing effect in drug formulations and also allow a controlled release of the drugs adsorbed on the silicates [294–296].

The main mechanism of interaction between drugs and natural clays resulting in hybrid materials is based on ion exchange, with the intercalation of the organic compounds in the interlamellar space of the silicates. Then, the release takes place by a similar process, with the exchange of the intercalated drug by ions present in biological fluids [294, 297–299]. For this purpose, usually smectites of high CEC like MMT and saponite are used. Some examples include the intercalation of 5-fluorouracil, a drug for treatment of colon cancer, into MMT in order to reduce its side effects [300] or the intercalation of the anti-Alzheimer drug donepezil into MMT, saponite, and the synthetic silicate Laponite<sup>®</sup> aiming to improve the thermal stability of the drug, as well as to provide a controlled release [301].

In other cases, hydrophobic interaction or hydrogen bonding can take place between the drug and the natural clay. For instance, fibrous silicates show a low CEC, but they offer a large external surface with high density of silanol groups, which can interact with the organic molecules by hydrogen bonding, as reported for timolol and 5-aminosalicylic acid (5ASA) [294]. Due to its high adsorption capacity, sepiolite is also very effective as odor adsorbent and exudates from wounds [302]. Some studies have reported the role of sepiolite in the lysis of erythrocytes [303], but the toxicity of fibrous clay minerals seems to be related to the fiber length, which depends on their geological origin [304]. In fact, other studies carried out on sepiolite from Taxus basin deposits in Spain confirmed its lack of toxicity [305].

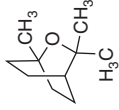
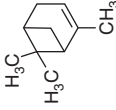
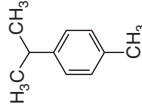
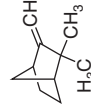
### 1.4.2.2 Clay-Based Hybrids for Drug Delivery Applications

Besides the use of natural clays in the preparation of drug–silicate hybrids, diverse types of organically modified clays can be used for drug delivery purposes. Such modification is usually carried out in order to enhance the surface reactivity of the clay, to increase hydrophobicity, or to profit from the properties

of the resulting nanocomposites when clays are combined with polymers [292]. Hydrophobic organoclays can help to stabilize certain drugs and bioactive compounds of organophilic nature. An example for this approach that reveals the very specific clay–organic interactions depending on the sorbate and the sorbent is demonstrated by the rate of evaporation of different components in rosemary oil [306]. Rosemary essential oil is extracted from the flowering tips of the rosemary plant and has been used since ancient times due to its therapeutic properties. The volatile composition of the essential oil of rosemary has been the subject of considerable research in recent years. Several studies [307–309] mention a mixture that includes among other compounds  $\alpha$ -pinene (vapor pressure 3 mm Hg), 1,8-cineole (eucalyptus oil, v.p. 1.9 mm Hg), *p*-cymene (v.p. 1.5 mm Hg), and camphene (v.p. 2.4 mm Hg). Evaporation of the different components from the rosemary oil mixture can be monitored by measuring the ATR-FTIR spectrum and quantifying the remaining amount from the relevant absorption bands of each component, related to the strength of the initial band as mentioned in Section 1.2.1.2, and calculating the half time life from the measurements as described in the appendix in [64]. It can be seen (Table 1.1) that half-life time of the different components in free oil are between 190 and 300 s. Adsorbing rosemary oil on SWy-1 MMT doubles and even triples half life times for part of the components, but does not have influence, for example, on  $\alpha$ -pinene. On the other hand, adsorption on an hydrophobic organoclay prepared from MMT with berberine adsorbed up to the CEC (Berb-SWy-1) changes the interaction for  $\alpha$ -pinene and slows more the release of 1,8-cineole and even more significantly that of camphene, but does not exhibit improvement on *p*-cymene when compared with raw MMT. Sepiolite, which offers neutral adsorption silanol sites, interacts relatively strongly with all the components, and half life times are increased 4–5 times as compared with free oil. But the most significant slow-release effect is observed on a hydrophobic organoclay prepared from MMT with CV adsorbed up to the CEC (CV-SWy-1), with half life times 6–8 times larger than in free oil. Results show that interaction of the different components of rosemary oil on clays and organoclays is very specific and not always fully understood. Thus, when preparing slow-release or controlled-release formulations (CRFs), optimization must be performed specifically on the compound of interest.

Organoclays have been typically used to improve the interaction of the clay with synthetic polymers. This is the case of the commercial organoclay Cloisite® 30B combined with poly(dimethylsiloxane), which was applied in the controlled delivery of metronidazole [310]. However, surfactants like quaternary ammonium compounds should be avoided in biomedical applications due to their reported cytotoxicity [311]. Biopolymer-based materials appear as a better alternative for drug delivery and other biomedical applications due to their biocompatible character [44]. Bionanocomposites can be used as carriers in DDS, allowing a gradual release of the drug in order to avoid periods of overdosing or underdosing during treatment [295]. The biopolymers can also prevent or reduce the tendency of unmodified clays to flocculate when the DDS is dispersed in physiological media [312].

**Table 1.1** Half life time of rosemary oil components in seconds.

Component	Structure	Free rosemary oil	Adsorbed on SWy-1	Adsorbed on Berb-SWy-1	Adsorbed on sepiolite	Adsorbed on CV-SWy-1
1,8-Cineole (845 $\text{cm}^{-1}$ )		253	764	974	1060	1953
$\alpha$ -Pinene (785 $\text{cm}^{-1}$ )		191	195	465	842	1185
<i>p</i> -Cymene (820 $\text{cm}^{-1}$ )		257	515	592	1228	2079
Camphene (886 $\text{cm}^{-1}$ )		300	527	1339	1257	1813

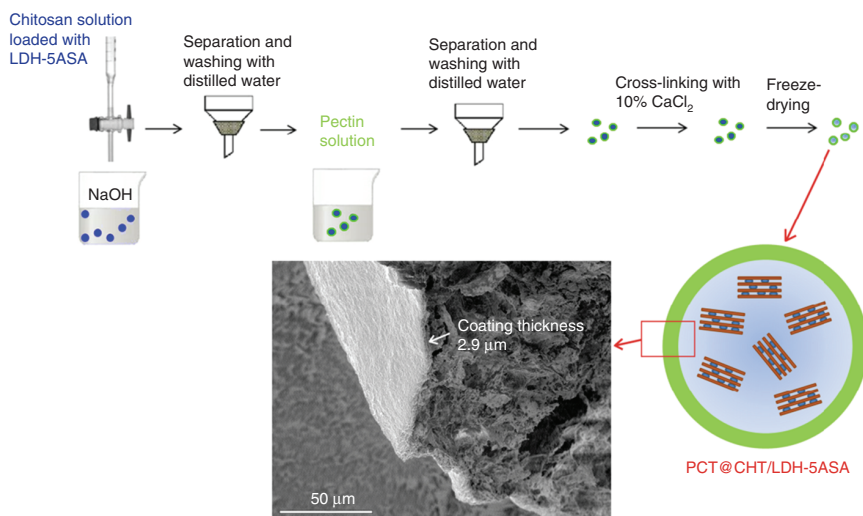


**Figure 1.11** Schematic illustration of the preparation of the pectin@chitosan/LDH-5ASA system, showing the pectin coating in the FE-SEM image of a bead cross section. (Ribeiro *et al.* 2014 [314]. Reproduced with permission of Elsevier.)

Most of the applications of bionanocomposites as DDS are based on layered silicates and related solids like the anionic clays known as LDH. In some cases the DDS is prepared by intercalation of the drug into the smectite clay, followed by encapsulation in a polymer or a blend of polymers. This is the case mentioned earlier of donepezil intercalated in smectites, which were then coated by the cationic polymer Eudragit<sup>®</sup> E-100 in order to improve the drug release rate [301]. A similar example is the coating of hybrid materials based on LDH and intercalated ibuprofen by a blend of alginate and zein, a hydrophobic protein extracted from corn [313]. In this case, zein reduces the swelling ability of the nanocomposite material, increasing the control in the release of entrapped ibuprofen. The coating of the hybrid material can be tailored in order to tune the delivery along the gastrointestinal tract. Thus, 5ASA intercalated in LDH was first embedded in chitosan, with mucoadhesive properties to afford a targeted delivery at the intestine, and then coated by a pectin layer to protect the DDS during its passage through the stomach (Figure 1.11) [314]. Similarly, the alginate coating of the hybrid based on the anticancer drug doxorubicin and Laponite<sup>®</sup> facilitated the transport through the cell membrane, releasing the drug due to the acidic environment of the endolysosomes [315].

In other cases, a bionanocomposite is formed by intercalation of the biopolymer in the interlamellar space of the silicate, and then the system is used as a carrier of the drug, as shown for carboxymethyl chitosan–MMT bionanocomposites loaded with isoniazid, an antibiotic used in the treatment of latent and active tuberculosis [316]. Cross-linkers like glutaraldehyde were also used in this case in order to enhance the control in swelling and the release rate. Similarly, chitosan–MMT nanocomposites were loaded with silver sulfadiazine and applied in wound healing [317].

In addition to layered solids, tubular and fibrous silicates have been also applied for drug delivery purposes. Chitosan-palygorskite bionanocomposites were loaded with the nonsteroidal anti-inflammatory drug diclofenac sodium (DS), and the resulting DDS showed an enhanced control in the release of DS at the intestinal fluid due to the presence of the fibrous silicate [318]. Analogous nanocomposites involving a second polymer component are prepared by addition of polyacrylic acid (PAA) or PAAm and are also widely studied as DDS. An illustrative example of these hydrogel materials with superabsorbent properties is the palygorskite–carboxymethyl cellulose–g-PAA material combined with alginate for the controlled release of DS at the intestinal tract, in which the presence of palygorskite reduces swelling, leading to a slower release rate [319].

As extensively reviewed by Lvov and Abdullayev [320], the nanotubular clay halloysite is also suitable as a container for entrapping drugs and many other active compounds (cosmetic additives, antiseptics, antibacterials, proteins, and DNA). The halloysite drug hybrid can be dispersed in polymers, giving rise to nanocomposites with slower release of the entrapped drug due to the polymer coating at both nanotube endings. Some examples are the use of a gentamicin-loaded halloysite–PMMA nanocomposite as bone cement in order to prepare implants with antibacterial effect [320] or the preparation of a halloysite–chitosan–poloxamer composite loaded with the antibiotic tetracycline for the treatment of animal periodontitis, which shows an extremely slow release of the antibiotic for up to 2.5 months [321]. Biopolymers like starch have been also used in DDS involving halloysite, as reported for the system loaded with 5ASA that was prepared by melt extrusion [322]. Given that starch is not pH dependent, the resulting DDS is resistant to acidic environment and would be able to protect the drugs during its passage through the stomach and transport them to the colon. Halloysite–chitosan nanocomposites have been proposed as nanocarriers for the anticancer drug curcumin, as they show good hemocompatibility and an enhanced anticancer efficacy in comparison with free curcumin [323].

Besides drug delivery, clay-based hybrids can be also applied as nonviral vectors for gene transfection. Hybrid materials based on intercalation of DNA in LDH were reported by Choy and coworkers [324], emphasizing the role of the LDH as a shield to minimize the repulsive interaction between DNA and the cell membranes, both negatively charged, and allowing the hybrid to penetrate into cells through endocytosis. The size of the LDH NP should be around 100–200 nm in order to allow cellular uptake, and after DNA or drug release, the LDH can be externalized through exocytosis, producing no harm on the cells [299]. The adsorption of DNA in layered silicates increases its stability against degradation by DNase I [325]. Studies carried out with plasmid and short linear amplified DNA adsorbed on MMT confirmed that although protection was not complete, the DNA was still able to transform *Escherichia coli* cells. Similarly, fibrous clays like sepiolite are being also applied in gene transfection, as DNA shows great affinity toward silicate, establishing hydrogen-bonding interactions with the silanol groups located at its surface [326]. When a mixture of the DNA–sepiolite hybrid and bacteria on agarose or gellan gum plates is stimulated through sliding friction on surface of the hydrogel, it may lead to the uptake



of the fibers by bacteria, allowing the transfection of the adsorbed DNA in the so-called Yoshida effect [327]. Recently, other studies are being carried out in order to extend the use of DNA–sepiolite hybrids for gene transfection into eukaryotic cells [328].

#### 1.4.2.3 Clay-Based Hybrids for Vaccine Applications

Recently, clays have been recognized as alternative immunogen support in vaccine formulations due to their large SSA, vector behavior, and inherent biocompatibility [107, 288]. One important aspect to increase the efficacy of vaccines is the stabilization of immunogens, that is, inactivated or live attenuated virus particles, viral vectors, proteins, or plasmids, on particulate carriers that can enable easy administration and protection from proteolysis and improved thermal storage performance [329]. However, it was observed in several studies that adsorption of antigens on the pristine clay surface can alter their protein structure possibly through strong electrostatic interactions with highly charged clay surfaces [107]. This resulted in decayed immunogenicity of the antigen and eventually compromised the vaccination efficacy [107, 288, 330]. Therefore, Rytwo *et al.* [107] explored the possibility of using clays with organo interfaces (MMT–berberine hybrids) in order to accommodate antigens while preventing adsorption-induced protein alterations. In that study, it could be shown that the organic modification of the clay permitted the co-adsorption of two antigenic proteins, heat-labile enterotoxin and viral protein 2, without conformational protein alterations, as evidenced from IR spectroscopy. The retained bioactivity of these organoclay-associated proteins enabled efficacious binding to cellular GM1 receptors, an important step in the stimulation of an immune response to the infectious bursal disease virus. An alternative approach was followed by using xanthan–sepiolite biohybrids to design an influenza vaccine [288]. Here, the governing idea was to provide a tissue-like environment for the adsorbed influenza virus similar to the nasal mucous membrane, the natural location of influenza virus entry into a body. Inactivated influenza A virus was adsorbed on sepiolite–xanthan, and immunization of mice and posterior challenge with infectious influenza A virus demonstrated high level of seroprotection elicited by this vaccine.

An important challenge in vaccination is the thermostability of vaccines, which becomes critical in stockpiling of pre-pandemic vaccines and in discontinuous cold chains, for example, in low-income countries [331]. The stability against accidental freezing during transportation and storage can also compromise vaccine efficacy (about 30% of all vaccines are freeze sensitive) [332]. Both scenarios represent economic and healthcare threats in the multimillion-dollar range [332]. Therefore, the Ruiz-Hitzky group explored sepiolite–lipid hybrids as novel adjuvants in thermostable influenza A vaccines [282]. Functional studies showed improved thermal stability at elevated temperatures up to 48 °C together with enhanced resistance against lyophilization-induced antigen denaturation as often seen for alum-stabilized antigens [333, 334]. This improvement in thermal stability was suggested to be related to the creation of a chemical microenvironment [334, 335] by the sepiolite–lipid biohybrid forming a kind of thermally protective scaffold for the adsorbed influenza virions.

A similar example of the thermo-protecting effect of organoclays toward sensitive biological species was reported by Fujimori *et al.* who fabricated multilayer films of organically (dimethyldioctadecylammonium) modified MMT platelets and lysozyme by a modified Langmuir–Blodgett method [336]. Mono- and bilayers of the enzyme were assembled onto the organoclay sheets or sandwiched in between them. This confinement of the enzyme results in surprisingly high thermal stability of lysozyme showing enzymatic activity until 160 °C.

The versatility of clay–lipid hybrids also allows for the immobilization of other biological molecules such as plasmid DNA vectors for genetic immunization. Layered double hydroxide-phosphatidylcholine (LDH-PC) hybrids were studied as nanocarrier of the plasmid pMAX-GFP (4.7 kb), which expresses the *Leishmania infantum* LACK antigen [337]. This antigen has shown to elicit protection against the tropical disease leishmaniasis [338]. The results suggested increased cytokine secretion of the DNA vaccine adjuvanted by the LDH-PC biohybrid as compared with the LDH-adjuvanted or non-adjuvanted DNA vaccine. LDH-PC also demonstrated high transfection efficacy of the pMAX-GFP plasmid into 293 T cells, which was even superior to the commercial transfection agent Lipofectamine<sup>®</sup>. Combined, these results suggest the expediency of the LDH-PC biohybrid to improve the efficacy of DNA vaccines.

#### 1.4.2.4 Clay-Based Hybrids in Regenerative Medicine

The use of clay minerals in regenerative medicine is generally related to reinforcement of natural or synthetic biodegradable polymers, but clays can also act as carriers of biomolecules in implants, can contribute to increase cell adhesion, or even can have influence on differentiation of stem cells (Figure 1.12), as recently reviewed by Ghadiri *et al.* [292]. For bone repair purposes, clay-based nanocomposites are commonly processed as cellular solids trying to mimic bone, which is in fact a natural porous bionanocomposite composed of type I collagen reinforced by hydroxyapatite (HAP) crystals as thin platelets. Although the first attempts to produce scaffolds or implants for hard biological tissue applications were focused on those materials present in the native bone composition [339], clays and a great variety of biocompatible and biodegradable polymers appear also as good components for bionanocomposite materials that reproduce the main characteristics of bone [292, 340, 341]. Collagen, gelatin, alginate, and chitosan among natural polymers and synthetic biodegradable polymers like PEG, poly(lactic acid) (PLA), poly( $\epsilon$ -caprolactone) (PCL), PEO, and poly(lactic-*co*-glycolic acid) (PLGA) are the most used polymer components in scaffolds for regenerative medicine.

3D supports with suitable porosity are required for tissue engineering applications. Usually, the preparation of bionanocomposite scaffolds proceeds by lyophilization or supercritical CO<sub>2</sub> foaming of the intermediate biopolymer–clay hydrogel. The result is a cellular material with highly interconnected pores of adequate size to accommodate cells, allowing the passage of nutrients and removal of metabolic wastes and leading to new tissue growth and vascularization. In this type of materials, clays play a crucial role acting as fillers of the polymer matrix in order to enhance compressive strength and stiffness of these highly porous scaffolds, which is of particular importance in bone repair [341].

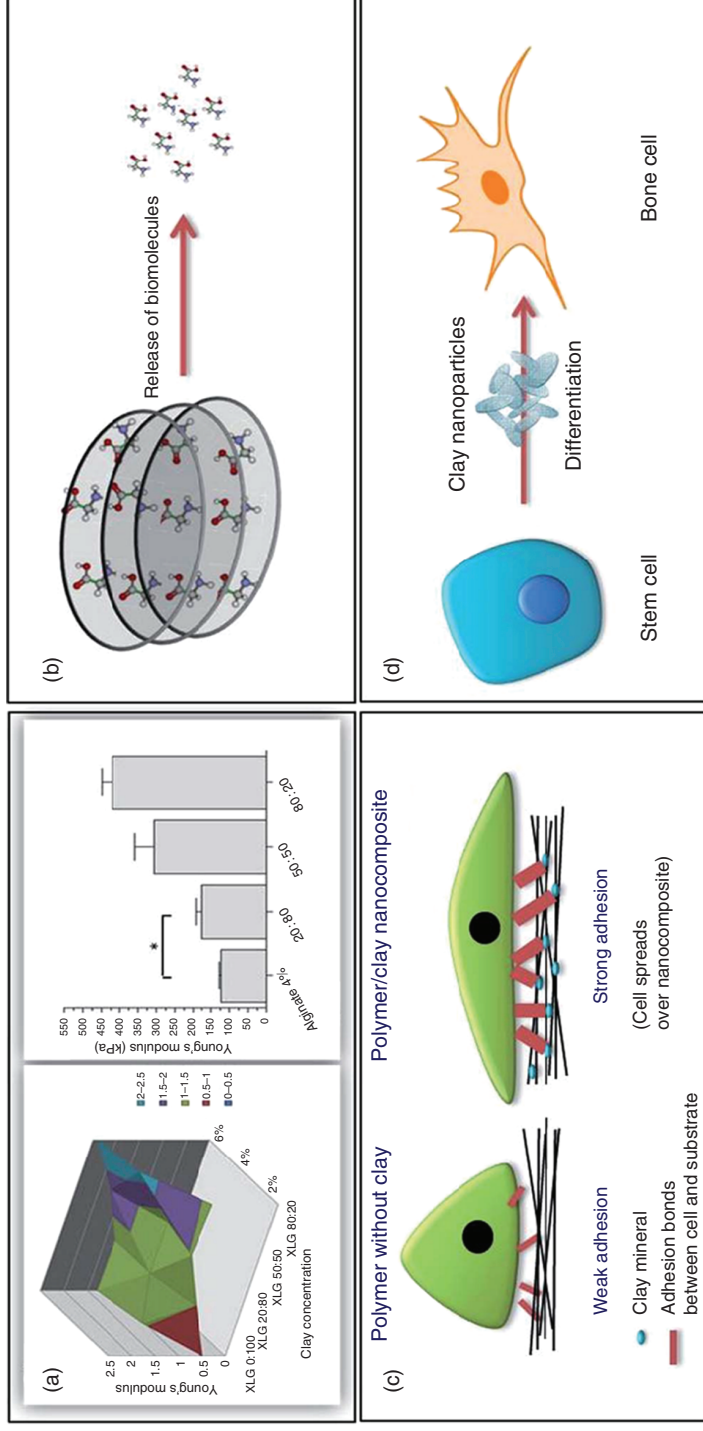


**Figure 1.12** Diverse uses of clay minerals in regenerative medicine: reinforcing fillers of biodegradable polymers (a), release of biomolecules (b), enhancement of cell adhesion (c), and proliferator and differentiator of stem cells to bone cells (d). (Ghadiri *et al.* 2015 [292]. Reproduced with permission of Royal Society of Chemistry.)

MMT and Laponite<sup>®</sup> are widely used in this type of applications. The dispersion of about 5% of MMT modified with dimethyl dihydrogenated tallow ammonium cations into PLA revealed the effect of the silicate NP on the biomaterial stiffness, leading to values of tensile modulus about 40% higher than that obtained for unmodified PLA [342]. A similar effect was observed in a 3D gelatin/MMT/chitosan nanocomposite scaffold with high porosity, in which the MMT layers acting as physical cross-linkers led to the improvement in mechanical stability, affording a good adhesion and proliferation of stem cells on the biohybrid scaffold [343]. Bioactive implants for bone repair were prepared by assembling chitosan to a PEO–laponite nanocomposite, where the Laponite<sup>®</sup> layers worked as cross-linkers bridging the PEO chains and chitosan increase cell adhesion and provided the nanocomposite with antimicrobial properties [344].

Several reports confirm that clays not only enhance the stiffness of the material but also can have a strong influence on the biodegradation rate. In the study of the biodegradability of a gelatin/MMT/chitosan nanocomposite, this behavior was attributed to the protection exerted by the clay platelets on the biopolymers against the action of lysozyme present in body fluids [345]. Similarly, biodegradation of materials involving PCL and chitosan-modified MMT was carried out at simulated physiological conditions over a period of 4 weeks, and the study confirmed the biodegradation of these scaffolds by hydrolysis at a slow rate [346].

Aiming to mimic the bone composition, HAP is sometimes incorporated in the preparation of scaffolds. Chitosan–MMT materials combined with HAP gave rise to better mechanical properties than the binary system, together with higher cell proliferation rate, as promising candidates for application in bone repair [347]. HAP was also incorporated in the interlayer space of nanoclays mimicking biomineralization process, and the resulting HA–clay hybrid was used in the preparation of PCL scaffolds [348]. The HA–clay hybrid provide the composite scaffolds with osteoinductive and osteoconductive properties that allowed the formation of bone nodules and mineralized extracellular matrix (ECM) by stem cells attached to the scaffold, confirming in this way the influence of nanoclays on stem cell differentiation.

The nanoclays forming part of a bionanocomposite scaffold can be loaded with a bioactive compound that can be slowly released during the permanence of the scaffold in the body. This is the case of a nanocomposite based on the co-intercalation of chitosan and the antibiotic vancomycin into the interlayer space of Laponite<sup>®</sup> [349]. This bionanocomposite was used as a coating of titanium implants for potential orthopedic applications, showing an improved cell attachment and proliferation together with slow release of the entrapped antibiotic to inhibit bacterial growth.

Besides layered clays, silicates with fibrous and tubular morphology are also involved in the development of nanocomposites for tissue repair. For instance, the study on sepiolite-reinforced collagen was initiated in the 1980s by Perez-Castells *et al.* [350]. Biomaterials based on the assembly of both components were tested *in vitro*, showing the lack of cytotoxicity together with good adhesion and proliferation of fibroblasts [351], as well as in *in vivo* tests in surgically created rat calvarial defects, where the biomaterial did not induce

inflammation or necrosis and promoted bone regeneration [352]. Biodegradation was tuned by cross-linking of the collagen-sepiolite scaffolds with glutaraldehyde in order to avoid resorption within the first days and extend the permanence of the scaffolds for several months, allowing the healing of the bone defect [353]. More recent studies have been carried out in order to understand the interaction established between collagen and gelatin with fibrous silicates [354, 355] and can be a starting point to address the development of bionanocomposite scaffolds for biomedical applications. Similarly, other biocompatible and biodegradable polymers like poly(butylene adipate-*co*-terephthalate) (PBAT) reinforced with sepiolite appear as promising candidates for tissue repair, as they show higher thermomechanical properties than analogous materials based on layered clays, together with good biological safety and almost non-cytotoxicity [356].

Bionanocomposites based on the nanotubular clay halloysite also offer potential application in tissue engineering. A recent example is the macroporous alginate/halloysite foam, which shows improved mechanical properties and decrease in the water swelling in comparison with pristine alginate [357]. These scaffolds showed good cytocompatibility, allowing the attachment and proliferation of mouse fibroblast cells, most likely due to the biocompatibility of halloysite nanotubes and the increase in the surface roughness in the bionanocomposite material. In a recent work, the biocompatibility and biodegradability of porous scaffolds produced by freeze-drying from chitosan/gelatin/agarose hydrogels doped with halloysite were tested *in vitro* and *in vivo* [358]. The evaluation in rats of these halloysite-doped scaffolds confirmed their capability to promote the formation of new connective tissue near the scaffold together with novel blood vessels, allowing the complete restoration of blood flow around the implantation sites, as well as full resorption of the scaffold within 6 weeks after implantation.

## 1.5 Clay Interfaces for Environmental Protection

Since ancient times, clays and derived hybrid materials have found application in environmental protection. The so-called environmental applications of clay–organic interactions may be traced since dawn of history: removal of polluting oil from wool, fining and purification of oils and wine, preparation of stable artisanal pigments, and even direct use as cheap and efficient construction materials or useful waste containment barriers. Several advantages endorse the direct use of natural clays in environmental remediation: their cationic exchange capacity and adsorption ability that make possible the removal of a great number of pollutants, mainly of cationic type, their abundance and low cost, and their lack of toxicity. In addition, the possibility of developing a wide variety of hybrid materials, in which the adsorption properties of natural clays are tuned by modification with molecular or polymeric organic species, enlarges considerably the number of potential applications in the environmental field. Thus, organoclays are commonly used for removal of anionic and hydrophobic pollutants, overcoming the limitations of natural clays. Water purification and treatment of polluted effluents and the preparation of better and less hazardous

formulations of pest management compounds are two important applications of clays and clay-derived hybrids within the topic of environmental remediation that will be revised in this section.

### 1.5.1 Natural Clays as Adsorbents of Organic Pollutants

Currently, the use of natural clays for removal of hazardous chemicals continues to be a widely explored research topic due to the important implications of remediation, mainly on health issues. For this purpose, silicates of layered morphology with ability to swell and accommodate organic species in the interlamellar space, as well as fibrous silicates provided with high porosity and SSA, tubular shape minerals (as halloysite) that might act as nanotubes, or specifically designed PILC that may act as molecular sieves due to the variable framework charge and porous structure have been widely used for removal of hazardous chemicals, including dyes and emerging pollutants like pharmaceuticals or biocides [359, 360]. As described in Section 1.2, due to the CEC of smectites, the exchangeable cations in their interlayer space can be easily replaced not only by other hazardous cations like heavy metal ions but also by positively charged organic molecules, forming hybrid interfaces and following an ion-exchange mechanism, mainly driven by electrostatic interaction [10, 11]. These silicates show also the ability to intercalate neutral organic species forming coordination compounds with exchangeable metal ions and surface oxygens of the tetrahedral sheets, which can act as proton acceptors for the formation of H bonds with adsorbates bearing  $-OH$  or  $-NH$  groups [14].

As mentioned earlier, dyes are typical pollutants that need to be removed from wastewater, mostly in the textile industry. Some of them can pose a considerable risk for the environment as well as for human health due to their very high toxicity. Thus, natural clay minerals have been used as geosorbents for certain dyes, mainly with cationic charge, since long time ago, as they offer a high adsorption capacity comparable to activated carbons [360]. MMT is one of the most commonly employed clays for this purpose. For instance, it has been applied in the removal of the cationic dye rhodamine B used in printing, textile, and photographic industries [361]. The maximum adsorption at an optimal pH of 4 was close to  $182 \text{ mg g}^{-1}$ , much higher than that obtained using kaolinite as adsorbent ( $22 \text{ mg g}^{-1}$ ), and did not improve by acid activation of the clay before the adsorption step.

Similarly, MMT has been applied in the removal of a great number of emerging pollutants like antibiotics and many other pharmaceuticals. An illustrative example is the case of ciprofloxacin, an antibiotic frequently used in human and veterinary medicine, which was removed by MMT mainly by intercalation mechanism under acid pH or by complexation with the interlayer cations when the molecule is negatively charged at higher pH values [362]. In both cases, the clay is able to retain high amounts of ciprofloxacin, showing adsorption capacities of  $400 \text{ mg g}^{-1}$  at pH 3 and  $520 \text{ mg g}^{-1}$  at pH 11. In contrast, other antibiotics like nalidixic acid do not show a similar complexation ability, and thus the adsorption capacity of MMT for this compound is strongly reduced at pH higher than its  $pK_a$  [363]. Several examples of the application of clays in the removal of other



hazardous chemicals like VOCs released in industrial operations or pest management compounds can be found in the literature, for instance, the application of beidellite to eliminate the herbicide simazine from aqueous solution [364]. In this case, the adsorption of simazine most likely takes place as protonated species, with protonation occurring by surface and interlayer hydrated protons.

The adsorption ability of clays like bentonites to remove organic and inorganic pollutants is the basis of their application as sealing systems, including horizontal technical base liners and cutoff walls, together with their ion-exchange capacity and swelling behavior as well as the low permeability of the bentonite-containing walls [365]. Studies are carried out in order to determine the best silicates for this type of application as geologic barriers in landfills. For instance, diverse clays from several locations in Spain were evaluated regarding their adsorption of organic pollutants like atrazine, benzamide, methomyl, paraquat, and toluene [366], and part of them showed promising results for application as multibarriers in controlled urban landfill.

#### 1.5.1.1 Clay-Based Hybrid Materials as Adsorbents of Pollutants

As mentioned earlier, clays minerals are generally ineffective in the adsorption of anionic and hydrophobic organic species. Thus, they are usually transformed into organoclays by modification with molecular or polymeric organic species in order to overcome these limitations and enlarge their applications in environmental protection [367, 368]. As described in previous reviews [29], organoclay formulations aiming to be used for environmental applications are based usually on three components:

1. *The substrate*: Clay mineral that due to its special mineralogical structure offers several binding sites available to different types of molecules. It can be compared with biological macromolecules with several kinds of active sites [369], each of them predominant in different clay–organic interactions, yielding overall unique results: (i) aluminol and silanol groups; (ii) isomorphic substitutions, yielding “lack” of positive charge; (iii) exchangeable cations that compensate the lack mentioned previously; (iv) hydrophobic siloxane surfaces; (v) hydration shell surrounding exchangeable cations mentioned in (iii); and (vi) hydrophobic sites on organic molecules adsorbed on clays.
2. *The “modifier”*: An organic molecule bound to the clay mineral. In several cases an organic cation with a hydrophobic moiety or a cationic polymer. In all cases the purpose is to exchange the originally bounded exchangeable inorganic cations attached to the surface due to the lack of positive charge in order to modify the substrate surface. In several cases the purpose is to form a hydrophobic non-charged surface to increase the affinity of the hybrid nanomaterial obtained to the additional component (pesticide, pollutant, etc.) of interest. Figure 1.13 presents an example of such modification. The added amounts of the organocation thiamin (vitamin B1) to SWy-2 MMT on the adsorbed amounts (triangles, left vertical axis) and the charge as measured by titration with a streaming current detector (squares, right vertical axis) exhibits a tight relationship between the amount of B1 adsorbed and the charge of the hybrid material. Such modifications aim to adapt the surface of the hybrid in order to optimize interactions with the molecule of interest.

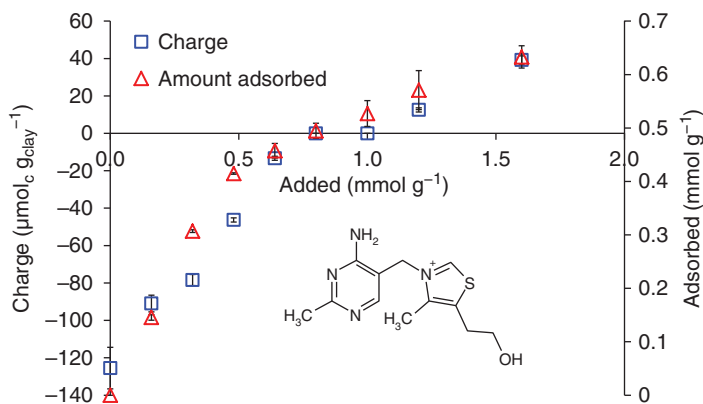


**Figure 1.13** Relationship between the amount of the organocation thiamin (vitamin B1) adsorbed on SWy-2 montmorillonite and the charge of the resulting hybrid material.

3. *The molecule of interest:* Depending on the case it can be a specific pollutant to be removed by the hybrid (e.g., [370]), a pesticide that is attached to the hybrid to avoid its leaching or decomposition (e.g., [371]) or any other environmental application of interest.

The organically modified substrates can facilitate the binding of hydrophobic organic compounds, either in the original preparation (in order to avoid leaching or degradation of pesticides) [60, 62] or by adsorbing organic unwanted compounds of pollutants that should be removed from effluents [58, 372]. Preparation of hybrid compounds exhibiting a net positive charge might also allow the binding of anionic pollutant. An example of such application is the removal of the  $^{125}\text{I}^-$  long-lived radioiodide by hexadecylpyridinium (HDPy)-modified vermiculite [373]. The HDPy modifier is incorporated in high amount into vermiculite, exceeding the CEC of the clay mineral, and part of HDPy is present as HDPyCl ion pairs, allowing the radioiodide adsorption through an anion-exchange mechanism. In contrast, intercalation of short-chain alkylammonium cations such as tetramethylammonium ( $\text{TMA}^+$ ) cannot exceed the CEC, and they are unable to form similar micellar systems with an excess of positive charge in the clay interlayer space, not allowing the adsorption of  $^{125}\text{I}^-$  [12]. Similarly, polymers can be adsorbed on the surface of silicates or intercalated in their interlayer space, producing a change in their original ion-exchange capacity. This fact was observed, for instance, after intercalation of chitosan into MMT at higher amounts exceeding the CEC of the clay [51, 374]. Thus, the resulting bionanocomposite showed an anion-exchange capacity (AEC) close to 57 mEq/100 g, due to the free protonated amino groups, which allowed its use as active phase in potentiometric sensors for determination of anions, as well as adsorbent of anionic organic pollutants like tannic acid [375] or anionic As(V) and Cr(VI) species [376]. Such charged nanocomposites can also be used for water purification as described in Section 1.5.3.1.

### 1.5.1.2 Environmental Applications of Hybrid Materials

The use of organoclays in diverse environmental applications like remediation of groundwater [377], encapsulation of solid wastes [378], or development of sensors for environmental control [379, 380] has been reported in the last years. Among all the possible applications, the main use of these clay-based hybrids seems to be related to removal of pollutants from drinking water and effluents as well as to the preparation of more efficient and less hazardous formulations of pest management compounds. Both types of application are reviewed in this section.

### 1.5.1.3 Water Purification and Treatment of Effluents

Organically modified clay materials are being widely employed in the removal of pollutants from water and effluents, not only for neutral or positively charged pollutants but also for anionic and hydrophobic organic compounds as mentioned in the previous section. For instance, organoclays resulting from the adsorption of certain dyes (CV and rhodamine B) were successfully applied to remove atrazine, phenol, and naphthalene [58]. A CV–MMT organoclay in which the CEC is saturated with the dye showed a similar efficiency than activated carbon in the removal of trichlorophenol (TCP), reaching values close to  $63 \text{ g kg}^{-1}$ , with the advantage of a rate of sorption ( $780 \times 10^{-4} \text{ kg g}^{-1} \text{ min}^{-1}$ ) about two orders of magnitude higher than that of activated carbon [381]. This type of clay-based organoclays were also proved as better adsorbents of oils from water and can be used as a pretreatment step before adsorption with activated carbon [382]. A recent work reporting the adsorption of the herbicides atrazine, alachlor, and trifluralin on TMA-based organoclays and other geosorbents reveals considerable differences between adsorption capacities from surface water and groundwater [377]. This fact can be related to the influence of the type and the content of dissolved organic carbon (DOC) in each water phase, which seems to be an important parameter in view of remediation of polluted areas.

Bionanocomposites prepared by modification of clays with biopolymers have been also evaluated as adsorbents in water treatment and environmental remediation. Among them, chitosan-based materials have been widely employed for the removal of anionic species like highly toxic species of As(V) and Cr(VI) [376], organic compounds like tannic acid [375], or certain dyes like reactive black 5 [383]. Chitosan–clay bionanocomposites can be also applied in the removal of hazardous cations. A recent example is the intercalation of chitosan in the inter-layer space of vermiculite by means of ultrasounds, and the application of this material conformed as a macroporous foam in the removal of cadmium ions from aqueous solution, showing a maximum adsorption capacity of  $125 \text{ mg g}^{-1}$  (Figure 1.14) [384]. Although vermiculite shows also certain ability to adsorb cadmium and other heavy metal ions, in this case the adsorption mechanism is also due to the complexation of cadmium ions by the chitosan chains. The clay layers also contribute to enhance the mechanical stability of the foam in the aqueous medium, facilitating its easy recovery from solution after the adsorption step. Similarly, bionanocomposites based on sepiolite and the polysaccharides chitosan, alginate, and starch, which showed good mechanical properties and

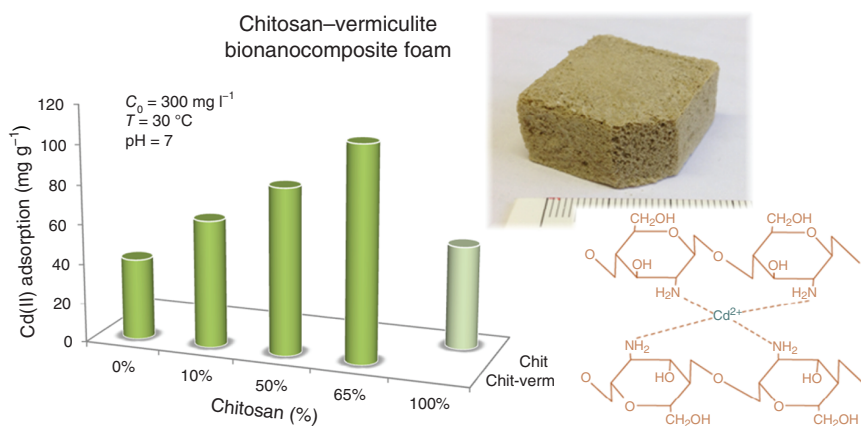


**Figure 1.14** Adsorption capacity of a chitosan–vermiculite bionanocomposite foam toward cadmium ions (II).

stability in water, were applied in the removal of copper and lead ions [385]. The best results in the removal of lead were obtained for alginate-based systems, while the chitosan-based material was the best adsorbent in the removal of copper ions. The recently discovered polysaccharide sacran is also used in environmental remediation. This anionic megamolecule extracted from the cyanobacterium *Aphanothece sacrum* was assembled to sepiolite, and those bionanocomposites with a sepiolite content around 27% showed an enhanced and selective retention of neodymium ions [386].

Other environmental applications of organoclays and nanocomposites are related to the treatment of wastewater by coagulation–flocculation processes. For instance, the brine wastewater from pickle industry, with low pH and high content in salt and organic matter, can be successfully pretreated with clays and berberine-based organoclays to remove the suspended solids and reduce the turbidity [90]. Some examples illustrating the use of bionanocomposites for this purpose are related to the application of highly charged nanocomposites based on commercial polymers as poly-DADMAC or biopolymers as chitosan combined with either fibrous clays like sepiolite or platelike clays like MMT for clarification of winery or olive mill wastewater [56] or to remove blooms of harmful cyanobacteria, which was successfully carried out in a field enclosure of Lake Taihu [387].

Other modifiers of biological origin such as PC are suitable to prepare eco-friendly alternatives to conventional alkylammonium-based organoclays. Thus, biohybrids based on PC and sepiolite or MMT were successfully applied in the uptake of aflatoxin B, a mycotoxin considered to be among the most carcinogenic substances known [30]. Another biohybrid material based on modification of the vermiculite surface with a microbial biofilm of *Pseudomonas putida* was applied as a barrier at the interface between water and sediments in order to prevent the adsorption of heavy metal ions on the sediments [388]. The biohybrid barrier showed the best results in the removal of zinc, while natural vermiculite offered the best behavior in the removal of copper ions.

An important issue in the study of organoclays in environmental remediation concerns the regeneration of the pollutant-loaded sorbents. In some cases the organoclay or nanocomposite can be used several times to interact with the polluted effluent before its activity is exhausted [56, 59, 389]. However, even in those cases in the end, a polluted sludge remains and requires additional considerations. Recent studies have addressed the regeneration process by diverse methods, including chemical extraction/desorption, thermal desorption, photoassisted oxidation, supercritical extraction, or biological degradation [390]. Extraction with suitable solvents is a common method to remove the pollutant from the adsorbent, allowing its use in a new adsorption cycle. For instance, cationic starch–MMT bionanocomposites used in the removal of hexavalent chromium were submitted to regeneration by extraction with solvents like sodium bicarbonate [391]. Such regeneration was effective and allowed the use of the hybrid material in several consecutive adsorption/regeneration cycles.

In contrast to alkylammonium-based organoclays, which show a low regeneration capability due to the low thermal stability of these organocations [116, 392], other organoclays involving dyes [393] or phosphonium species [394] can be submitted to thermal desorption of the pollutants as they show considerably higher thermal stability, with thermal decomposition starting at 400 °C in the case of tetraphenylphosphonium (TPP)-modified clays. This behavior allows preserving the hybrid material while the pollutant is thermally destroyed. Nevertheless, it is important to control the temperature for thermal degradation in order to preserve the adsorption capacity of the organoclay. This fact is well illustrated with a CV–organoclay used for removal of TCP, which showed similar adsorption capacities after heating to 120 or 200 °C, while the adsorption capability was completely lost at temperatures higher than 350 °C due to the transformation of CV.

Another method for regeneration of the organoclays is based on the biodegradation of the retained pollutant by microorganisms. An illustrative example is the rapid and effective (about 82% within 24 h) biodegradation of the organophosphorous pesticide fenamiphos adsorbed on cetyltrimethylammonium-based organoclay using the bacterium *Brevibacterium* [395], which takes place by extracellular enzymes released by bacteria that hydrolyze the sorbed pesticide. More recently, another work has reported the biodegradation by the bacterium *Arthrobacter* sp. 4H $\beta$  of *p*-nitrophenol (PNP) adsorbed onto a CV-modified MMT, in which the toxicity of CV to bacteria is minimized due to the dye–silicate interaction [396].

#### 1.5.1.4 Formulations of Pest Management Compounds

Pest management compounds are usually applied as part of formulations aiming to reduce the leaching of these compounds to minimize environmental problems, ensuring their physical and chemical stability and improving their efficiency. The use of CRFs was proposed as a way to avoid overdosing and keep a constant release of the diverse pesticides [397], and clay-based systems have been widely studied for this purpose [371]. Typically, organically modified clays showing hydrophobic interfaces are required for developing these formulations due to the organophilic nature of most pest management compounds. The

interactions established between organoclays and pesticides contribute to reduce their leaching, providing a constant release, and also to minimize decomposition of the entrapped pesticides by photodegradation or volatilization. For example, [109] showed that the efficacy of a PM herbicide formulation based on the binding of PM to MMT particles pre-adsorbed with the organocation DZ was considerably increased and an efficient herbicide control was obtained with 30% less active ingredient. An additional approach is the release of biological pesticides with high vapor pressure to avoid, for example, development of fungi or other pests in packaged agricultural. For example, evaporation of tea tree or mustard oil from organoclays has been shown to be 4–40 times slower than from free applications [64].

Most of the first clay-based hybrids developed for CRFs included toxic chemicals as modifiers, which limited their commercial application. Thus, the current trend envisages the use of less hazardous or eco-friendly modifiers, such as the agriculturally allowed cationic pesticides mepiquat or DZ [109], food-grade cationic compounds like berberine [60], surfactants of biological origin like PC, or a great variety of biopolymers. In PC-based formulations, the pest management compound was incorporated in the PC vesicles adsorbed on the external surface of MMT, as is the case of a formulation for slow release of the herbicide diuron [398]. In the last decades, polymers began to be evaluated for CRF preparation, as they can afford certain advantages such as increase of the water holding capacity of soil or their biodegradable character in the case of natural polymers [399]. Nanocomposites based on smectites and cationic polymers were used in CRFs as the charge reversal allowed the retention of anionic herbicides. This was the case of CRFs involving polydiallyldimethylammonium, which were used for the controlled release of imazapyr [400]. Similarly, proteins like gelatin are useful for this purpose due to the presence of positively charged protein side groups that can form complexes with anionic herbicides as in the case of gelatin–MMT materials used for the slow release of 4-chloro-2-methylphenoxyacetic acid (MCPA) [401]. The anionic herbicide imazamox was adsorbed on chitosan-based CRFs mainly by ionic interactions at pH values where chitosan is partially protonated, but also some hydrophobic interactions could be established due to the presence of uncharged amino groups [402]. An additional advantage of polymer–clay nanocomposites is the protective effect they can provide to the entrapped herbicide. An illustrative example is the use of starch–MMT composites in CRFs to reduce the UV-induced degradation and the volatilization of ametryne [403].

## 1.6 Concluding Remarks

The synthesis and uses of organic–inorganic interfaces based on both layered and fibrous clays have been discussed in this chapter. The surface properties of these clay minerals offer many opportunities to prepare organic–inorganic interfaces based on ionic, molecular, and polymeric species of diverse origin including biological components. The interaction mechanism in these interfaces is determined by the features of the silicate substrate and the involved organic species,



leading to diverse properties in the resulting hybrid materials. The main group among these materials is the so-called organoclays, mainly employed as compatible interfaces in the development of reinforced polymer nanocomposites. A novelty within this field is the increasing use of organoclays based on sepiolite and palygorskite fibrous clays as nanofiller of diverse types of polymers. In this case, modification of the clay is of critical importance in producing convenient organic–inorganic interfaces, as their highly hydrophilic external surface makes difficult their distribution within most of the polymeric matrices. It is worthy to mention also the relevance of clay modification with species of biological origin as could be certain amphiphilic molecules (e.g., PC) to produce more ecological organoclays, also called by some authors as bio-organoclays, and biocompatible interfaces of interest in biomedicine and other applications.

The analysis of hybrid nanostructures formed by the organic compounds and clay minerals is a key point to elucidate the exact composition as for amounts of constituents, spatial structure, chemical binding, physical properties, and so on. In order to do that, a series of analytical methods is used, most of them conventional and widely adopted in other disciplines, but some of them resulting from the ingenuity of the researchers in this inter- and multidisciplinary field. The most widely used methods have been reviewed in this chapter, and a short review on some less common analytical approaches has been also introduced. To that we must add the fact that ingenious material scientists will all the time seek for better methods that will be more accurate, less expensive and/or time/work consuming and elucidate in a more effective way the characterization, structure, and properties of the new hybrid material they engineered.

The organic–inorganic interface of organoclays, both based on layered and fibrous clays, are prone to associate and stabilize alkoxysilanes and other metal alkoxides that could be further hydrolyzed and polycondensated to produce diverse type of porous clay nanoarchitectures. When using layered clays, the nature of the hybrid interface and the methodology employed to produce the controlled hydrolysis and polycondensation of the alkoxide determine the generation of organized pillars separating the silicate layers, as in PCH, or the delamination of the silicate platelets within the polycondensated matrix, as in the so-called DPCH. In the case of organoclays based on fibrous clays, the characteristics of the organic modifier at the hybrid interfaces control the growth of polycondensated species at the external surface of fibrous clays, resulting in materials with diverse textural properties. Most of these porous nanoarchitectures are used as catalysts and/or sorbents, but other fields of applications may be related to their use as nanofiller in polymer–clay nanocomposites.

Other important applications of hybrid materials are related to the biomedical and environmental fields. In the first case, the possibility of developing biointerfaces by supporting biomimetic layers on clay minerals gives rise to biocompatible environments for immobilization of functional guest species, providing them with thermal and structural protection and preserving their bioactivity, which is of great interest in biocatalysis. The application of these biocompatible hybrid systems as carriers of drugs, DNA, or viral particles for controlled release, gene therapy, or vaccination purposes has been also

reviewed in this chapter, together with the application of hybrid systems processed as scaffolds, mainly those derived from bionanocomposite hydrogels, in regenerative medicine. Finally, clay–organic interfaces are of great interest in environmental protection due to the possibility of tuning the adsorption properties of clays by modification with molecular or polymeric organic species. The resulting organoclays and nanocomposite materials have found application in water purification and remediation of polluted areas, as well as carriers of pest management compounds in CRFs. The current trend is the development of less hazardous organoclay-based pesticide formulations by using eco-friendly modifiers like phospholipids or biopolymers, which can minimize environmental pollution resulting from conventional formulations.

## List of Abbreviations

2D	two-dimensional
3D	three-dimensional
5ASA	5-aminosalicylic acid
AEC	anion-exchange capacity
AFM	atomic force microscopy
APTMS	aminopropyltrimethoxysilane
ATR	attenuated total reflectance
BET	Brunauer–Emmett–Teller
CEC	cation-exchange capacity
CP	chlorpheniramine
CRF	controlled-release formulations
CTAB	cetyltrimethylammonium (or hexadecyltrimethylammonium) bromide
CV	crystal violet
DPCH	delaminated porous clay heterostructures
DDS	drug delivery systems
DOC	dissolved organic carbon
DS	diclofenac sodium
DSC	differential scanning calorimetry
DTA	differential thermal analysis
DTG	differential thermogravimetric analysis
DZ	difenzoquat
ECM	extracellular matrix
EGME	ethyl glycol methyl ether
ESEM	environmental scanning electron microscopy
FRET	Forster or fluorescence resonance energy transfer
FTIR	Fourier transform infrared spectroscopy
HA	hemagglutinin
HAP	hydroxyapatite
HDPy	hexadecylpyridinium

HDTMA	hexadecyltrimethylammonium
HPLC	high-performance liquid chromatography
HRTEM	high-resolution transmission electron microscopy
IR	infrared
LDH	layered double hydroxides
MCM	mobile composition of matter material
MCPA	4-chloro-2-methylphenoxyacetic acid
MTBE	methyl <i>tert</i> -butyl ether
MWCNTs	multi-walled carbon nanotubes
NMR	nuclear magnetic resonance
NP	nanoparticles
O	octahedral
ODTMA	octadecyltrimethylammonium
PAA	polyacrylic acid
PAAm	polyacrylamide
PAH	(poly)allylamine hydrochloride
PBAT	poly(butylene adipate- <i>co</i> -terephthalate)
PC	phosphatidylcholine
PCL	poly( $\epsilon$ -caprolactone)
PCH	porous clay heterostructures
PEG	poly(ethylene glycol)
PEO	poly(ethylene oxide)
PILC	pillared clays
PLA	poly(lactic acid)
PLGA	poly(lactic- <i>co</i> -glycolic acid)
PM	pendimethalin
PNP	<i>p</i> -nitrophenol
Poly-DADMAC	polydiallyldimethylammonium chloride
PP	polypropylene
PS	polystyrene
SBA	Santa Barbara Amorphous type material
SEM	scanning electron microscopy
SSA	specific surface area
T	tetrahedral
TCP	trichlorophenol
TEM	transmission electron microscopy
TMA	tetramethylammonium
TMOS	tetramethyl orthosilicate
TEOS	tetraethyl orthosilicate
TGA	thermal gravimetric analysis
TPP	tetraphenylphosphonium chloride
VOCs	volatile organic compounds
v.p.	vapor pressure
WAXD	wide-angle X-ray diffraction
XRD	X-ray diffraction
XRF	X-ray fluorescence

## References

- 1 Ruiz-Hitzky, E., Aranda, P., Darder, M., and Fernandes, F.M. (2013) in *Handbook of Clay Science. Part A: Fundamentals*, 2nd edn (eds F. Bergaya and G. Lagaly), Elsevier, Amsterdam & Oxford, pp. 721–741.
- 2 Kutilek, M. and Nielsen, D.R. (2015) *Soil: The Skin of the Planet Earth*, Springer.
- 3 Ponnampuruma, C., Shimoyama, A., and Friebele, E. (1982) Clay and the origin of life. *Origins of Life*, **12**, 9–40.
- 4 Martin, R.T., Bailey, S.W., Eberl, D.D., Fanning, D.S., Guggenheim, S., Kodama, H., Pevear, D.R., Środoń, J., and Wicks, F.J. (1991) Report of the clay minerals society nomenclature committee: revised classification of clay materials. *Clays Clay Miner.*, **39**, 333–335.
- 5 Lvov, Y.M., Shchukin, D.G., Möhwald, H., and Price, R.R. (2008) Halloysite clay nanotubes for controlled release of protective agents. *ACS Nano*, **2**, 814–820.
- 6 Guggenheim, S. and Eggleton, R.A. (1988) in *Hydrous Phyllosilicates (Exclusive of the Micas)* (ed. S.W. Bailey), Mineralogical Society of America, Washington, DC, pp. 675–725.
- 7 Brauner, K. and Pressinger, A. (1956) Struktur und Entstehung des Sepioliths. *Contrib. Mineral. Petrol.*, **6**, 120–140.
- 8 Ruiz-Hitzky, E. (2001) Molecular access to intracrystalline tunnels of sepiolite. *J. Mater. Chem.*, **11**, 86–91.
- 9 Ahlrichs, J.L., Serna, C.J., and Serratos, J.M. (1975) Structural hydrolysis in sepiolites. *Clays Clay Miner.*, **23**, 119–124.
- 10 Gieseking, J.E. (1939) The mechanism of cation exchange in the montmorillonite-beidellite-nontronite type of clay minerals. *Soil Sci.*, **47**, 1–13.
- 11 Hendricks, S.B. (1941) Base exchange of the clay mineral montmorillonite for organic cations and its dependence upon adsorption due to van der Waals forces. *J. Phys. Chem.*, **45**, 65–81.
- 12 Ruiz-Hitzky, E., Aranda, P., and Serratos, J.M. (2004) in *Handbook of Layered Materials* (eds S.M. Auerbach, K.A. Carrado, and P.K. Dutta), Marcel Dekker, pp. 91–154.
- 13 MacEwan, D.M.C. (1948) Complexes of clays with organic compounds. I. Complex formation between montmorillonite and halloysite and certain organic liquids. *Trans. Faraday Soc.*, **44**, 349–367.
- 14 Ruiz-Hitzky, E., Aranda, P., and Darder, M. (2015) in *Tailored Organic–Inorganic Materials* (eds E. Brunet, J.L. Colón, and A. Clearfield), John Wiley & Sons, Inc., pp. 245–298.
- 15 Serratos, J.M. (1965) Use of infra-red spectroscopy to determine the orientation of pyridine sorbed on montmorillonite. *Nature*, **208**, 679–681.
- 16 Serratos, J.M. (1966) Infrared analysis of the orientation of pyridine molecules in clay complexes. *Clays Clay Miner.*, **14**, 385–391.
- 17 Dedzo, G.K., Ngnie, G., and Detellier, C. (2016) PdNP decoration of halloysite lumen via selective grafting of ionic liquid onto the aluminol surfaces and catalytic application. *ACS Appl. Mater. Interfaces*, **8**, 4862–4869.

- 18 Kuang, W., Facey, G.A., Detellier, C., Casal, B., Serratosa, J.M., and Ruiz-Hitzky, E. (2003) Nanostructured hybrid materials formed by sequestration of pyridine molecules in the tunnels of sepiolite. *Chem. Mater.*, **15**, 4956–4967.
- 19 Ruiz-Hitzky, E. and Fripiat, J.J. (1976) Organomineral derivatives obtained by reacting organochlorosilanes with surface of silicates in organic solvents. *Clays Clay Miner.*, **24**, 25–30.
- 20 Fernandez Hernandez, M.N. and Ruiz Hitzky, E. (1979) Interaccion de isocianatos con sepiolita. *Clay Miner.*, **14**, 295–305.
- 21 Van Meerbeek, A. and Ruiz-Hitzky, E. (1979) Mechanism of the grafting of organosilanes on mineral surfaces. *Colloid. Polym. Sci.*, **257**, 178–181.
- 22 Aznar, A.J. and Ruiz-Hitzky, E. (1988) Arylsulphonic resins based on organic/inorganic macro-molecular systems. *Mol. Cryst. Liq. Cryst. Inc. Nonlinear Opt.*, **161**, 459–469.
- 23 Gutierrez, E., Aznar, A.J., and Ruiz-Hitzky, E. (1991) in *Heterogeneous Catalysis and Fine Chemicals II* (eds M. Guisnet, J. Barrault, C. Bouchoule, D. Duprez, G. Perot, R. Maurel, and C. Montassier), Elsevier, Amsterdam, pp. 539–547.
- 24 Alvarez, A., Santaren, J., Perez-Castells, R., Casal, B., Ruiz-Hitzky, E., Levitz, P., and Fripiat, J.J. (1985) Surfactant adsorption and rheological behavior of surface modified sepiolite, in *Proceedings of the International Clay Conference, Denver* (eds L.G. Schultz, H. van Olphen, and F.A. Mumpton), The Clay Minerals Society, Denver, Bloomington, IN, pp. 370–374.
- 25 Ruiz-Hitzky, E., Aranda, P., Alvarez, A., Santarén, J., and Esteban-Cubillo, A. (2011) in *Developments in Palygorskite-Sepiolite Research. A New Outlook on these Nanomaterials* (eds E. Galán and A. Singer), Elsevier B.V., Oxford, UK, pp. 393–452.
- 26 Ruiz-Hitzky, E. and Casal, B. (1978) Crown ether intercalations with phyllosilicates. *Nature*, **276**, 596–597.
- 27 Ruiz-Hitzky, E., Casal, B., Aranda, P., and Galván, J.C. (2001) Inorganic–organic nanocomposite materials based on macrocyclic compounds. *Rev. Inorg. Chem.*, **21**, 125.
- 28 Doner, H.E. and Mortland, M.M. (1969) Benzene complexes with copper(II) montmorillonite. *Science*, **166**, 1406–1407.
- 29 Ruiz-Hitzky, E., Aranda, P., Darder, M., and Rytwo, G. (2010) Hybrid materials based on clays for environmental and biomedical applications. *J. Mater. Chem.*, **20**, 9306–9321.
- 30 Wicklein, B., Darder, M., Aranda, P., and Ruiz-Hitzky, E. (2010) Bio-organoclays based on phospholipids as immobilization hosts for biological species. *Langmuir*, **26**, 5217–5225.
- 31 Wicklein, B., Darder, M., Aranda, P., and Ruiz-Hitzky, E. (2008) Organically modified clays for uptake of mycotoxins. *Macla*, **9**, 257–258.
- 32 Fukushima, Y. and Inagaki, S. (1987) Synthesis of an intercalated compound of montmorillonite and 6-polyamide. *J. Inclusion Phenom.*, **5**, 473–482.
- 33 Pinnavaia, T.J. and Beall, G.W. (Eds.) (2000) *Polymer–Clay Nanocomposites*, John Wiley & Sons, New York.
- 34 Alexandre, M. and Dubois, P. (2000) Polymer-layered silicate nanocomposites: preparation, properties and uses of a new class of materials. *Mater. Sci. Eng., R*, **28**, 1–63.

- 35 Sinha Ray, S. and Okamoto, M. (2003) Polymer/layered silicate nanocomposites: a review from preparation to processing. *Prog. Polym. Sci.*, **28**, 1539–1641.
- 36 Ruiz-Hitzky, E. and Van Meerbeek, A. (2006) in *Handbook of Clay Science. Development in Clay Science* (eds F. Bergaya, B.K.G. Theng, and G. Lagaly), Elsevier, Amsterdam, pp. 583–621.
- 37 Bergaya, F. and Lagaly, G. (2007) in *Clay-Based Polymer Nanocomposites (CPN). CMS Workshop Lecture*, vol. 15 (eds K. Carrado and F. Bergaya), The Clay Minerals Society, Chantilly, pp. 61–97.
- 38 Kiliaris, P. and Papaspyrides, C.D. (2010) Polymer/layered silicate (clay) nanocomposites: an overview of flame retardancy. *Prog. Polym. Sci.*, **35**, 902–958.
- 39 Bergaya, F., Detellier, C., Lambert, J.-F., and Lagaly, G. (2013) in *Handbook of Clay Science* (eds F. Bergaya and G. Lagaly), Elsevier Science Ltd, Oxford, pp. 655–677.
- 40 Ruiz-Hitzky, E. and Fernandes, F.M. (2013) Progress in bionanocomposites: from green plastics to biomedical applications. *Prog. Polym. Sci.*, **38**, 1391.
- 41 Ruiz-Hitzky, E. and Aranda, P. (1990) Polymer-salt intercalation complexes in layer silicates. *Adv. Mater.*, **2**, 545–547.
- 42 Aranda, P. and Ruiz-Hitzky, E. (1992) Poly(ethylene oxide)-silicate intercalation materials. *Chem. Mater.*, **4**, 1395–1403.
- 43 Vaia, R.A., Ishii, H., and Giannelis, E.P. (1993) Synthesis and properties of two-dimensional nanostructures by direct intercalation of polymer melts in layered silicates. *Chem. Mater.*, **5**, 1694–1696.
- 44 Ruiz-Hitzky, E., Darder, M., Fernandes, F.M., Wicklein, B., Alcántara, A.C.S., and Aranda, P. (2013) Fibrous clays based bionanocomposites. *Prog. Polym. Sci.*, **38**, 1392–1414.
- 45 Ruiz-Hitzky, E., Darder, M., Alcántara, A.C.S., Wicklein, B., and Aranda, P. (2015) Recent advances on fibrous clay-based nanocomposites, in *Organic–Inorganic Hybrid Nanomaterials* (eds S. Kalia and Y. Haldorai), Springer International Publishing, Cham, pp. 39–86.
- 46 Ruiz-Hitzky, E., Darder, M., Wicklein, B., Alcántara, A.C.S., and Aranda, P. (2017) in *Functional Polymer Composites with Nanoclays* (eds Y. Lvov, B. Guo, and R. Fakhruddin), Royal Society of Chemistry, Cambridge, UK, pp. 1–53.
- 47 Shafiq, M., Yasin, T., and Saeed, S. (2012) Synthesis and characterization of linear low-density polyethylene/sepiolite nanocomposites. *J. Appl. Polym. Sci.*, **123**, 1718–1723.
- 48 Wang, R., Li, Z., Wang, Y., Liu, W., Deng, L., Jiao, W., and Yang, F. (2013) Effects of modified attapulgite on the properties of attapulgite/epoxy nanocomposites. *Polym. Compos.*, **34**, 22–31.
- 49 Zhu, L., Liu, P., and Wang, A. (2014) High clay-content attapulgite/poly(acrylic acid) nanocomposite hydrogel via surface-initiated redox radical polymerization with modified attapulgite nanorods as initiator and cross-linker. *Ind. Eng. Chem. Res.*, **53**, 2067–2071.
- 50 Ruiz-Hitzky, E., Aranda, P., and Darder, M. (2008) *Kirk-Othmer Encyclopedia of Chemical Technology*, John Wiley & Sons, Inc, Hoboken, NJ, pp. 1–28.



- 51 Darder, M., Colilla, M., and Ruiz-Hitzky, E. (2003) Clay-based biopolymer nanocomposites based on chitosan intercalated in montmorillonite. *Chem. Mater.*, **15**, 3774–3780.
- 52 Darder, M., Lopez-Blanco, M., Aranda, P., Aznar, A.J., Bravo, J., and Ruiz-Hitzky, E. (2006) Microfibrous chitosan-sepiolite nanocomposites. *Chem. Mater.*, **18**, 1602–1610.
- 53 Usuki, A., Kawasumi, M., Kojima, Y., Okada, A., Kurauchi, T., and Kamigaito, O. (1993) Swelling behavior of montmorillonite cation exchanged for  $\omega$ -amino acids by  $\epsilon$ -caprolactam. *J. Mater. Res.*, **8**, 1174–1178.
- 54 Rytwo, G. (2017) Hybrid clay-polymer nanocomposites for the clarification of water and effluents, *Recent Patents on Nanotechnology*, **11** (1), <http://dx.doi.org/10.2174/1872210511666170125125928>
- 55 Rytwo, G. (2012) The use of clay-polymer nanocomposites in wastewater pretreatment. *Scientific World J.*, **2012**, 1–7.
- 56 Rytwo, G., Lavi, R., Rytwo, Y., Monchase, H., Dultz, S., and König, T.N. (2013) Clarification of olive mill and winery wastewater by means of clay-polymer nanocomposites. *Sci. Total Environ.*, **442**, 134–142.
- 57 Bauer, C., Jacques, P., and Kalt, A. (1999) Investigation of the interaction between a sulfonated azo dye (AO7) and a  $\text{TiO}_2$  surface. *Chem. Phys. Lett.*, **307**, 397–406.
- 58 Borisover, M., Graber, E.R., Bercovich, F., and Gerstl, Z. (2001) Suitability of dye-clay complexes for removal of non-ionic organic compounds from aqueous solutions. *Chemosphere*, **44**, 1033–1040.
- 59 Rytwo, G., Kohavi, Y., Botnick, I., and Gonen, Y. (2007) Use of CV- and TPP-montmorillonite for the removal of priority pollutants from water. *Appl. Clay Sci.*, **36**, 182–190.
- 60 Rytwo, G., Gonen, Y., and Afuta, S. (2008) Preparation of Berberine-montmorillonite-metolachlor formulations from hydrophobic/hydrophilic mixtures. *Appl. Clay Sci.*, **41**, 47–60.
- 61 Tha-in, S., Dau, H.A., and Dumri, K. (2013) The enhanced carbamate adsorption of modified bentonite with coscinium fenestratum. *Int. J. Environ. Sci. Dev.*, **4**, 415–418.
- 62 Mishael, Y.G., Undabeytia, T., Rabionovitz, O., Rubin, B., and Nir, S. (2003) Sulfosulfuron incorporated in micelles adsorbed on montmorillonite for slow release formulations. *J. Agric. Food. Chem.*, **51**, 2253–2259.
- 63 Mishael, Y.G., Undabeytia, T., Rytwo, G., Papahadjopoulos-Sternberg, B., Rubin, B., and Nir, S. (2002) Sulfometuron incorporation in cationic micelles adsorbed on montmorillonite. *J. Agric. Food. Chem.*, **50**, 2856–2863.
- 64 Rytwo, G., Zakai, R., and Wicklein, B. (2015) The use of ATR-FTIR spectroscopy for quantification of adsorbed compounds. *J. Spectro.*, **2015**, 8.
- 65 Rytwo, G., Gonen, Y., and Huterer-Shveky, R. (2009) Evidence of degradation of triarylmethine dyes on Texas vermiculite. *Clays Clay Miner.*, **57**, 555–565.
- 66 Cohen, E., Joseph, T., Lapides, I., and Yariv, S. (2005) The adsorption of berberine by montmorillonite and thermo-XRD analysis of the organo-clay complex. *Clay Miner.*, **40**, 223–232.

- 67 Rytwo, G., Varman, H., Bluvshstein, N., König, T.N., Mendelovits, A., and Sandler, A. (2011) Adsorption of berberine on commercial minerals. *Appl. Clay Sci.*, **51**, 43–50.
- 68 Battu, S.K., Repka, M.A., Maddineni, S., Chittiboyina, A.G., Avery, M.A., and Majumdar, S. (2010) Physicochemical characterization of berberine chloride: a perspective in the development of a solution dosage form for oral delivery. *AAPS PharmSciTech*, **11**, 1466–1475.
- 69 Margalit, S. (2015) Examination a combined adsorption model using adsorption experiments with pharmaceutical on clay and organo-clay M.Sc. Thesis, Tel Hai College, Hebrew.
- 70 Aznar, A.J., Casal, B., Ruiz-Hitzky, E., Lopez-Arbeloa, I., Lopez-Arbeloa, F., Santaren, J., and Alvarez, A. (1992) Adsorption of methylene blue on sepiolite gels: spectroscopic and rheological studies. *Clay Miner.*, **27**, 101–108.
- 71 Ganigar, R., Rytwo, G., Gonen, Y., Radian, A., and Mishael, Y.G. (2010) Polymer-clay nanocomposites for the removal of trichlorophenol and trinitrophenol from water. *Appl. Clay Sci.*, **49**, 311–316.
- 72 Bezrodna, T.V., Klishevich, G.V., Melnyk, V.I., Nesprava, V.V., Puchkovska, G.A., and Chashechnikova, I.T. (2011) Photoluminescence of montmorillonite clay minerals modified by cetyltrimethylammonium bromide. *J. Appl. Spectrosc.*, **77**, 784–789.
- 73 Vaia, R.A., Jandt, K.D., Kramer, E.J., and Giannelis, E.P. (1996) Microstructural evolution of melt intercalated polymer – organically modified layered silicates nanocomposites. *Chem. Mater.*, **8**, 2628–2635.
- 74 Sanz, J. and Serratos, J.M. (2002) in *NMR spectroscopy Organo-, organo-clay complexes* (eds S. Yariv and S. Cross), Marcel Dekker Inc., New York, pp. 223–272.
- 75 Simpson, A.J., McNally, D.J., and Simpson, M.J. (2011) NMR spectroscopy in environmental research: from molecular interactions to global processes. *Prog. Nucl. Magn. Reson. Spectrosc.*, **58**, 97–175.
- 76 Borsacchi, S., Sudhakaran, U.P., Geppi, M., Ricci, L., Liuzzo, V., and Ruggeri, G. (2013) Synthesis, characterization, and solid-state NMR investigation of organically-modified bentonites and their composites with LDPE. *Langmuir*, **29** (29), 9164–9172.
- 77 Bryar, T.R. and Knight, R.J. (2008) NMR relaxation measurements to quantify immiscible organic contaminants in sediments. *Water Resour. Res.*, **44**, W02401, doi:10.1029/2006WR005635.
- 78 Grandjean, J. (2006) Solid-state NMR study of modified clays and polymer/clay nanocomposites. *Clay Miner.*, **41**, 567–586.
- 79 Coates, J. (2000) in *Interpretation of Infrared Spectra, a Practical Approach* (ed. R.A. Meyers), John Wiley & Sons Ltd, Chichester, UK, pp. 10815–10837.
- 80 Madejová, J. (2003) FTIR techniques in clay mineral studies. *Vib. Spectro.*, **31**, 1–10.
- 81 Madejová, J. and Komadel, P. (2001) Baseline studies of the clay minerals society source clays: infrared methods. *Clays Clay Miner.*, **49**, 410–432.

- 82 Bertaux, J., Frohlich, F., and Ildefonse, P. (1998) Multicomponent analysis of FTIR spectra: quantification of amorphous and crystallized mineral phases in synthetic and natural sediments. *J. Sediment. Res.*, **68**, 440–447.
- 83 Kaufhold, S., Hein, M., Dohrmann, R., and Ufer, K. (2012) Quantification of the mineralogical composition of clays using FTIR spectroscopy. *Vib. Spectrosc.*, **59**, 29–39.
- 84 Clarke, C.E., Aguilar-Carrillo, J., and Roychoudhury, A.N. (2011) Quantification of drying induced acidity at the mineral–water interface using ATR-FTIR spectroscopy. *Geochim. Cosmochim. Acta*, **75**, 4846–4856.
- 85 Dowding, C.E., Borda, M.J., Fey, M.V., and Sparks, D.L. (2005) A new method for gaining insight into the chemistry of drying mineral surfaces using ATR-FTIR. *J. Colloid Interface Sci.*, **292**, 148–151.
- 86 Boyd, S.A., Sheng, G., Teppen, B.J., and Johnston, C.T. (2001) Mechanisms for the adsorption of substituted nitrobenzenes by smectite clays. *Environ. Sci. Technol.*, **35**, 4227–4234.
- 87 Rytwo, G., Nir, S., and Margulies, L. (1995) Interactions of monovalent organic cations with montmorillonite: adsorption studies and model calculations. *Soil Sci. Soc. Am. J.*, **59**, 554–564.
- 88 Gutman, R. and Rytwo, G. (2015) Acicular clays and bio-composites based thereon for use in treatment of metabolic syndrome and related disorders, US Patent 62/237593.
- 89 Rytwo, G., Nir, S., Margulies, L., Casal, B., Merino, J., Ruiz-Hitzky, E., and Serratos, J.M. (1998) Adsorption of monovalent organic cations on sepiolite; experimental results and model calculations. *Clays Clay Miner.*, **46**, 340–348.
- 90 König, T.N., Shulami, S., and Rytwo, G. (2012) Brine wastewater pretreatment using clay minerals and organoclays as flocculants. *Appl. Clay Sci.*, **67–68**, 119–124.
- 91 Rytwo, G., Tropp, D., and Serban, C. (2002) Adsorption of diquat, paraquat and methyl green on sepiolite: experimental results and model calculations. *Appl. Clay Sci.*, **20**, 273–282.
- 92 Szabó, T., Wang, J., Volodin, A., van Haesendonck, C., Dekany, I., and Schoonheydt, R.A. (2009) AFM study of smectites in hybrid langmuir–blodgett films: saponite, wyoming bentonite, hectorite, and laponite. *Clays Clay Miner.*, **57**, 706–714.
- 93 Cadene, A., Durand-Vidal, S., Turq, P., Brendle, J., Dekany, I., and Schoonheydt, R.A. (2005) Study of individual Na-montmorillonite particles size, morphology, and apparent charge. *J. Colloid Interface Sci.*, **285**, 719–730.
- 94 Chua, Y.C., Lu, X., and Wan, T. (2006) Polymorphism behavior of poly(ethylene naphthalate)/clay nanocomposites. *J. Polym. Sci., Part B: Polym. Phys.*, **44**, 1040–1049.
- 95 Malwitz, M.M., Dundigalla, A., Ferreira, V., Butler, P.D., Henk, M.C., and Schmidt, G. (2004) Layered structures of shear-oriented and multilayered PEO/silicate nanocomposite films. *Phys. Chem. Chem. Phys.*, **6**, 2977.

- 96 Ratna, D., Divekar, S., Samui, A.B., Chakraborty, B.C., and Banthia, A.K. (2006) Poly(ethylene oxide)/clay nanocomposite: thermomechanical properties and morphology. *Polymer*, **47**, 4068–4074.
- 97 Vijayan, P.P., Puglia, D., Vijayan, P.P., Kenny, J.M., and Thomas, S. (2016) The role of clay modifier on cure characteristics and properties of epoxy/clay/carboxyl-terminated poly(butadiene-co-acrylonitrile) (CTBN) hybrid. *Mater. Technol.*, **32**, 1–7.
- 98 Rytwo, G. (2017) Method for Pretreatment of Wastewater and Recreational Water with Nanocomposites, US Patent 9,546,102, <https://www.google.com/patents/US9546102>
- 99 Manias, E., Polizos, G., Nakajima, H., and Heidecker, M.J. (2007) in *Fundamentals of Polymer Nanocomposite Technology* (eds A.B. Morgan and C.A. Wilkie), John Wiley & Sons, Ltd., pp. 31–66.
- 100 Coiai, S., Passaglia, E., Pucci, A., and Ruggeri, G. (2015) Nanocomposites based on thermoplastic polymers and functional nanofiller for sensor applications. *Materials*, **8**, 3377–3427.
- 101 Klocek, J., Kolanek, K., and Schmeißer, D. (2012) Spectroscopic and atomic force microscopy investigations of hybrid materials composed of fullerenes and 3-aminopropyltrimethoxysilane. *J. Phys. Chem. Solids*, **73**, 699–706.
- 102 John Innes Centre (2012) Microscopy.
- 103 Yaron-Marcovich, D., Chen, Y., Nir, S., and Prost, R. (2005) High resolution electron microscopy structural studies of organo-clay nanocomposites. *Environ. Sci. Technol.*, **39**, 1231–1238.
- 104 Tazaki, K., Kimura, S., Yoshimura, T., Akai, J., and Fyfe, W.S. (1989) Clay–organic complexes as a cementing agent in the arahama sand dune, Japan. *Clays Clay Miner.*, **37**, 219–226.
- 105 Chung, Y.-L., Ansari, S., Estevez, L., Hayrapetyan, S., Giannelis, E.P., and Lai, H.-M. (2010) Preparation and properties of biodegradable starch–clay nanocomposites. *Carbohydr. Polym.*, **79**, 391–396.
- 106 Herrera, P., Burghardt, R.C., and Phillips, T.D. (2000) Adsorption of *Salmonella enteritidis* by cetylpyridinium-exchanged montmorillonite clays. *Veterinary Microbiol.*, **74**, 259–272.
- 107 Rytwo, G., Mendelovits, A., Eliyahu, D., Pitcovski, J., and Aizenshtein, E. (2010) Adsorption of two vaccine-related proteins to montmorillonite and organo-montmorillonite. *Appl. Clay Sci.*, **50**, 569–575.
- 108 Thostenson, E.T., Li, C., and Chou, T.W. (2005) Nanocomposites in context. *Compos. Sci. Technol.*, **65**, 491–516.
- 109 Rytwo, G., Gonen, Y., Afuta, S., and Dultz, S. (2005) Interactions of pendimethalin with organo-montmorillonite complexes. *Appl. Clay Sci.*, **28**, 67–77.
- 110 Brindley, G.W. (1955) Identification of clays mineralogy by X-ray diffraction analysis. 1st National Conference on Clays and Clay Technology, Bull. 169, pp. 319–328.
- 111 Dutrow, B.L. and Clark, M.C. (2016) X-ray powder diffraction (XRD), [https://serc.carleton.edu/research\\_education/geochemsheets/techniques/XRD.html](https://serc.carleton.edu/research_education/geochemsheets/techniques/XRD.html). Accessed on July 6th 2017.

- 112 Chipera, S.J. and Bish, D.L. (2001) Baseline studies of the clay minerals society source clays: powder X-ray diffraction analyses. *Clays Clay Miner.*, **49**, 398–409.
- 113 Darder, M., Aranda, P., Ruiz, A.I., Fernandes, F.M., and Ruiz-Hitzky, E. (2008) Design and preparation of bionanocomposites based on layered solids with functional and structural properties. *J. Mater. Sci. Technol.*, **24**, 1100–1110.
- 114 LeBaron, P.C., Wang, Z., and Pinnavaia, T.J. (1999) Polymer-layered silicate nanocomposites: an overview. *Appl. Clay Sci.*, **15**, 11–29.
- 115 Srinivasan, R. (2011) Advances in application of natural clay and its composites in removal of biological, organic, and inorganic contaminants from drinking water. *Adv. Mater. Sci. Eng.*, **2011**, 1–7.
- 116 Beall, G.W. and Goss, M. (2004) Self-assembly of organic molecules on montmorillonite. *Appl. Clay Sci.*, **27**, 179–186.
- 117 Schampera, B. and Dultz, S. (2011) The effect of surface charge and wettability on H<sub>2</sub>O self diffusion in compacted clays. *Clays Clay Miner.*, **59**, 42–57.
- 118 Yariv, S., Müller-Vonmoos, M., Kahr, G., and Rub, A. (1989) Thermal analytic study of the adsorption of crystal violet by montmorillonite. *Thermochim. Acta*, **148**, 457–466.
- 119 Grim, R.E. and Rowland, R.A. (1942) Differential thermal analysis of clay minerals and other hydrous materials. Part 1 and Part 2. *Am. Mineral.*, **27**, 746–818.
- 120 Földvári, M. (2011) *Handbook of thermogravimetric system of minerals and its use in geological practice*, Occasional Papers of the Geological Institute of Hungary, vol. 213, Budapest.
- 121 Coats, A.W. and Redfern, J.P. (1963) Thermogravimetric analysis. A review. *Analyst*, **88**, 906.
- 122 Bhadeshia, H.K.D.H. (2016) An introduction to thermal analysis techniques.
- 123 Yariv, S., Lapidés, I., and Borisover, M. (2012) Thermal analysis of tetraethylammonium and benzyltrimethylammonium montmorillonites. *J. Therm. Anal. Calorim.*, **110**, 385–394.
- 124 Bujdák, J. (2015) Hybrid systems based on organic dyes and clay minerals: fundamentals and potential applications. *Clay Miner.*, **50**, 549–571.
- 125 Sauer, M., Hofkens, J., and Enderlein, J. (2011) Basic Principles of Fluorescence Spectroscopy. *Handbook of Fluorescence Spectroscopy and Imaging: From Single Molecules to Ensembles*, pp. 1–30. <https://doi.org/10.1002/9783527633500.ch1>
- 126 Bergmann, K. and O’Konski, C.T. (1963) A spectroscopic study of methylene blue monomer, dimer, and complexes with montmorillonite. *J. Phys. Chem.*, **67**, 2169–2177.
- 127 Bujdak, J. and Iyi, N. (2002) Visible spectroscopy of cationic dyes in dispersions with reduced-charge montmorillonites. *Clays Clay Miner.*, **50**, 446–454.
- 128 Cenens, J. and Schoonheydt, R.A. (1988) Visible spectroscopy of methylene blue on hectorite, laponite b, and barasym in aqueous suspension. *Clays Clay Miner.*, **36**, 214–224.

- 129 Samuels, M., Mor, O., and Rytwo, G. (2013) Metachromasy as an indicator of photostabilization of methylene blue adsorbed to clays and minerals. *J. Photochem. Photobiol., B*, **121**, 23–26.
- 130 Dobrogowska, C., Hepler, L.G., Ghosh, D.K., and Yariv, S. (1991) Metachromasy in clay mineral systems. *J. Therm. Anal. Calorim.*, **37**, 1347–1356.
- 131 Garfinkel-Shweky, D. and Yariv, S. (1997) The determination of surface basicity of the oxygen planes of expanding clay minerals by acridine orange. *J. Colloid Interface Sci.*, **188**, 168–175.
- 132 Yariv, S., Ghosh, D.K., and Hepler, L.G. (1991) Metachromasy in clay-mineral systems: adsorption of cationic dyes crystal violet and ethyl violet by kaolinite from aqueous and organic solutions. *J. Chem. Soc., Faraday Trans.*, **87**, 1201–1207.
- 133 Chiu, C.-W., Huang, T.-K., Wang, Y.-C., Alamani, B.G., and Lin, J.-J. (2014) Intercalation strategies in clay/polymer hybrids. *Prog. Polym. Sci.*, **39**, 443–485.
- 134 Binder, H., Kohlstrunk, B., Brenn, U., Schwieger, W., and Klose, G. (1998) Infrared dichroism measurements on the alkyl chain packing of an ionic detergent intercalated between silicate layers. *Colloid. Polym. Sci.*, **276**, 1098–1109.
- 135 Margulies, L. and Rozen, H. (1986) Adsorption of methyl green on montmorillonite. *J. Mol. Struct.*, **141**, 219–226.
- 136 Specht, C.H., Frimmel, F.H., Tipping, E., Tipping, E., Cooke, D., Vermeer, A.W.P., Riemsdijk, W.H.v., Koopal, L.K., Ballinger, T.H., Wong, J.C.S., Yates, J.T.J., Gong, W.Q., Parentich, A., Warren, L.J., Sperline, R.P., Song, Y., Degenhardt, J., McQuillan, A.J., Peak, D., Ford, R.G., Sparks, D.L., Kesselman-Truttmann, J.M., Hug, S.J., Gu, B., Schmitt, J., Chem, Z., Liang, L., McCarthy, J.F., Wershaw, R.L., Llaguno, E.C., Leenheer, J.A., Sperline, R.P., Song, Y., Martin, S.T., Kesselman, J.M., Park, D.S., Lewis, N.S., Hoffmann, M.R., Weissmahr, K., Haderlein, S.B., Schwarzenbach, R.P., Hany, R., Nüesch, R., Frost, R.L., Kristof, J., Mako, E., Klopogge, J.T., Frost, R.L., Kristof, J., Mako, E., Klopogge, J.T., Yost, E.C., Tejedor-Tejedor, M.I., Anderson, M.A., Tejedor-Tejedor, M.I., Yost, E.C., Anderson, M.A., Tejedor-Tejedor, M.I., Yost, E.C., Anderson, M.A., Biber, M.V., Stumm, W., Hug, S.J., Sulzberger, B., Frost, R.L., Johnston, C., Sposito, G., Birge, R.R., Tunesi, S., and Anderson, S.A. (2001) An in situ ATR-FTIR study on the adsorption of dicarboxylic acids onto kaolinite in aqueous suspensions dedicated to Professor F. Dörr on the occasion of his 80th birthday. *Phys. Chem. Chem. Phys.*, **3**, 5444–5449.
- 137 Arrondo, J.L., Muga, A., Castresana, J., and Goñi, F.M. (1993) Quantitative studies of the structure of proteins in solution by Fourier-transform infrared spectroscopy. *Prog. Biophys. Mol. Biol.*, **59**, 23–56.
- 138 Vedantham, G., Sparks, H.G., Sane, S.U., Tzannis, S., and Przybycien, T.M. (2000) A holistic approach for protein secondary structure estimation from infrared spectra in H<sub>2</sub>O solutions. *Anal. Biochem.*, **285**, 33–49.
- 139 Schmidt, M.P. and Martinez, C.E. (2016) Kinetic and conformational insights of BSA adsorption onto montmorillonite revealed using in-situ ATR-FTIR/2D-COS. *Langmuir*, **32**, 7719–7729.



- 140 Servagent-Noinville, S., Revault, M., Quiquampoix, H., and Baron, M.H. (2000) Conformational changes of bovine serum albumin induced by adsorption on different clay surfaces: FTIR analysis. *J. Colloid Interface Sci.*, **221**, 273–283.
- 141 Wang, Y. (2012) Processing, structure and properties of layered films and clay aerogel composites by 2012.
- 142 Gilman, J.W. (1999) Flammability and thermal stability studies of polymer layered-silicate (clay) nanocomposites. *Appl. Clay Sci.*, **15**, 31–49.
- 143 Gilman, J.W., Jackson, C.L., Morgan, B., Harris, R., Giannelis, E.P., Wuthenow, M., Hilton, D., and Phillips, S.H. (2000) Flammability properties of polymer – layered-silicate. *Chem. Mater.*, **12**, 1866–1873.
- 144 Zhao, Z., Gou, J., Bietto, S., Ibeh, C., and Hui, D. (2009) Fire retardancy of clay/carbon nanofiber hybrid sheet in fiber reinforced polymer composites. *Compos. Sci. Technol.*, **69**, 2081–2087.
- 145 Lebovka, N., Goncharuk, A., Bezrodna, T., Chashechnikova, I., and Nesprava, V. (2012) Microstructure and electrical conductivity of hybrid liquid crystalline composites including 5CB, carbon nanotubes and clay platelets. *Liq. Cryst.* **39**, 531–538. doi: 10.1080/02678292.2012.660201
- 146 Tachibana, H., Yamanuka, Y., Kumai, R., Asamitsu, A., Matsumoto, M., and Tokura, Y. (1999) Electrical conductivity of hybrid langmuir–blodgett films of transition metal dichalcogenide and amphiphilic cations. *Synth. Met.*, **102**, 1485–1486.
- 147 Suzuki, Y., Tenma, Y., Nishioka, Y., and Kawamata, J. (2012) Efficient nonlinear optical properties of dyes confined in interlayer nanospaces of clay minerals. *Chem. Asian J.*, **7**, 1170–1179.
- 148 Ogawa, M., Sohmiya, M., and Watase, Y. (2011) Stabilization of photosensitizing dyes by complexation with clay. *Chem. Commun.*, **47**, 8602–8604.
- 149 Iyi, N., Sasai, R., Fujita, T., Deguchi, T., Sota, T., López Arbeloa, F., and Kitamura, K. (2002) Orientation and aggregation of cationic laser dyes in a fluoromica: polarized spectrometry studies. *Appl. Clay Sci.*, **22**, 125–136.
- 150 Belušáková, S., Lang, K., and Bujdák, J. (2015) Hybrid systems based on layered silicate and organic dyes for cascade energy transfer. *J. Phys. Chem. C*, **119**, 21784–21794.
- 151 Delgado, A.V., González-Caballero, F., Hunter, R.J., Koopal, L.K., and Lyklema, J. (2007) Measurement and interpretation of electrokinetic phenomena. *J. Colloid Interface Sci.*, **309**, 194–224.
- 152 Rytwo, G., Chorsheed, L., Avidan, L., and Lavi, R. (2016) in CMS Workshop Lectures Series “Surface Modification of Clays and Nanocomposites”, vol. **20** (eds G. Beall and C.E. Powell), The Clay Minerals Society, Chantilly, VA, pp. 73–86.
- 153 Etzler, F.M. and Deanne, R. (1997) Particle size analysis: a comparison of various methods II. *Part. Part. Syst. Char.*, **14**, 278–282.
- 154 Reynolds, R.A., Stramski, D., Wright, V.M., and Woźniak, S.B. (2010) Measurements and characterization of particle size distributions in coastal waters. *J. Geophys. Res. C: Oceans*, **115**, C08024.

- 155 Horiba Scientific (2014) A Guidebook to Particle Size Analysis, [https://www.horiba.com/fileadmin/uploads/Scientific/Documents/PSA/PSA\\_Guidebook.pdf](https://www.horiba.com/fileadmin/uploads/Scientific/Documents/PSA/PSA_Guidebook.pdf). Accessed on July 6th, 2017.
- 156 Kaya, M., Onganer, Y., and Tabak, A. (2015) Preparation and characterization of “green” hybrid clay-dye nanopigments. *J. Phys. Chem. Solids*, **78**, 95–100.
- 157 Unuabonah, E.I., Günter, C., Weber, J., Lubahn, S., and Taubert, A. (2013) Hybrid clay: a new highly efficient adsorbent for water treatment. *ACS Sustainable Chem. Eng.*, **1**, 966–973.
- 158 Malvern Instruments Ltd (2013) Laser diffraction, <http://www.malvern.com/en/products/technology/laser-diffraction/>. Accessed on July 6th, 2017.
- 159 Etzler, F. and Sanderson, M. (1995) Particle size analysis: a comparative study of various methods. *Part. Part. Syst. Char.*, **12**, 217–224.
- 160 Eshel, G., Levy, G.J., Mingelgrin, U., and Singer, M.J. (2004) Critical evaluation of the use of laser diffraction for particle-size distribution analysis. *Soil Sci. Soc. Am. J.*, **68**, 736.
- 161 Detloff, T., Böddeker, M., and Lerche, D. (2011) Algorithms to determine the volume based particle size distributions from multi wavelength extinction profiles of separating dispersions. *Dispersion Lett.*, **2**, 28–31.
- 162 Petersen, L.W., Moldrup, P., Jacobsen, O.H., and Rolston, D.E. (1996) Relations between specific surface area and soil physical and chemical properties. *Soil Sci.*, **161**, 9–21.
- 163 Davis, P.J., Gallegos, D.P., and Smith, D.M. (1987) Rapid surface area determination via NMR spin-lattice relaxation measurements. *Powder Technol.*, **53**, 39–47.
- 164 Helmy, A.K., Ferreiro, E.A., and de Bussetti, S.G. (1999) Surface area evaluation of montmorillonite. *J. Colloid Interface Sci.*, **210**, 167–171.
- 165 Greene-Kelly, R. (1964) Montmorillonite surface areas specific surface area determinations preparation of mixed samples. *Clay Min. Bull.*, **5**, 392–400.
- 166 Macht, F., Eusterhues, K., Pronk, G.J., and Totsche, K.U. (2011) Specific surface area of clay minerals: comparison between atomic force microscopy measurements and bulk-gas (N<sub>2</sub>) and -liquid (EGME) adsorption methods. *Appl. Clay Sci.*, **53**, 20–26.
- 167 Cerato, A.B. and Lutenegeger, A.J. (2002) Determination of surface area of fine-grained soils by the ethylene glycol monoethyl ether (EGME) method. *Geotech. Test. J.*, **25**, 10035.
- 168 Santamarina, J.C., Klein, K.A., Wang, Y.H., and Prencke, E. (2002) Specific surface: determination and relevance. *Can. Geotech. J.*, **39**, 233–241.
- 169 Braschi, I., Gatti, G., Bisio, C., Berlier, G., Sacchetto, V., Cossi, M., and Marchese, L. (2012) The role of silanols in the interactions between methyl tert -butyl ether and high-silica faujasite: an infrared spectroscopy and computational model study. *J. Phys. Chem. C*, **116**, 6943–6952.
- 170 Sacchetto, V., Gatti, G., Paul, G., Braschi, I., Berlier, G., Cossi, M., Marchese, L., Bagatin, R., and Bisio, C. (2013) Physical chemistry chemical physics

- the interactions of methyl tert-butyl ether on high silica zeolites: a combined experimental and computational study. *Phys. Chem. Chem. Phys.*, **15**, 13275–13287.
- 171 Glaves, C.L., Davis, P.J., and Smith, D.M. (1988) Surface area determination via NMR: fluid and frequency effects. *Powder Technol.*, **54**, 261–269.
  - 172 Delville, A. and Letellier, M. (1995) Structure and dynamics of simple liquids in heterogeneous condition: an NMR study of the clay–water interface. *Langmuir*, **11**, 1361–1367.
  - 173 Fairhurst, D. and Prescott, S. (2011) The use of nuclear magnetic resonance as an analytical tool in the characterisation of dispersion behaviour. *Spectrosc. Eur.*, **23**, 13–16.
  - 174 Gangoli, V.S. and Barron, A. (2010) Measuring the specific surface area of nanoparticle suspensions using NMR, pp. 1-11, <http://cnx.org/contents/E7PbEjn9@1/Measuring-the-Specific-Surface>. Accessed on July 6th, 2017.
  - 175 Ariga, K. (ed.) (2012) *Manipulation of Nanoscale Materials: An Introduction to Nanoarchitectonics*, Royal Society of Chemistry, Wakefield.
  - 176 Gil, A., Korili, S., Trujillano, R. and M.A. Vicente (eds.) (2010) *Pillared Clays and Related Catalysts*, Springer, New York.
  - 177 Ruiz-Hitzky, E., Aranda, P., and Belver, C. (2012) in *Manipulation of Nanoscale Materials: an Introduction to Nanoarchitectonics* (ed. K. Ariga), Royal Society of Chemistry, Cambridge, pp. 87–111.
  - 178 Aranda, P., Belver, C., and Ruiz-Hitzky, E. (2014) in CMS Workshop Lectures Series, “Clays and Materials”, vol. **18** (ed. L.F. Drummy), The Clay Minerals Society, Chantilly, VA, pp. 21–40.
  - 179 Ruiz-Hitzky, E. and Aranda, P. (2014) Novel architectures in porous materials based on clays. *J. Sol-Gel Sci. Technol.*, **70**, 307–316.
  - 180 Aranda, P., Belver, C., and Ruiz-Hitzky, E. (2015) in *The Sol-Gel Handbook: Synthesis, Characterization and Applications*, 1st edn (eds D. Levy and M. Zayat), Weinheim, John Wiley & Sons, Inc., pp. 443–470.
  - 181 Aranda, P. and Ruiz-Hitzky, E. (2016) in CMS Workshop Lectures Series “Surface Modification of Clays and Nanocomposites”, Vol. **20** (eds G. Beall and C.E. Powell), The Clay Minerals Society, Chantilly, VA, pp. 87–100.
  - 182 Michot, L.J. and Pinnavaia, T.J. (1992) Improved synthesis of alumina-pillared montmorillonite by surfactant modification. *Chem. Mater.*, **4**, 1433–1437.
  - 183 Michot, L.J., Barres, O., Hegg, E.L., and Pinnavaia, T.J. (1993) Cointercalation of aluminum (Al<sup>III</sup>) polycations and nonionic surfactants in montmorillonite clay. *Langmuir*, **9**, 1794–1800.
  - 184 Montarges, E., Michot, L., Lhote, F., and Fabien, T. (1995) Intercalation of Al<sup>III</sup>-polyethyleneoxide complexes into montmorillonite clay. *Clays Clay Miner.*, **43**, 417–426.
  - 185 Suchithra, P.S., Vazhayal, L., Peer Mohamed, A., and Ananthakumar, S. (2012) Mesoporous organic–inorganic hybrid aerogels through ultrasonic assisted sol–gel intercalation of silica–PEG in bentonite for effective removal of dyes, volatile organic pollutants and petroleum products from aqueous solution. *Chem. Eng. J.*, **200–202**, 589–600.

- 186 Han, Y.-S. and Choy, J.-H. (1998) Modification of the interlayer pore structure of silica iron oxide sol pillared clay using organic templates. *J. Mater. Chem.*, **8**, 1459–1463.
- 187 Li, B., Liu, Z., Liu, J., Zhou, Z., Gao, X., Pang, X., and Sheng, H. (2011) Preparation, characterization and application in deep catalytic ODS of the mesoporous silica pillared clay incorporated with phosphotungstic acid. *J. Colloid Interface Sci.*, **362**, 450–456.
- 188 Yoda, S., Nagashima, Y., Endo, A., Miyata, T., Yanagishita, H., Otake, K., and Tsuchiya, T. (2005) Nanoscale architecture of metal-oxide-pillared clays using supercritical CO<sub>2</sub>. *Adv. Mater.*, **17**, 367–369.
- 189 Mao, H., Li, B., Li, X., Yue, L., Xu, J., Ding, B., Gao, X., and Zhou, Z. (2010) Facile synthesis and catalytic properties of titanium containing silica-pillared clay derivatives with ordered mesoporous structure through a novel intra-gallery templating method. *Microporous Mesoporous Mater.*, **130**, 314–321.
- 190 Yang, S., Liang, G., Gu, A., and Mao, H. (2013) Synthesis of TiO<sub>2</sub> pillared montmorillonite with ordered interlayer mesoporous structure and high photocatalytic activity by an intra-gallery templating method. *Mater. Res. Bull.*, **48**, 3948–3954.
- 191 Yoda, S., Sakurai, Y., Endo, A., Miyata, T., Otake, K., Yanagishita, H., and Tsuchiya, T. (2002) TiO<sub>2</sub>-montmorillonite composites via supercritical intercalation. *Chem. Commun.*, 1526–1527.
- 192 Hsu, R.-S., Chang, W.-H., and Lin, J.-J. (2010) Nanohybrids of magnetic iron-oxide particles in hydrophobic organoclays for oil recovery. *ACS Appl. Mater. Interfaces*, **2**, 1349–1354.
- 193 Xu, Z., Lv, F., Zhang, Y., and Fu, L. (2013) Synthesis and characterization of CPC modified magnetic MMT capable of using as anisotropic nanoparticles. *Chem. Eng. J.*, **215–216**, 755–762.
- 194 Skoutelas, A.P., Karakassides, M.A., and Petridis, D. (1999) Magnetically modified Al<sub>2</sub>O<sub>3</sub> pillared clays. *Chem. Mater.*, **11**, 2754–2759.
- 195 Ruiz-Hitzky, E., Aranda, P., and González-Alfaro, Y. (2010) Procedimiento de obtención de materiales con comportamiento superparamagético, Spanish Patent ES2365082.
- 196 González-Alfaro, Y., Aranda, P., Fernandes, F.M., Wicklein, B., Darder, M., and Ruiz-Hitzky, E. (2011) Multifunctional porous materials through ferrofluids. *Adv. Mater.*, **23**, 5224–5228.
- 197 Akkari, M., Aranda, P., Ben Rhaïem, H., Ben Haj Amara, A., and Ruiz-Hitzky, E. (2016) ZnO/clay nanoarchitectures: synthesis, characterization and evaluation as photocatalysts. *App. Clay Sci.*, **131**, 131–139.
- 198 Fatimah, I., Wang, S., and Wulandari, D. (2011) ZnO/montmorillonite for photocatalytic and photochemical degradation of methylene blue. *Appl. Clay Sci.*, **53**, 553–560.
- 199 Khumchoo, N., Khaorapapong, N., and Ogawa, M. (2015) Formation of zinc oxide particles in cetyltrimethylammonium-smectites. *Appl. Clay Sci.*, **105–106**, 236–242.

- 200 Wang, J., Merino, J., Aranda, P., Galvan, J.-C., and Ruiz-Hitzky, E. (1999) Reactive nanocomposites based on pillared clays. *J. Mater. Chem.*, **9**, 161–167.
- 201 Zhu, L., Tian, S., Zhu, J., and Shi, Y. (2007) Silylated pillared clay (SPILC): a novel bentonite-based inorgano–organo composite sorbent synthesized by integration of pillaring and silylation. *J. Colloid Interface Sci.*, **315**, 191–199.
- 202 Galarneau, A., Barodawalla, A., and Pinnavaia, T.J. (1995) Porous clay heterostructures formed by gallery-templated synthesis. *Nature*, **374**, 529–531.
- 203 Galarneau, A., Barodawalla, A., and Pinnavaia, T.J. (1997) Porous clay heterostructures (PCH) as acid catalysts. *Chem. Commun.*, 1661–1662.
- 204 Ahenach, J., Cool, P., and Vansant, E.F. (2000) Enhanced Bronsted acidity created upon Al-grafting of porous clay heterostructures [italic v (to differentiate from times ital nu)]ia aluminium acetylacetonate adsorption. *Phys. Chem. Chem. Phys.*, **2**, 5750–5755.
- 205 Pichowicz, M. and Mokaya, R. (2001) Porous clay heterostructures with enhanced acidity obtained from acid-activated clays. *Chem. Commun.*, (21), 2100–2101.
- 206 Benjelloun, M., Cool, P., Van Der Voort, P., and Vansant, E.F. (2002) Template extraction from porous clay heterostructures: influence on the porosity and the hydrothermal stability of the materials. *Phys. Chem. Chem. Phys.*, **4**, 2818–2823.
- 207 Maghear, A., Etienne, M., Tertiş, M., Săndulescu, R., and Walcarius, A. (2013) Clay-mesoporous silica composite films generated by electro-assisted self-assembly. *Electrochim. Acta*, **112**, 333–341.
- 208 Yuan, P., Yin, X., He, H., Yang, D., Wang, L., and Zhu, J. (2006) Investigation on the delaminated-pillared structure of TiO<sub>2</sub>-PILC synthesized by TiCl<sub>4</sub> hydrolysis method. *Microporous Mesoporous Mater.*, **93**, 240–247.
- 209 Polverejan, M., Pauly, T.R., and Pinnavaia, T.J. (2000) Acidic porous clay heterostructures (PCH): intragallery assembly of mesoporous silica in synthetic saponite clays. *Chem. Mater.*, **12**, 2698–2704.
- 210 Pálková, H., Madejová, J., Zimowska, M., Bielańska, E., Olejniczak, Z., Lityńska-Dobrzyńska, L., and Serwicka, E.M. (2010) Laponite-derived porous clay heterostructures: I. Synthesis and physicochemical characterization. *Microporous Mesoporous Mater.*, **127**, 228–236.
- 211 Park, K.-W., Jung, J.H., Seo, H.-J., and Kwon, O.-Y. (2009) Mesoporous silica-pillared kenyaite and magadiite as catalytic support for partial oxidation of methane. *Microporous Mesoporous Mater.*, **121**, 219–225.
- 212 Perdigon, A.C., Li, D., Pesquera, C., Gonzalez, F., Ortiz, B., Aguado, F., and Blanco, C. (2013) Synthesis of porous clay heterostructures from high charge mica-type aluminosilicates. *J. Mater. Chem. A*, **1**, 1213–1219.
- 213 Polverejan, M., Liu, Y., and Pinnavaia, T.J. (2002) Aluminated derivatives of porous clay heterostructures (PCH) assembled from synthetic saponite clay: properties as supermicroporous to small mesoporous acid catalysts. *Chem. Mater.*, **14**, 2283–2288.
- 214 Zhou, C., Li, X., Ge, Z., Li, Q., and Tong, D. (2004) Synthesis and acid catalysis of nanoporous silica/alumina-clay composites. *Catal. Today*, **93–95**, 607–613.

- 215 Cecilia, J.A., García-Sancho, C., and Franco, F. (2013) Montmorillonite based porous clay heterostructures: influence of Zr in the structure and acidic properties. *Microporous Mesoporous Mater.*, **176**, 95–102.
- 216 Pinto, M.L., Marques, J., and Pires, J. (2012) Porous clay heterostructures with zirconium for the separation of hydrocarbon mixtures. *Sep. Purif. Technol.*, **98**, 337–343.
- 217 Choy, J.-H., Jung, H., Han, Y.-S., Yoon, J.-B., Shul, Y.-G., and Kim, H.-J. (2002) New CoO – SiO<sub>2</sub>-sol pillared clays as catalysts for NO<sub>x</sub> conversion. *Chem. Mater.*, **14**, 3823–3828.
- 218 Bunnak, N., Ummartyotin, S., Laoratanakul, P., Bhalla, A.S., and Manuspiya, H. (2014) Synthesis and characterization of magnetic porous clay heterostructure. *J. Porous Mater.*, **21**, 1–8.
- 219 Kuzniarska-Biernacki, I., Silva, A., Carvalho, A., Pires, J., and Freire, C. (2010) Anchoring of chiral manganese(III) salen complex onto organo clay and porous clay heterostructure and catalytic activity in alkene epoxidation. *Catal. Lett.*, **134**, 63–71.
- 220 Kuźniarska-Biernacka, I., Pereira, C., Carvalho, A.P., Pires, J., and Freire, C. (2011) Epoxidation of olefins catalyzed by manganese(III) salen complexes grafted to porous heterostructured clays. *Appl. Clay Sci.*, **53**, 195–203.
- 221 Pereira, C., Biernacki, K., Rebelo, S.L.H., Magalhães, A.L., Carvalho, A.P., Pires, J., and Freire, C. (2009) Designing heterogeneous oxovanadium and copper acetylacetonate catalysts: effect of covalent immobilisation in epoxidation and aziridination reactions. *J. Mol. Catal. A: Chem.*, **312**, 53–64.
- 222 Nunes, C.D., Pires, J., Carvalho, A.P., Calhorda, M.J., and Ferreira, P. (2008) Synthesis and characterisation of organo-silica hydrophobic clay heterostructures for volatile organic compounds removal. *Microporous Mesoporous Mater.*, **111**, 612–619.
- 223 Wei, L., Tang, T., and Huang, B. (2004) Novel acidic porous clay heterostructure with highly ordered organic–inorganic hybrid structure: one-pot synthesis of mesoporous organosilica in the galleries of clay. *Microporous Mesoporous Mater.*, **67**, 175–179.
- 224 Mao, H., Gao, X., Yang, J., and Li, B. (2011) A novel one-step synthesis of mesostructured silica-pillared clay with highly ordered gallery organic–inorganic hybrid frame. *Appl. Surf. Sci.*, **257**, 4655–4662.
- 225 Letaïef, S. and Ruiz-Hitzky, E. (2003) Silica-clay nanocomposites. *Chem. Commun.*, 2996–2997.
- 226 Letaïef, S., Martín-Luengo, M.A., Aranda, P., and Ruiz-Hitzky, E. (2006) A colloidal route for delamination of layered solids: novel porous-clay nanocomposites. *Adv. Funct. Mater.*, **16**, 401–409.
- 227 Zapata, P.A., Belver, C., Quijada, R., Aranda, P., and Ruiz-Hitzky, E. (2013) Silica/clay organo-heterostructures to promote polyethylene–clay nanocomposites by in situ polymerization. *Appl. Catal., A*, **453**, 142–150.
- 228 Akkari, M., Aranda, P., Ben Haj Amara, A., and Ruiz-Hitzky, E. Novel silica-clay porous heterostructures doped with ZnO nanoparticles as photocatalysts, in preparation.



- 229 Manova, E., Aranda, P., Angeles Martín-Luengo, M., Letaïef, S., and Ruiz-Hitzky, E. (2010) New titania-clay nanostructured porous materials. *Microporous Mesoporous Mater.*, **131**, 252–260.
- 230 Bouna, L., Rhouta, B., Amjoud, M., Maury, F., Jada, A., Daoudi, L., Senocq, F., Lafont, M.-C., and Drouet, C. (2012) Synthèse, caractérisations et tests photocatalytiques d'un matériau argileux d'origine naturelle à base de beidellite fonctionnalisée par TiO<sub>2</sub>. *Mater. Tech.*, **100**, 241–252.
- 231 Rhouta, B., Bouna, L., Maury, F., Senocq, F., Lafont, M.C., Jada, A., Amjoud, M., and Daoudi, L. (2015) Surfactant-modifications of Na<sup>+</sup>-beidellite for the preparation of TiO<sub>2</sub>-Bd supported photocatalysts: I-organobeidellite precursor for nanocomposites. *Appl. Clay Sci.*, **115**, 260–265.
- 232 Rhouta, B., Bouna, L., Maury, F., Senocq, F., Lafont, M.C., Jada, A., Amjoud, M., and Daoudi, L. (2015) Surfactant-modifications of Na<sup>+</sup>-beidellite for the preparation of TiO<sub>2</sub>-Bd supported photocatalysts: II – Physico-chemical characterization and photocatalytic properties. *Appl. Clay Sci.*, **115**, 266–274.
- 233 Belver, C., Bedia, J., and Rodriguez, J.J. (2015) Titania – clay heterostructures with solar photocatalytic applications. *Appl. Catal., B*, **176–177**, 278–287.
- 234 Belver, C., Bedia, J., Álvarez-Montero, M.A., and Rodriguez, J.J. (2016) Solar photocatalytic purification of water with Ce-doped TiO<sub>2</sub>/clay heterostructures. *Catal. Today*, **266**, 36–45.
- 235 Pérez-Carvajal, J., Aranda, P., Obregón, S., Colón, G., and Ruiz-Hitzky, E. (2016) TiO<sub>2</sub>-clay based nanoarchitectures for enhanced photocatalytic hydrogen production. *Microporous Mesoporous Mater.*, **222**, 120–127.
- 236 Belver, C., Aranda, P., Martín-Luengo, M.A., and Ruiz-Hitzky, E. (2012) New silica/alumina-clay heterostructures: properties as acid catalysts. *Microporous Mesoporous Mater.*, **147**, 157–166.
- 237 Belver, C., Aranda, P., Martín-Luengo, M.A., and Ruiz-Hitzky, E. (2010) *Nouveaux matériaux poreux à partir d'argiles délaminiées*, Matériaux Nantes, Fédération Française pour les Sciences de la Chimie, Nantes, pp. 1–4.
- 238 Belver, C., Molinero, L., Ladero, M., Aranda, P., and Ruiz-Hitzky, E. (2010) *Silica/alumina Clay Nanocomposites as Heterogeneous Acid Catalysts*, SEA-CSSJ-CMS Trilateral Meeting on Clays, Seville, Seville, pp. 345–346.
- 239 Belver, C., Esteban, J., Ladero, M., Aranda, P., and Ruiz-Hitzky, E. (2011) Silica/alumina-clay heterostructures as catalysts for production of glycerol-derived chemicals, in *European Congress on Catalysis*, Glasgow.
- 240 Gómez-Avilés, A., Aranda, P., Fernandes, F.M., Belver, C., and Ruiz-Hitzky, E. (2013) Silica-sepiolite nanoarchitectures. *J. Nanosci. Nanotechnol.*, **13**, 2897–2907.
- 241 Aranda, P., Kun, R., Martín-Luengo, M.A., Letaïef, S., Dékány, I., and Ruiz-Hitzky, E. (2008) Titania – sepiolite nanocomposites prepared by a surfactant templating colloidal route. *Chem. Mater.*, **20**, 84–91.
- 242 Bouna, L., Rhouta, B., Amjoud, M., Maury, F., Lafont, M.C., Jada, A., Senocq, F., and Daoudi, L. (2011) Synthesis, characterization and photocatalytic activity of TiO<sub>2</sub> supported natural palygorskite microfibers. *Appl. Clay Sci.*, **52**, 301–311.

- 243 Bouna, L., Rhouta, B., and Maury, F. (2013) Physicochemical study of photocatalytic activity of TiO<sub>2</sub> supported palygorskite clay mineral. *Int. J. Photoenergy*, **2013**, 6.
- 244 Belver, C., Aranda, P., and Ruiz-Hitzky, E. (2013) Silica-alumina/sepiolite nanoarchitectures. *J. Mater. Chem. A*, **1**, 7477–7487.
- 245 Stathatos, E., Papoulis, D., Aggelopoulos, C.A., Panagiotaras, D., and Nikolopoulou, A. (2012) TiO<sub>2</sub>/palygorskite composite nanocrystalline films prepared by surfactant templating route: synergistic effect to the photocatalytic degradation of an azo-dye in water. *J. Hazard. Mater.*, **211–212**, 68–76.
- 246 Barrios-Neira, J., Rodrique, L., and Ruiz-Hitzky, E. (1974) Mise en évidence de groupements organiques insaturés greffés sur la sepiolite. *J. Microscopie*, **20**, 295–298.
- 247 Casal, B., Bergaya, F., Challal, D., Fripiat, J.J., Ruiz-Hitzky, E., and Van Damme, H. (1985) Photooxidation of water mediated by a clay-anchored Os-catalyst. *J. Mol. Catal.*, **33**, 83–86.
- 248 Letaief, S., Grant, S., and Detellier, C. (2011) Phenol acetylation under mild conditions catalyzed by gold nanoparticles supported on functional pre-acidified sepiolite. *Appl. Clay Sci.*, **53**, 236–243.
- 249 Park, D.-H., Cho, J., Kwon, O.-J., Yun, C.-O., and Choy, J.-H. (2016) Biodegradable inorganic nanovector: passive versus active tumor targeting in siRNA transportation. *Angew. Chem. Int. Ed.*, **55**, 4612.
- 250 Bhushan, B. (2009) Biomimetics: lessons from nature – an overview. *Philos. Trans. R. Soc. London, Ser. A*, **367**, 1445–1486.
- 251 Liu, K. and Jiang, L. (2011) Bio-inspired design of multiscale structures for function integration. *Nano Today*, **6**, 155–175.
- 252 Zhao, J., Zhao, X., Jiang, Z., Li, Z., Fan, X., Zhu, J., Wu, H., Su, Y., Yang, D., Pan, F., and Shi, J. (2014) Biomimetic and bioinspired membranes: preparation and application. *Prog. Polym. Sci.*, **39**, 1668–1720.
- 253 Alberts, B., Johnson, A., Lewis, J., Raff, M., Roberts, K., and Walter, P. (2014) *Molecular Biology of the Cell*, 5th edn, Garland Science, New York.
- 254 Simons, K. and Toomre, D. (2000) Lipid rafts and signal transduction. *Nat. Rev. Mol. Cell Biol.*, **1**, 31–39.
- 255 Shan, Y. and Wang, H. (2015) The structure and function of cell membranes examined by atomic force microscopy and single-molecule force spectroscopy. *Chem. Soc. Rev.*, **44**, 3617–3638.
- 256 Shen, Y.-x., Saboe, P.O., Sines, I.T., Erbakan, M., and Kumar, M. (2014) Biomimetic membranes: a review. *J. Membr. Sci.*, **454**, 359–381.
- 257 Lehn, J.M. (2002) Toward self-organization and complex matter. *Science*, **295**, 2400–2403.
- 258 Ariga, K., Hill, J.P., Lee, M.V., Vinu, A., Charvet, R., and Acharya, S. (2008) Challenges and breakthroughs in recent research on self-assembly. *Sci. Technol. Adv. Mater.*, **9**, 014109.
- 259 Rapuano, R. and Carmona-Ribeiro, A.M. (1997) Physical adsorption of bilayer membranes on silica. *J. Colloid Interface Sci.*, **193**, 104–111.
- 260 Anderson, T.H., Min, Y.J., Weirich, K.L., Zeng, H.B., Fygenon, D., and Israelachvili, J.N. (2009) Formation of supported bilayers on silica substrates. *Langmuir*, **25**, 6997–7005.

- 261 Petty, M.C. (1996) *Langmuir–Blodgett Films. An Introduction*, Cambridge University Press, Cambridge.
- 262 Szabo, T., Mitea, R., Leeman, H., Premachandra, G.S., Johnston, C.T., Szekeres, M., Dekany, I., and Schoonheydt, R.A. (2008) Adsorption of protamine and papain proteins on saponite. *Clays Clay Miner.*, **56**, 494–504.
- 263 Davis, S.A., Dujardin, E., and Mann, S. (2003) Biomolecular inorganic materials chemistry. *Curr. Opin. Solid State Mater. Sci.*, **7**, 273–281.
- 264 Angelatos, A.S., Katagiri, K., and Caruso, F. (2006) Bioinspired colloidal systems via layer-by-layer assembly. *Soft Matter*, **2**, 18–23.
- 265 Becker, A.L., Johnston, A.P.R., and Caruso, F. (2010) Peptide nucleic acid films and capsules: assembly and enzymatic degradation. *Macromol. Biosci.*, **10**, 488–495.
- 266 Lu, J.R., Zhao, X.B., and Yaseen, M. (2007) Biomimetic amphiphiles: biosurfactants. *Curr. Opin. Colloid Interface Sci.*, **12**, 60–67.
- 267 Carnero Ruiz, C. (2009) *Sugar-Based Surfactants. Fundamentals and applications*, CRC Press, Taylor & Francis Group, Boca Raton, FL.
- 268 Pacwa-Plociniczak, M., Plaza, G.A., Piotrowska-Seget, Z., and Cameotra, S.S. (2011) Environmental applications of biosurfactants: recent advances. *Int. J. Mol. Sci.*, **12**, 633–654.
- 269 Lang, S. (2002) Biological amphiphiles (microbial biosurfactants). *Curr. Opin. Colloid Interface Sci.*, **7**, 12–20.
- 270 Ruiz-Hitzky, E., Darder, M., Aranda, P., and Ariga, K. (2010) Advances in biomimetic and nanostructured biohybrid materials. *Adv. Mater.*, **22**, 323–336.
- 271 Wicklein, B., Darder, M., Aranda, P., and Ruiz-Hitzky, E. (2011) Phospholipid–sepiolite biomimetic interfaces for the immobilization of enzymes. *ACS Appl. Mater. Interfaces*, **3**, 4339–4348.
- 272 Konnova, S.A., Sharipova, I.R., Demina, T.A., Osin, Y.N., Yarullina, D.R., Ilinskaya, O.N., Lvov, Y.M., and Fakhrullin, R.F. (2013) Biomimetic cell-mediated three-dimensional assembly of halloysite nanotubes. *Chem. Commun.*, **49**, 4208–4210.
- 273 Fakhrullin, R.F., Zamaleeva, A.I., Minullina, R.T., Konnova, S.A., and Paunov, V.N. (2012) Cyborg cells: functionalisation of living cells with polymers and nanomaterials. *Chem. Soc. Rev.*, **41**, 4189–4206.
- 274 Hederos, M., Konradsson, P., and Liedberg, B. (2005) Synthesis and self-assembly of galactose-terminated alkanethiols and their ability to resist proteins. *Langmuir*, **21**, 2971–2980.
- 275 Fyrner, T., Lee, H.-H., Mangone, A., Ekblad, T., Pettitt, M.E., Callow, M.E., Callow, J.A., Conlan, S.L., Mutton, R., Clare, A.S., Konradsson, P., Liedberg, B., and Ederth, T. (2011) Saccharide-functionalized alkanethiols for fouling-resistant self-assembled monolayers: synthesis, monolayer properties, and antifouling behavior. *Langmuir*, **27**, 15034–15047.
- 276 Stubbs, G.W., Smith, H.G., and Litman, B.J. (1976) Alkyl glucosides as effective solubilizing agents for bovine rhodopsin – comparison with several commonly used detergents. *BBA*, **426**, 46–56.
- 277 Privé, G.G. (2007) Detergents for the stabilization and crystallization of membrane proteins. *Methods*, **41**, 388–397.

- 278 Mukherjee, D., May, M., and Khomami, B. (2011) Detergent–protein interactions in aqueous buffer suspensions of Photosystem I (PS I). *J. Colloid Interface Sci.*, **358**, 477–484.
- 279 Evans, D.G. and Slade, R.C.T. (2005) Structural aspects of layered double hydroxides, in *Layered Double Hydroxides* (eds D.G. Evans and X. Duan), Springer, Berlin Heidelberg.
- 280 Leroux, F. and Besse, J.-P. (2001) Polymer interleaved layered double hydroxide: a new emerging class of nanocomposites. *Chem. Mater.*, **13**, 3507–3515.
- 281 Rogez, G., Massobrio, C., Rabu, P., and Drillon, M. (2011) Layered hydroxide hybrid nanostructures: a route to multifunctionality. *Chem. Soc. Rev.*, **40**, 1031–1058.
- 282 Wicklein, B., Martín del Burgo, M.Á., Yuste, M., Darder, M., Escrig Llavata, C., Aranda, P., Ortín, J., del Real, G., and Ruiz-Hitzky, E. (2012) Lipid-based bio-nanohybrids for functional stabilisation of influenza vaccines. *Eur. J. Inorg. Chem.*, **2012**, 5186–5191.
- 283 Thasneem, Y.M., Rekha, M.R., Sajeesh, S., and Sharma, C.P. (2013) Biomimetic mucin modified PLGA nanoparticles for enhanced blood compatibility. *J. Colloid Interface Sci.*, **409**, 237–244.
- 284 Sandberg, T., Karlsson Ott, M., Carlsson, J., Feiler, A., and Caldwell, K.D. (2009) Potential use of mucins as biomaterial coatings. II. Mucin coatings affect the conformation and neutrophil-activating properties of adsorbed host proteins – toward a mucosal mimic. *J. Biomed. Mater. Res. Part A*, **91A**, 773–785.
- 285 Cook, M.T., Smith, S.L., and Khutoryanskiy, V.V. (2015) Novel glycopolymer hydrogels as mucosa-mimetic materials to reduce animal testing. *Chem. Commun.*, **51**, 14447–14450.
- 286 Cook, M.T. and Khutoryanskiy, V.V. (2015) Mucoadhesion and mucosa-mimetic materials – a mini-review. *Int. J. Pharm.*, **495**, 991–998.
- 287 Viebke, C., Al-Assaf, S., and Phillips, G.O. (2014) Food hydrocolloids and health claims. *Bioact. Carbohydr. Dietary Fibre*, **4**, 101–114.
- 288 Ruiz-Hitzky, E., Darder, M., Aranda, P., Martín del Burgo, M.Á., and del Real, G. (2009) Bionanocomposites as new carriers for influenza vaccines. *Adv. Mater.*, **21**, 4167–4171.
- 289 Zhou, Y., Hu, N., Zeng, Y., and Rusling, J.F. (2002) Heme protein–clay films: direct electrochemistry and electrochemical catalysis. *Langmuir*, **18**, 211–219.
- 290 Chen, X., Hu, N., Zeng, Y., Rusling, J.F., and Yang, J. (1999) Ordered electrochemically active films of hemoglobin, didodecyldimethylammonium ions, and clay. *Langmuir*, **15**, 7022–7030.
- 291 Wicklein, B., Aranda, P., Ruiz-Hitzky, E., and Darder, M. (2013) Hierarchically structured bioactive foams based on polyvinyl alcohol-sepiolite nanocomposites. *J. Mater. Chem. B*, **1**, 2911–2920.
- 292 Ghadiri, M., Chrzanowski, W., and Rohanizadeh, R. (2015) Biomedical applications of cationic clay minerals. *RSC Adv.*, **5**, 29467–29481.

- 293 Carretero, M.I. and Pozo, M. (2009) Clay and non-clay minerals in the pharmaceutical industry Part I. Excipients and medical applications. *Appl. Clay Sci.*, **46**, 73–80.
- 294 Aguzzi, C., Cerezo, P., Viseras, C., and Caramella, C. (2007) Use of clays as drug delivery systems: possibilities and limitations. *Appl. Clay Sci.*, **36**, 22–36.
- 295 Viseras, C., Cerezo, P., Sanchez, R., Salcedo, I., and Aguzzi, C. (2010) Current challenges in clay minerals for drug delivery. *Appl. Clay Sci.*, **48**, 291–295.
- 296 Rodrigues, L.A.d.S., Figueiras, A., Veiga, F., de Freitas, R.M., Nunes, L.C.C., da Silva Filho, E.C., and da Silva Leite, C.M. (2013) The systems containing clays and clay minerals from modified drug release: a review. *Colloids Surf., B*, **103**, 642–651.
- 297 Choy, J.H., Choi, S.J., Oh, J.M., and Park, T. (2007) Clay minerals and layered double hydroxides for novel biological applications. *Appl. Clay Sci.*, **36**, 122–132.
- 298 Joshi, G.V., Kevadiya, B.D., Patel, H.A., Bajaj, H.C., and Jasra, R.V. (2009) Montmorillonite as a drug delivery system: intercalation and in vitro release of timolol maleate. *Int. J. Pharm.*, **374**, 53–57.
- 299 Oh, J.-M., Biswick, T.T., and Choy, J.-H. (2009) Layered nanomaterials for green materials. *J. Mater. Chem.*, **19**, 2553–2563.
- 300 Lin, F.H., Lee, Y.H., Jian, C.H., Wong, J.-M., Shieh, M.-J., and Wang, C.-Y. (2002) A study of purified montmorillonite intercalated with 5-fluorouracil as drug carrier. *Biomaterials*, **23**, 1981–1987.
- 301 Park, J.K., Choy, Y.B., Oh, J.-M., Kim, J.Y., Hwang, S.-J., and Choy, J.-H. (2008) Controlled release of donepezil intercalated in smectite clays. *Int. J. Pharm.*, **359**, 198–204.
- 302 Kose, A.A., Karabagli, Y., Kurkcuoglu, M., and Cetin, C. (2005) Alpha sepiolite: an old clay mineral a new dressing material. *Wounds*, **17**, 114–121.
- 303 Oscarson, D.W., Van Scoyoc, G.E., and Ahlrichs, J.L. (1986) Lysis of erythrocytes by silicate minerals. *Clays Clay Miner.*, **34**, 74–80.
- 304 Carretero, M. and Pozo, M. (2007) *Mineralogía aplicada: salud y medio ambiente*, Paraninfo, Madrid, p. 406.
- 305 Santarén, J. and Alvarez, A. (1994) Assessment of the health effects of mineral dust. The sepiolite case. *Ind. Miner.*, 101–114.
- 306 Rytwo, G. (2014) The use of hybrid organoclays and nanocomposites for slow release of high vapor pressure compounds. HINT Workshop Working Group 1 & 4 Meeting: Role of Interface in Synthesis and Applications, Turku, Finland.
- 307 Jamshidi, R., Afzali, Z., and Afzali, D. (2009) Chemical composition of hydrodistillation essential oil of rosemary in different origins in Iran and comparison with other countries. *American-Eurasian J. Agric. Environ. Sci.*, **5**, 78–81.
- 308 Jiang, Y., Wu, N., Fu, Y.-J., Wang, W., Luo, M., Zhao, C.-J., Zu, Y.-G., and Liu, X.-L. (2011) Chemical composition and antimicrobial activity of the essential oil of Rosemary. *Eur. J. Pharmacol. Environ. Toxicol. Pharm.*, **32**, 63–68.

- 309 Szumny, A., Figiel, A., Gutiérrez-Ortíz, A., and Carbonell-Barrachina, Á.A. (2010) Composition of rosemary essential oil (*Rosmarinus officinalis*) as affected by drying method. *J. Food Eng.*, **97**, 253–260.
- 310 Vasilakos, S.P. and Tarantili, P.A. (2012) In vitro drug release studies from organoclay/poly(dimethyl siloxane) nanocomposite matrices. *J. Biomed. Mater. Res. Part B*, **100B**, 1899–1910.
- 311 Styan, K.E., Martin, D.J., and Poole-Warren, L.A. (2008) In vitro fibroblast response to polyurethane organosilicate nanocomposites. *J. Biomed. Mater. Res. Part A*, **86A**, 571–582.
- 312 Luckham, P.F. and Rossi, S. (1999) The colloidal and rheological properties of bentonite suspensions. *Adv. Colloid Interface Sci.*, **82**, 43–92.
- 313 Alcantara, A.C.S., Aranda, P., Darder, M., and Ruiz-Hitzky, E. (2010) Bio-nanocomposites based on alginate-zein/layered double hydroxide materials as drug delivery systems. *J. Mater. Chem.*, **20**, 9495–9504.
- 314 Ribeiro, L.N.M., Alcântara, A.C.S., Darder, M., Aranda, P., Araújo-Moreira, F.M., and Ruiz-Hitzky, E. (2014) Pectin-coated chitosan–LDH bionanocomposite beads as potential systems for colon-targeted drug delivery. *Int. J. Pharm.*, **463**, 1–9.
- 315 Gonçalves, M., Figueira, P., Maciel, D., Rodrigues, J., Qu, X., Liu, C., Tomás, H., and Li, Y. (2014) pH-sensitive Laponite<sup>®</sup>/doxorubicin/alginate nanohybrids with improved anticancer efficacy. *Acta Biomater.*, **10**, 300–307.
- 316 Banik, N., Ramteke, A., and Maji, T.K. (2014) Carboxymethyl chitosan-montmorillonite nanoparticles for controlled delivery of isoniazid: evaluation of the effect of the glutaraldehyde and montmorillonite. *Polym. Adv. Technol.*, **25**, 1580–1589.
- 317 Aguzzi, C., Sandri, G., Bonferoni, C., Cerezo, P., Rossi, S., Ferrari, F., Caramella, C., and Viseras, C. (2014) Solid state characterisation of silver sulfadiazine loaded on montmorillonite/chitosan nanocomposite for wound healing. *Colloids Surf., B*, **113**, 152–157.
- 318 Wang, Q., Wu, J., Wang, W., and Wang, A. (2011) Preparation, characterization and drug-release behaviors of crosslinked chitosan/attapulgitite hybrid microspheres by a facile spray-drying technique. *J. Biomater. Nanobiotechnol.*, **2**, 250–257.
- 319 Wang, Q., Wang, W., Wu, J., and Wang, A. (2012) Effect of attapulgitite contents on release behaviors of a pH sensitive carboxymethyl cellulose-g-poly(acrylic acid)/attapulgitite/sodium alginate composite hydrogel bead containing diclofenac. *J. Appl. Polym. Sci.*, **124**, 4424–4432.
- 320 Lvov, Y. and Abdullayev, E. (1690-1719) Functional polymer–clay nanotube composites with sustained release of chemical agents. *Prog. Polym. Sci.*, **2013**, 38.
- 321 Kelly, H.M., Deasy, P.B., Ziaka, E., and Claffey, N. (2004) Formulation and preliminary in vivo dog studies of a novel drug delivery system for the treatment of periodontitis. *Int. J. Pharm.*, **274**, 167–183.
- 322 Schmitt, H., Creton, N., Prashantha, K., Soulestin, J., Lacrampe, M.F., and Krawczak, P. (2015) Melt-blended halloysite nanotubes/wheat starch nanocomposites as drug delivery system. *Polym. Eng. Sci.*, **55**, 573–580.
- 323 Liu, M., Chang, Y., Yang, J., You, Y., He, R., Chen, T., and Zhou, C. (2016) Functionalized halloysite nanotube by chitosan grafting for drug delivery



- of curcumin to achieve enhanced anticancer efficacy. *J. Mater. Chem. B*, **4**, 2253–2263.
- 324 Choy, J.-H., Kwak, S.-Y., Jeong, Y.-J., and Park, J.-S. (2000) Inorganic layered double hydroxides as nonviral vectors. *Angew. Chem. Int. Ed.*, **39**, 4041–4045.
- 325 Paget, E., Monrozier, L.J., and Simonet, P. (1992) Adsorption of DNA on clay minerals: protection against DNaseI and influence on gene transfer. *FEMS Microbiol. Lett.*, **97**, 31–39.
- 326 Castro-Smirnov, F.A., Piétrement, O., Aranda, P., Bertrand, J.R., Ayache, J., Le Cam, E., Ruiz-Hitzky, E. and Lopez, B.S. (2016) Physical interactions between DNA and sepiolite nanofibers, and potential application for DNA transfer into mammalian cells. *Sci. Rep.*, **6**, 36341.
- 327 Naoto, Y. (2007) Discovery and application of the yoshida effect: nano-sized acicular materials enable penetration of bacterial cells by sliding friction force. *Recent Pat. Biotechnol.*, **1**, 194–201.
- 328 Castro-Smirnov, F.A. (2014) *Physicochemical Characterization of DNA-Based Bionanocomposites Using Nanofibrous Clay Minerals. Biological Applications*, Université Paris XI, Versailles (France).
- 329 Heegaard, P., Dedieu, L., Johnson, N., Le Potier, M.-F., Mockey, M., Mutinelli, F., Vahlenkamp, T., Vascellari, M., and Sørensen, N. (2011) Adjuvants and delivery systems in veterinary vaccinology: current state and future developments. *Arch. Virol*, **156**, 183–202.
- 330 Patil, V., Venkatesh, M.D., Krishnappa, G.K., and Srinivasa Gouda, R.N. (2004) Immune response of calves to bentonite and alum adjuvanted combined vaccine against haemorrhagic septicaemia and black quarter. *Indian J. Ani. Sci.*, **74**, 845–847.
- 331 Brandau, D.T., Jones, L.S., Wiethoff, C.M., Rexroad, J., and Middaugh, C.R. (2003) Thermal stability of vaccines. *J. Pharm. Sci.*, **92**, 218–231.
- 332 Chen, D. and Kristensen, D. (2009) Opportunities and challenges of developing thermostable vaccines. *Expert Rev. Vaccines*, **8**, 547–557.
- 333 Maa, Y.-F., Zhao, L., Payne, L.G., and Chen, D. (2003) Stabilization of alum-adjuvanted vaccine dry powder formulations: mechanism and application. *J. Pharm. Sci.*, **92**, 319–332.
- 334 Clapp, T., Siebert, P., Chen, D., and Jones Braun, L. (2011) Vaccines with aluminum-containing adjuvants: optimizing vaccine efficacy and thermal stability. *J. Pharm. Sci.*, **100**, 388–401.
- 335 Wittayanukuluk, A., Jiang, D., Regnier, F.E., and Hem, S.L. (2004) Effect of microenvironment pH of aluminum hydroxide adjuvant on the chemical stability of adsorbed antigen. *Vaccine*, **22**, 1172–1176.
- 336 Fujimori, A., Arai, S., Soutome, Y., and Hashimoto, M. (2014) Improvement of thermal stability of enzyme via immobilization on Langmuir–Blodgett films of organo-modified aluminosilicate with high coverage. *Colloids Surf, A*, **448**, 45–52.
- 337 Wicklein, B., Darder, M., Aranda, P., Martín del Burgo, M.A., del Real, G., Esteban, M., and Ruiz-Hitzky, E. (2016) Clay–lipid nanohybrids: toward influenza vaccines and beyond. *Clay Miner.*, **51**, 529–538.

- 338 Sánchez-Sampedro, L., Gómez, C.E., Mejías-Pérez, E., Sorzano, C.O.S., and Esteban, M. (2012) High quality long-term CD4+ and CD8+ effector memory populations stimulated by DNA-LACK/MVA-LACK regimen in leishmania major BALB/c model of infection. *PLoS One*, **7**, e38859.
- 339 Ruiz-Hitzky, E., Darder, M., Fernandes, F.M., Wicklein, B., Alcântara, A.C.S., and Aranda, P. (2015) in *Natural Mineral Nanotubes: Properties and Applications* (eds P. Pasbakhsh and G.J. Churchman), Apple Academic Press.
- 340 Wu, C.-J., Gaharwar, A.K., Schexnailder, P.J., and Schmidt, G. (2010) Development of biomedical polymer-silicate nanocomposites: a materials science perspective. *Materials*, **3**, 2986.
- 341 Dawson, J.I. and Oreffo, R.O.C. (2013) Clay: new opportunities for tissue regeneration and biomaterial design. *Adv. Mater.*, **25**, 4069–4086.
- 342 Lee, J.H., Park, T.G., Park, H.S., Lee, D.S., Lee, Y.K., Yoon, S.C., and Nam, J.-D. (2003) Thermal and mechanical characteristics of poly(l-lactic acid) nanocomposite scaffold. *Biomaterials*, **24**, 2773–2778.
- 343 Zheng, J.P., Wang, C.Z., Wang, X.X., Wang, H.Y., Zhuang, H., and Yao, K.D. (2007) Preparation of biomimetic three-dimensional gelatin/montmorillonite–chitosan scaffold for tissue engineering. *React. Funct. Polym.*, **67**, 780–788.
- 344 Gaharwar, A.K., Schexnailder, P.J., Jin, Q., Wu, C.-J., and Schmidt, G. (2010) Addition of chitosan to silicate cross-linked PEO for tuning osteoblast cell adhesion and mineralization. *ACS Appl. Mater. Interfaces*, **2**, 3119–3127.
- 345 Zhuang, H., Zheng, J.P., Gao, H., and De Yao, K. (2007) In vitro biodegradation and biocompatibility of gelatin/montmorillonite-chitosan intercalated nanocomposite. *J. Mater. Sci. - Mater. Med.*, **18**, 951–957.
- 346 Mkhabela, V. and Ray, S.S. (2015) Biodegradation and bioresorption of poly( $\epsilon$ -caprolactone) nanocomposite scaffolds. *Int. J. Biol. Macromol.*, **79**, 186–192.
- 347 Kalpana, S.K., Dinesh, R.K., and Rajalaxmi, D. (2008) Synthesis and characterization of a novel chitosan/montmorillonite/hydroxyapatite nanocomposite for bone tissue engineering. *Biomed. Mater.*, **3**, 034122.
- 348 Ambre, A.H., Katti, D.R., and Katti, K.S. (2015) Biomineralized hydroxyapatite nanoclay composite scaffolds with polycaprolactone for stem cell-based bone tissue engineering. *J. Biomed. Mater. Res. Part A*, **103**, 2077–2101.
- 349 Ordikhani, F., Dehghani, M., and Simchi, A. (2015) Antibiotic-loaded chitosan–Laponite films for local drug delivery by titanium implants: cell proliferation and drug release studies. *J. Mater. Sci. - Mater. Med.*, **26**, 1–12.
- 350 Perez-Castells, R., Alvarez, A., Gavilanes, J., Lizarbe, M.A., Martínez Del Pozo, A., Olmo, N., and Santaren, J. (1985) Adsorption of collagen by sepiolite, in *Proceedings of the International Clay Conference Denver* (eds L.G. Schultz, H. van Olphen, and F.A. Mumpton), The Clay Minerals Society, Bloomington, IN, pp. 359–362.
- 351 Lizarbe, M.A., Olmo, N., and Gavilanes, J.G. (1987) Adhesion and spreading of fibroblasts on sepiolite-collagen complexes. *J. Biomed. Mater. Res.*, **21**, 137–144.

- 352 Herrera, J.I., Olmo, N., Turnay, J., Sicilia, A., Bascones, A., Gavilanes, J.G., and Lizarbe, M.A. (1995) Implantation of sepiolite-collagen complexes in surgically created rat calvaria defects. *Biomaterials*, **16**, 625–631.
- 353 Olmo, N., Turnay, J., Herrera, J.I., Gavilanes, J.G., and Lizarbe, M.A. (1996) Kinetics of in vivo degradation of sepiolite-collagen complexes: effect of glutaraldehyde treatment. *J. Biomed. Mater. Res.*, **30**, 77–84.
- 354 Fernandes, F.M., Manjubala, I., and Ruiz-Hitzky, E. (2011) Gelatin renaturation and the interfacial role of fillers in bionanocomposites. *Phys. Chem. Chem. Phys.*, **13**, 4901–4910.
- 355 Su, D., Wang, C., Cai, S., Mu, C., Li, D., and Lin, W. (2012) Influence of palygorskite on the structure and thermal stability of collagen. *Appl. Clay Sci.*, **62–63**, 41–46.
- 356 Fukushima, K., Wu, M.-H., Bocchini, S., Rasyida, A., and Yang, M.-C. (2012) PBAT based nanocomposites for medical and industrial applications. *Mater. Sci. Eng., C*, **32**, 1331–1351.
- 357 Liu, M., Dai, L., Shi, H., Xiong, S., and Zhou, C. (2015) In vitro evaluation of alginate/halloysite nanotube composite scaffolds for tissue engineering. *Mater. Sci. Eng., C*, **49**, 700–712.
- 358 Naumenko, E.A., Guryanov, I.D., Yendluri, R., Lvov, Y.M., and Fakhrullin, R.F. (2016) Clay nanotube-biopolymer composite scaffolds for tissue engineering. *Nanoscale*, **8**, 7257–7271.
- 359 Grassi, M., Kaykioglu, G., Belgiorno, V., and Lofrano, G. (2012) in *Emerging Compounds Removal from Wastewater: Natural and Solar Based Treatments* (ed. G. Lofrano), Springer Netherlands, Dordrecht, pp. 15–37.
- 360 Ismadji, S., Soetaredjo, F.E., and Ayucitra, A. (2015) *Clay Materials for Environmental Remediation*, Springer International Publishing, Cham, pp. 5–37.
- 361 Bhattacharyya, K.G., SenGupta, S., and Sarma, G.K. (2014) Interactions of the dye, Rhodamine B with kaolinite and montmorillonite in water. *Appl. Clay Sci.*, **99**, 7–17.
- 362 Wu, Q., Li, Z., Hong, H., Yin, K., and Tie, L. (2010) Adsorption and intercalation of ciprofloxacin on montmorillonite. *Appl. Clay Sci.*, **50**, 204–211.
- 363 Wu, Q., Li, Z., and Hong, H. (2013) Adsorption of the quinolone antibiotic nalidixic acid onto montmorillonite and kaolinite. *Appl. Clay Sci.*, **74**, 66–73.
- 364 Paul, B., Yang, D., Yang, X., Ke, X., Frost, R., and Zhu, H. (2010) Adsorption of the herbicide simazine on moderately acid-activated beidellite. *Appl. Clay Sci.*, **49**, 80–83.
- 365 Koch, D. (2002) Bentonites as a basic material for technical base liners and site encapsulation cut-off walls. *Appl. Clay Sci.*, **21**, 1–11.
- 366 Sánchez-Jiménez, N., Sevilla, M.T., Cuevas, J., Rodríguez, M., and Procopio, J.R. (2012) Interaction of organic contaminants with natural clay type geosorbents: potential use as geologic barrier in urban landfill. *J. Environ. Manage.*, **95** (Supplement), S182–S187.
- 367 Shen, Y.H. (2004) Phenol sorption by organoclays having different charge characteristics. *Colloids Surf., A*, **232**, 143–149.

- 368 Lee, S.M. and Tiwari, D. (2012) Organo and inorgano-organo-modified clays in the remediation of aqueous solutions: an overview. *Appl. Clay Sci.*, **59–60**, 84–102.
- 369 Johnston, C.T. (1996) in *Sorption of Organic Compounds on Clay Minerals: A Surface Functional Group Approach* (ed. B. Sahwney), The Clay Mineral Society, Boulder CO, pp. 1–44.
- 370 Srinivasan, R. (2011) Advances in application of natural clay and its composites in removal of biological, organic, and inorganic contaminants from drinking water. *Adv. Mater. Sci. Eng.*, **2011**, 1–17.
- 371 Nir, S., El-Nahhal, Y., Undabeytia, T., Rytwo, G., Polubesova, T., Mishael, Y., Rabinovitz, O., and Rubin, B. (2013) *Clays, Clay Minerals, and Pesticides*, vol. 5, Elsevier, pp. 645–662, Chapter 5.2, .
- 372 Nafees, M. and Waseem, A. (2014) Organoclays as sorbent material for phenolic compounds: a review. *CLEAN – Soil, Air, Water*, **42**, 1500–1508.
- 373 Bors, J., Gorny, A., and Dultz, S. (1997) Iodide, caesium and strontium adsorption by organophilic vermiculite. *Clay Miner.*, **32**, 21–28.
- 374 Darder, M., Colilla, M., and Ruiz-Hitzky, E. (2005) Chitosan–clay nanocomposites: application as electrochemical sensors. *Appl. Clay Sci.*, **28**, 199–208.
- 375 An, J.-H. and Dultz, S. (2007) Adsorption of tannic acid on chitosan-montmorillonite as a function of pH and surface charge properties. *Appl. Clay Sci.*, **36**, 256–264.
- 376 An, J.H. and Dultz, S. (2008) Adsorption of Cr(VI) and As(V) on chitosan-montmorillonite: selectivity and ph dependence. *Clays Clay Miner.*, **56**, 549–557.
- 377 Leovac, A., Vasyukova, E., Ivancev-Tumbas, I., Uhl, W., Kragulj, M., Trickovic, J., Kerkez, D., and Dalmacija, B. (2015) Sorption of atrazine, alachlor and trifluralin from water onto different geosorbents. *RSC Adv.*, **5**, 8122–8133.
- 378 Dultz, S., Riebe, B., and Bunnenberg, C. (2005) Temperature effects on iodine adsorption on organo-clay minerals: II. *Structural effects. Appl. Clay Sci.*, **28**, 17–30.
- 379 Darder, M., Valera, A., Nieto, E., Colilla, M., Fernández, C.J., Romero-Aranda, R., Cuartero, J., and Ruiz-Hitzky, E. (2009) Multisensor device based on case-based reasoning (CBR) for monitoring nutrient solutions in fertigation. *Sens. Actuators, B*, **135**, 530–536.
- 380 Jović-Jovičić, N., Mojović, Z., Darder, M., Aranda, P., Ruiz-Hitzky, E., Banković, P., Jovanović, D., and Milutinović-Nikolić, A. (2016) Smectite-chitosan-based electrodes in electrochemical detection of phenol and its derivatives. *Appl. Clay Sci.*, **124–125**, 62–68.
- 381 Rytwo, G. and Gonen, Y. (2006) Very fast sorbent for organic dyes and pollutants. *Colloid. Polym. Sci.*, **284**, 817–820.
- 382 Alther, G. (2002) Using organoclays to enhance carbon filtration. *Waste Manage.*, **22**, 507–513.
- 383 Umpuch, C. and Sakaew, S. (2015) Adsorption characteristics of reactive black 5 onto chitosan-intercalated montmorillonite. *Desalin. Water Treat.*, **53**, 2962–2969.

- 384 Padilla-Ortega, E., Darder, M., Aranda, P., Figueredo Gouveia, R., Leyva-Ramos, R., and Ruiz-Hitzky, E. (2016) Ultrasound assisted preparation of chitosan–vermiculite bionanocomposite foams for cadmium uptake. *Appl. Clay Sci.*, **130**, 40–49.
- 385 Alcântara, A.C.S., Darder, M., Aranda, P., and Ruiz-Hitzky, E. (2014) Polysaccharide-fibrous clay bionanocomposites. *Appl. Clay Sci.*, **96**, 2–8.
- 386 Alcántara, A.C.S., Darder, M., Aranda, P., Tateyama, S., Okajima, M.K., Kaneko, T., Ogawa, M., and Ruiz-Hitzky, E. (2014) Clay-bionanocomposites with sacran megamolecules for the selective uptake of neodymium. *J. Mater. Chem. A*, **2**, 1391–1399.
- 387 Pan, G., Zhang, M.M., Chen, H., Zou, H., and Yan, H. (2006) Removal of cyanobacterial blooms in Taihu Lake using local soils. I. Equilibrium and kinetic screening on the flocculation of microcystis aeruginosa using commercially available clays and minerals. *Environ. Pollut.*, **141**, 195–200.
- 388 Ferronato, C., Silva, B., Costa, F., and Tavares, T. (2016) Vermiculite bio-barriers for Cu and Zn remediation: an eco-friendly approach for fresh-water and sediments protection. *Int. J. Environ. Sci. Technol.*, **13**, 1219–1228.
- 389 Rytwo, G., Rettig, A., and Gonen, Y. (2011) Organo-sepiolite particles for efficient pretreatment of organic wastewater: application to winery effluents. *Appl. Clay Sci.*, **51**, 390–394.
- 390 Zhu, R., Zhu, J., Ge, F., and Yuan, P. (2009) Regeneration of spent organo-clays after the sorption of organic pollutants: a review. *J. Environ. Manage.*, **90**, 3212–3216.
- 391 Koriche, Y., Darder, M., Aranda, P., Semsari, S., and Ruiz-Hitzky, E. (2014) Bionanocomposites based on layered silicates and cationic starch as eco-friendly adsorbents for hexavalent chromium removal. *Dalton Trans.*, **43**, 10512–10520.
- 392 Xue, S. and Pinnavaia, T.J. (2007) in *CMS Workshop Lectures Series*, vol. **15** (ed. K.A.C.A.F. Bergaya), The Clay Minerals Society, Chantilly VA, pp. 1–32.
- 393 Rytwo, G., Huterer-Harari, R., Dultz, S., and Gonen, Y. (2006) Adsorption of fast green and erythrosin-B to montmorillonite modified with crystal violet. *J. Therm. Anal. Calorim.*, **84**, 225–231.
- 394 Riebe, B., Bunnenberg, C., and Dultz, S. (2005) Studies on organophilic clays as adsorbents for anions in engineered barriers. Final Report (in German). Reference Number 02E9481.
- 395 Singh, N., Megharaj, M., Gates, W.P., Churchman, G.J., Anderson, J., Kookana, R.S., Naidu, R., Chen, Z., Slade, P.G., and Sethunathan, N. (2003) Bioavailability of an organophosphorus pesticide, fenamiphos, sorbed on an organo clay. *J. Agric. Food. Chem.*, **51**, 2653–2658.
- 396 Masaphy, S., Zohar, S., and Jander-Shagug, G. (2014) Biodegradation of p-nitrophenol sorbed onto crystal violet-modified organoclay by *Arthrobacter* sp. 4H $\beta$ . *Appl. Microbiol. Biotechnol.*, **98**, 1321–1327.
- 397 Scher, H.B. (1999) *Controlled-Release Delivery Systems for Pesticides*, Marcel Dekker, New York.
- 398 Undabeytia, T., Recio, E., Maqueda, C., Sánchez-Verdejo, T., and Balek, V. (2012) Slow diuron release formulations based on clay–phosphatidylcholine complexes. *Appl. Clay Sci.*, **55**, 53–61.

- 399 Singh, B., Sharma, D.K., Dhiman, A., and Gupta, A. (2011) Applications of natural polysaccharide-based beads for slow release herbicide formulation. *Toxicol. Environ. Chem.*, **93**, 616–622.
- 400 Radian, A. and Mishael, Y.G. (2008) Characterizing and designing poly-cation – clay nanocomposites as a basis for imazapyr controlled release formulations. *Environ. Sci. Technol.*, **42**, 1511–1516.
- 401 Alromeed, A.A., Scrano, L., Bufo, S.A., and Undabeytia, T. (2015) Slow-release formulations of the herbicide MCPA by using clay-protein composites. *Pest Manage. Sci.*, **71**, 1303–1310.
- 402 Cabrera, A., Celis, R., and Hermosín, M.C. (2016) Imazamox–clay complexes with chitosan- and iron(III)-modified smectites and their use in nanoformulations. *Pest Manage. Sci.*, **72**, 1285–1294.
- 403 Giroto, A.S., de Campos, A., Pereira, E.I., Ribeiro, T.S., Marconcini, J.M., and Ribeiro, C. (2015) Photoprotective effect of starch/montmorillonite composites on ultraviolet-induced degradation of herbicides. *React. Funct. Polym.*, **93**, 156–162.